ENHANCEMENT OF DISPERSIBILITY OF ZERO-VALENT IRON NANOPARTICLES FOR ENVIRONMENTAL REMEDIATION: ENTRAPMENT AND SURFACE MODIFICATION WITH POLYMERS

A Dissertation
Submitted to the Graduate Faculty
of the
North Dakota State University
of Agriculture and Applied Science

By

Sita Krajangpan

In Partial Fulfillment
for the Degree of
DOCTOR OF PHILOSOPHY

Major Department:
Civil Engineering

January 2012

Fargo, North Dakota

North Dakota State University
Graduate School

Title

Enhancement of Dispersibility of Zero-valent Iron nanoparticles for Environmental Remediation: Entrapment and Surface Modification with Polymers

By

Sita Krajangpan

The Supervisory Committee certifies that this ***disquisition*** complies with North Dakota State University's regulations and meets the accepted standards for the degree of

DOCTOR OF PHILOSOPHY

SUPERVISORY COMMITTEE:

Dr. Achintya Bezbaruah
Co-Chair

Dr. Bret Chishlom
Co-Chair

Dr. Eakalak Khan

Dr. Senay Simsek

Dr. G. Padmanabhan

Approved by Department Chair:

Jan 24, 2012
Date

Dr. Eakalak Khan
Signature

ABSTRACT

Nanoscale zero-valent iron (NZVI) particles have been used for contaminant remediation. NZVI tend to agglomerate due to magnetic and van der Waals forces and form larger particles that settle down in aqeous media. Agglomerated particles increase in size and have decreased specific surface area and that lead to decrease in their reactivity. In this research, polymer-based surface modifiers were used to increase dispersibility of NZVI for environmental remediation. Ca-alginate was selected to entrap NZVI in beads and used to remove aqueous nitrate. The two-way ANOVA test indicates that there was no significant difference between reactivities (towards nitrate) of entrapped NZVI and bare NZVI. While the reactivity of entrapped NZVI was comparable to bare NZVI, the NZVI particles were found to remain agglomerated or clustered together within the alginate beads.

A novel amphiphilic polysiloxane graft copolymers (APGC) was designed, synthesized and used to coat NZVI to overcome the agglomeration problem. APGC was composed of hydrophobic polysilosin, hydrophilic polyethylene glycol (PEG), and carboxylic acid. The APGC was successfully adsorbed onto the NZVI surfaces via the carboxylic acid anchoring groups and PEG grafts provided dispersibility in water. Coating of NZVI particles with APGC was found to enhance their colloidal stability in water. The APGC possessing the highest concentration of carboxylic acid anchoring group (AA) provided the highest colloidal stability. It was also found that the colloidal stability of the APGC coated NZVI remained effectively unchanged up to 12 months. The sedimentation characteristics of APGC coated NZVI (CNZVI) under different ionic strength conditions (0-10 mM NaCl and $CaCl_2$) did not change significantly. Degradation studies were

conducted with trichloroethylene (TCE) and arsenic (V) [As (V)] as the model contaminants. TCE degradation rates with CNZVI were determined to be higher as compared to bare NZVI. Shelf-life studies indicated no change on TCE degradation by CNZVI over a 6-month period. As (V) removal batch studies with CNZVI were conducted to in both aerobic and anaerobic conditions. Increase in arsenic removal efficiency was observed with CNZVI as compare to bare NZVI in both aerobic and anaerobic conditions. Ionic strengths showed minimal inhibiting effect on arsenic removal by CNZVI.

ACKNOWLEDGMENTS

I would like to express my deepest gratitude to my advisor, Dr. Achintya Bezbaruah, for his guidance, advice, and support during my study at NDSU. Without him this work would not be accomplished. My gratitude is also extended to Dr. Bret Chisholm for providing me his valuable suggestions and laboratory facility throughout my research. I would like to specially thank Dr. Eakalak Khan for supporting and helping me overcome every difficulty. Sincere thanks to Dr. Senay Simsek for laboratory facility and comments and suggestions. My appreciation is also extended to Dr. G. Padmanabhan for encouragement and serving on my research committee.

I gratefully thank Department of Civil Engineering, North Dakota State University, Center for Nanoscale Science and Engineering, and North Dakota Water Resources Research Institute for my stipend support. My sincere appreciation is extended to Dr. Kalpana Katti and Scott Payne for their help with electron microscopy analyses. I would also like to thank Dr. Donna Jacob and Curt Doetkott for their assistance on using ICP-OES and statistical analysis. I would like to acknowledge Laura Jarabek and John Jepperson for their help in polymer synthesis. I am very grateful help and input from my colleagues, especially, Dr. Harjyoti Kalita and Dr. Sreerama Murthy Kasi Somayajula. I would like to express my deep gratitude to Jan Lofberg and Milka Singha for their help during my entire doctoral study at NDSU. Thank you to all of my Thai friends and former and present colleagues in the Environmental Engineering Laboratory. Special thanks goes out to the Khan Family and Tu Le. Fargo is too cold without sincere friendship from them.

I am most thankful to unconditional love, support, and encouragement from my family, Wallapa, Prasit, Sirinart, and Satri Krajangpan, throughout my study.

TABLE OF CONTENTS

LIST OF TABLES

Table **Page**

LIST OF FIGURES

Figure **Page**

LIST OF APPENDIX TABLES

CHAPTER 1. INTRODUCTION

1.1. Background

The zero-valent iron (ZVI) remediation process is generally a two-electron redox reaction. The standard electrode potential of the zero-valent iron/ferrous iron system is -0.44 V (Milazzo et al., 1978). A number of environmentally relevant compounds, most notably chlorinated aliphatic compounds, are sufficiently reduced to yield a thermodynamically favorable oxidation-reduction reaction with zero-valent iron (Johnson et al., 1996). Matheson and Tratnyek (1994) have proposed the following reactions (Eqs. 1-1 and 1-2) to represent reactions involving ZVI and chlorinated compound (R-X):

$$Fe^0 \rightarrow Fe^{2+} + 2e^- \quad (1\text{-}1)$$

$$R\text{-}X + 2e^- + H^+ \rightarrow R\text{-}H + X^- \quad (1\text{-}2)$$

The advantages of iron metal for remediation include its non-toxicity and economy. Lab-scale studies on iron (in the form of filings or microscale powder) have been successful in treating chlorinated ethanes (Orth and Gillham, 1996; Hara et al., 2005), chlorinated methanes (Matheson and Tratnyek, 1994), and arsenic (Kanel et al., 2005; Luepin et al., 2005). Zero-valent iron has been employed in hundreds of sites, usually in the form of permeable reactive barriers (PRB) (Rock et al., 1998). The first field application of Fe^0 in PRB for insitu remediation was for groundwater contaminated with trichloroethylene (TCE) and tetrachloroethylene (PCE) at the Canadian Forces Base, Borden, Ontario in 1991. It showed about 95% and 91% removal of TCE and PCE, respectively (Orth and Gillham, 1996). After that the first commercial Fe^0 PRB was

installed at an industrial site in Sunnyvale, California to remove chlorinated hydrocarbons in groundwater in 1995. In 1996, another Fe^0 PRB was installed at the United States Coast Guard (USGS) Support Center near Elizabeth City, North Carolina for removal of both chlorinated hydrocarbons and hexavalent chromium in groundwater (Powell et al., 1998).

Zero-valent iron reactions are surface mediated processes (Matheson and Tratnyek, 1994; Li et al., 2006). Higher specific surface area (i.e. surface area per unit mass of ZVI) is expected to lead to higher degradation of contaminants, while conventionally used nanosacled zero-valent iron (NZVI) has very low specific surface area. For example microscale ZVI has a surface area of 1-2 m^2/g (Thompson et al., 2010) while NZVI has a surface area of 25-54 m^2/g (Chen et al., 2004; Li et al., 2006; Bezbaruah et al., 2009). The NZVI with higher reactive surface area are expected to work better and these nanoparticles react approximately 1,000 times faster than micro scaled zero-valent iron (MZVI) (Kanel et al., 2005; Kanel et al., 2006). In addition to having higher reactive surface area, NZVI have other unique physicalchemical properties such as smaller size (<100 nm), and higher interparticle interactions and magnetic properrties. NZVI have been used for the removal of various groundwater contaminants including chlorinated compounds (Liu and Lowry, 2006; Cheng et al., 2007; Katsenovich and Miralles-Wilhelm, 2009, Bezbaruah et al., 2011), pesticides (Feitz et al., 2005; Joo et al., 2008; Thompson et al., 2010), heavy metals (Ponder et al., 2000; Alowitz and Scherer, 2002; Xi et al., 2010; Klimkova et al., 2011), non-metallic inorganics (Bezbaruah et al., 2009) and explosives (Gregory et al., 2004; Oh et al., 2005; Zhang et al., 2010).

1.2. Need statement

While NZVI particles have been used for groundwater remediation, NZVI tend to agglomerate due to magnetic and van der Waals forces and form larger particles that settle into aquifer media pores. Agglomerated particles have decreased specific surface area. As NZVI based reactions are surface mediated, the loss of specific surface area leads to decrease in reactivity of NZVI (Krajangpan et al., 2008; Tiraferri et al., 2008; Krajangpan et al., 2009). To overcome these problems, it is necessary to ensure that each NZVI particle can disperse independently and the particles have reduced interparticle attractions.

NZVI particles should be easily injectable to the aquifer matrix for groundwater contaminant remediation. Injecting NZVI into the aquifer is considered a standard practice for groundwater remediation (Figure 1.1). However, NZVI particles have a high sticking coefficient and they get attached to aquifer materials (Saleh et al., 2007). Nanoscale iron subsurface mobility is limited by particle-soil grain attachment and particle-particle agglomeration (Quinn et al., 2005; Saleh et al., 2007; Phenrat et al, 2009). To increase subsurface mobility nanoparticles (including NZVI) in groundwater and stabilize them in aqueous media, the particles have been surface modified by researchers (Table 1.1).

Considerable research has been done to improve dispersibility and mobility of NZVI on aquifer media. The most relevant research is reported by Saleh et al. (2007) who use triblock copolymers to surface modify NZVI. While the dispersibility of NZVI increased markedly, the reactivity of the NZVI coated with the triblock copolymer decreasesd by 24 times as compared to bare NZVI while treating trichloroethylene.

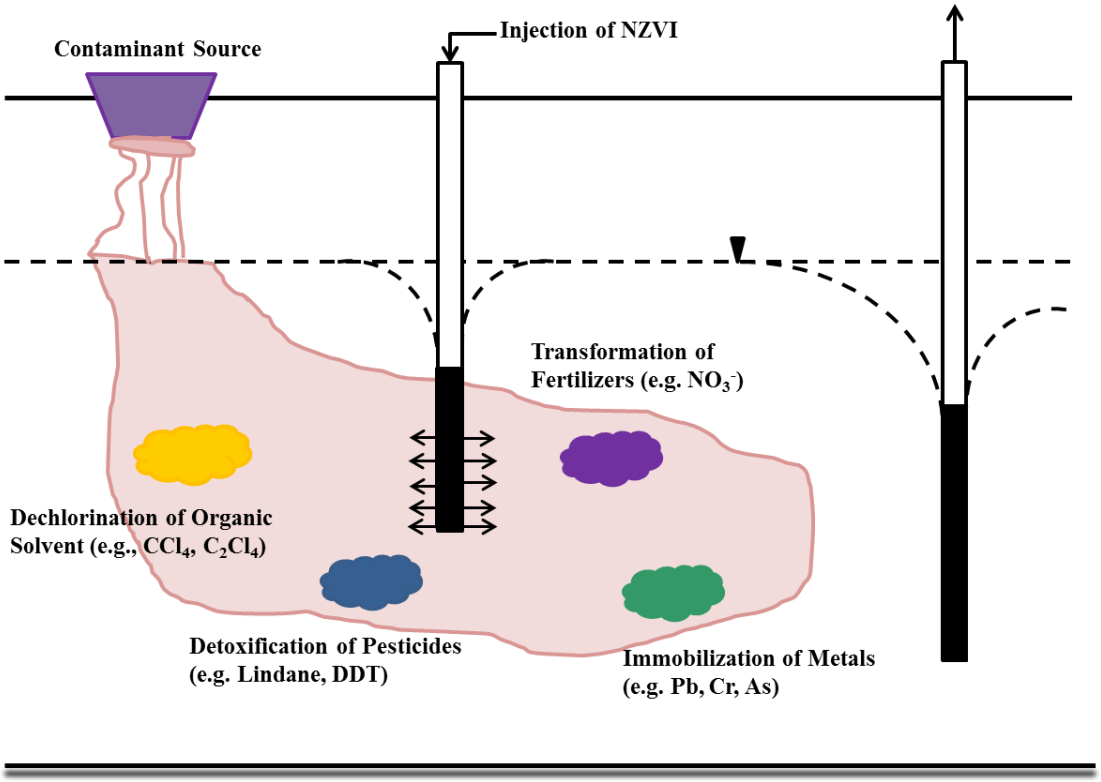

Figure 1.1. Schematic of a remediation project where NZVI particles are used (reproduced after Zhang, 2003)

Based on the discussion above, there is a need for further research to improve NZVI dispersibility and mobility without sacrificing its reactivity. The following needs have been identified for further research:

1. NZVI should disperse more efficiently
2. NZVI should have the ability avoid attachment to aquifer materials
3. Surface modified NZVI should be able to react more efficiently with contaminants

Table 1.1. Surface modifiers for enhancing NZVI dispersibility and remediation efficiency

Surface Modifiers	Uses	Source
Iron-on-resin Ferragels	Iron-on-resin Ferragels supported NZVI was used to remove Cr(VI) and Pb(II)	Ponder et al. (2000)
Polyacrylic acid (PAA)	PAA supported NZVI was used to remove chlorinated hydrocarbon	Schrick et al. (2004)
Poly(vinyl alcohol phosphate) (PVAP)	PVAP was used to increase the dispersibility of metal oxide nanoparticles	Mohapatra et al. (2006)
Amphiphilic triblock copolymers poly(methacrylic acid)-block-poly(methylmethacrylate)-block-poly(styrenesulfonate)	The triblock copolymers were used to modify iron nanoparticles to promote their colloidal stability in aqueous suspension	Saleh et al. (2008)
Carboxymethyl cellulose (CMC)	CMC modified NZVI had high mobility in soil matrix	He et al. (2009)
CMC	Synthesized colloidal ZVI with CMC for Cr(VI) removal	Franco et al. (2009)
Guar gum	Guar gum was used to reduce of NZVI sedimentation and aggregation	Tiraferri et al. (2009)
Poly(ethylene oxide) and poly(propylene oxide)	Di- and tri-block copolymers poly(ethylene oxide) and poly(propylene oxide) were used to stabilize gold nanoparticles (~12 nm) in aqueous media	Rahme et al. (2009)
Tween 80	Nonionic surfactant (Tween 80) was used to mobilize perchloroethylene in the aquifer. It enhanced the remediation performance of perchloroethylene contaminated groundwater by the NZVI reactive barrier.	Chen et al. (2010)
Polyvinylpyrrolidone (PVP-K30)	PVP-K30 was used for the removal of tetracycline from aqueous solutions	Chen et al. (2011)

1.3. Hypotheses

Use of polymeric surface modifiers or entrapment media will increase dispersibility of NZVI particles and specific surface area available. Dispersed particles will have more specific surface area available for reaction to take place compared to unmodified NZVI.

1.4. Objectives

The broad objective of this study is to modify NZVI particles using polymers to achieve better groundwater remediation.

The specific objectives of this research are as follows:

- Entrapment of NZVI particles in polymer matrix to increase their dispersibility.
- Design a new polymeric surface modifier for NZVI to achieve increased dispersibility of the particles.
- Test polymer entrapped and modified NZVI for groundwater remediation.

1.5. Experimental plan

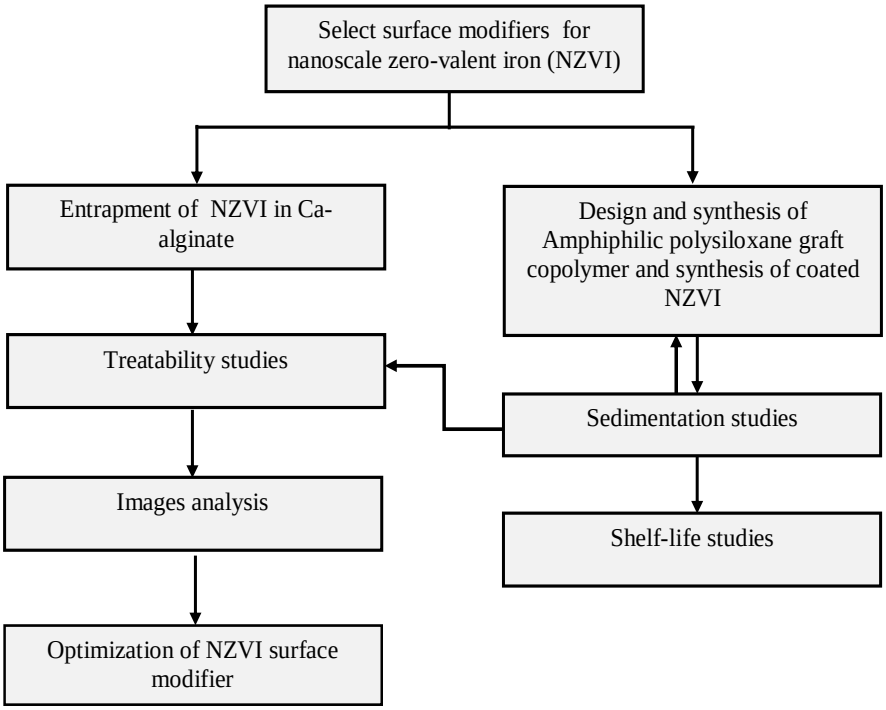

Figure 1.2. Schematic of research approach

1.6. Dissertation organization

This dissertation is divided into eight chapters. Chapter 1 is the introduction which includes background of this research, need statement, research hypothesis, research objectives, experimental plan, and dissertation organization. Chapter 2 contains literature review that is relevent to the research topic of this study. Chapter 3 is based on a manuscript entitled "Entrapment of iron nanoparticles in calcium alginate beads for groundwater remediation applications" published in 2009 (Bezbaruah et al., 2009). Chapter 4 covers design, preparation, characterization of amphiphilic polysiloxane graft copolymer (APGC) and APGC coated nanoscale zero-valent iron (CNZVI) including shelf-life study of CNZVI over a 12-month period. This chapter is an expanded version of a conference preprint published in 2008 entitled "Polymer modified iron nanoparticles for environmental remediation" (Krajangpan et al., 2008) and a book chapter entitled "Challenges in groundwater remediation with iron nanoparticles: Enhancement colloidal stability" (Krajangpan et al., 2009). Chapter 5 describes treatability study of a model contaminant (Trichloroethylene, TCE) using APGC coated NZVI (CNZVI). The chaper also incluses results and discussion on shelf-life of CNZVI over a 6-month period. Chapter 6 focuses on treatability study of arsenic(V) by CNZVI under aerobic and anaerobic conditions. Chapter 7 presents general conclusions. Chapter 8 discusses the potential areas of future research to improve upon this study.

CHAPTER 2. LITERATURE REVIEW

An extensive literature review was perform as part of this research. The literature review includes peer-reviewed papers related to increasing dispersibility of metal particles by using different kinds of surface modifiers.

Environmental nanotechnology is considered to play a key role in shaping current environmental engineering and science. Looking at the nanoscale has stimulated the development and use of novel and cost-effective technologies for catalytic degradation, adsorptive removal and detection of contaminants as well as other environmental concerns. Polymer-based nanocomposites incorporate advantages of both nanoparticles and polymers, have received increasing attention in both academia and industry. Surface modification and functionalization by polymers are widely practiced on nanoparticles used for biomedical applications. Different types of modifiers such as carboxylate-functional compounds (Sahoo et al., 2005), phosphate-functional compounds (Portet et al., 2001; Mutin et al., 2003), silica (Johnson et al., 1996; Alcala and Real, 2006), gold (Lin et al., 2001), dextran (Lee et al., 2002), polyethylene glycol (Kim et al., 2001; Paul et al., 2004), polyvinyl alcohol (Nishio et al., 2004), alginate (Kroll et al., 1996), and chitosan (Lee et al., 2005) have been used to surface modify nanoparticles for biomedical purposes. To avoid agglomeration, surfactants or polymers can provide electrosteric repulsion to reduce magnetic and van-der-Waals attraction forces between particles and, hence, increase colloidal stability (Saleh et al., 2008; Tiraferri et al., 2008; Lin et al., 2010).

Papell invented the ferrofluids (Papell, 1965) which are now used to increase the colloidal stability of magnetic nanoparticles. Water or oil-based ferrofluids are commercially available and they are usually stable at pH < 5 (acidic ferrofluid) or pH > 8

(alkaline ferrofluid). By controlling the surface charge and using specific surfactants, stability of ferrofluids can be enhanced. (Lu et al., 2007). Kim et al. (2005) coated iron oxide nanoparticles (~15 nm) with oleic acid before dispersing them in chitosan biopolymer to make ferrofluids. The mean hydrodynamic diameter of their coated particles in the chitosan solution was estimated to be 65 nm. The stabilized ferrofluids with different iron concentrations were stable for 30 d without precipitation.

Surfactants have been used with a varying degree of success for colloidal stabilization of nanoparticles (Rosen, 2002). The hydrophobic "tails" of the surfactants physically absorb on the NZVI surface while the hydrophilic "heads" inhibit flocculation and allow for suspension in the aqueous medium. While surfactants enable colloidal stability in water, the highly reversible nature of surfactant absorption limits its application as a delivery system for groundwater decontamination since desorption will be favored when the nanoparticles are transported through surfactant-free groundwater. Schrick et al. (2004) used poly(acrylic acid) and anionic hydrophilic carbon supported NZVI for the removal of chlorinated hydrocarbons (Schrick et al., 2004; Saleh et al., 2005). The delivery vehicle was able to lower the aggregation and sticking coefficient of NZVI. However, poly(acrylic acid) has limited application due to its reversible adsorption characteristics (Schrick et al., 2004; Saleh et al., 2005). Sun et al. (2007) used polyvinyl alcohol-co-vinyl acetate-co-itaconic acid (PV3A), a biodegradable surfactant, as a dispersant for NZVI. PV3A with a molecular weight of 4300-4400 proved to be the best. PV3A is food grade and nontoxic. It is also biodegradable because of the presence of –OH, -CO-, and –COOH groups. The addition of PV3A led to significant enhancements in particle stability and subsurface mobility of NZVI. Other effects of application of the surfactant included

reduction of mean NZVI particle size from 105 nm to 15 nm, reduction of the zeta (ζ)-potential from +20 mV to −80 mV at neutral pH, and a shift of the isoelectric point from pH ~8.1 to 4.5. They also found that PV3A-stabilized iron nanoparticles were capable of effectively decomposing trichloroethene (TCE). While bare NZVI (prepared without PV3A, median diameter 59.4 nm and mean diameter 105.7 nm) settled in less than 1 min no sedimentation of the PV3A-stabilized NZVI (median diameter 7.9 nm and mean diameter 15.5 nm) was observed for over a 6-month period (Sun et al., 2007).

Song et al. (2008) stabilized CeO_2-Coated SiO_2 nanoparticles with the anionic surfactant, sodium dodecyl benzene sulfonate (SDBS), and the nonionic surfactant, polyethylene glycol (PEG). The dispersion characteristics observed under different conditions indicated better dispersion of surface modified nanoparticles as compared to unmodified analogs. PEG is hydrophilic and the hydrated film that develops around the PEG molecule gives rise to steric stabilization (Song et al., 2008).

He and Zhao (2005) reported on the use of water-soluble starch for the stabilization of palladized iron (Fe-Pd) nanoparticles. The modified nanoparticles were used for the dechlorination of TCE and polychlorinated biphenyls (He and Zhao, 2005). The starched-modified nanoparticles showed less agglomeration and were present as discrete particles as opposed to dendritic flocs for unmodified particles. The starch-modified nanoparticles remained suspended in water after 24 h and only partial precipitation was observed after 48 h. In contrast, the bare nanoparticles agglomerated and precipitated within a few minutes. Starch is a branched, hydrophilic polymer containing ~20% amylase units. It was hypothesized that iron-starch interactions and formation of intra-starch iron clusters played a fundamental role in nanoparticle dispersion and stabilization. A significant improvement

in the reactivity of the starch-modified Pd-Fe nanoparticles towards TCE and polychlorinated biphenyls (PCB) was observed. The researchers reported a 37-fold increase in the surface area normalized reaction rate (k_{SA}) for TCE degradation using starch-modified Fe-Pd nanoparticles compared to bare particles..

Gu et al. (2005) examined a method to produce monodispersed submicron-sized polymer coated Fe_2O_3 particles referred to as "magnetic polymer particles." They conducted soap-free emulsion polymerization during which Fe_2O_3 nanoparticles were heterocoagulated onto precipitated polymer nuclei and attached to the nuclei through the introduction of vinyl groups on to the Fe_2O_3 surface. To chemically fix the nanoparticles to the polymer, a vinyl group was introduced into the primary surface modification reaction with methacryloxypropyltrimethoxysilane and methacryloxypropyldimethoxysilane (MPDMS). The colloidal stability of the polymer coated particles was improved by adding the ionic monomer, sodium p-styrenesulfonate (NaSS), during polymerization. The researchers concluded that the addition of the ionic surfactant to the soap-free emulsion polymerization might have improved the surface potential and raised the dispersion stability of the polymer coated Fe_2O_3 particles. Further, it was observed that the NaSS addition changed the zeta-potential and consequently raised the stability of the particles.

Jun et al. (2005) targeted coating magnetite nanocrystals (4-12 nm) with a multifunctional ligand system that provided for high stability of the particles. The ligand, 2,3-dimercaptosuccinic acid (DMSA), was used for the synthesis of the coated nanocrystals. They found that the DMSA coated Fe_2O_3 nanocrystals were fairly well dispersed in aqueous media. DMSA forms a stable coating on the Fe_2O_3 surface by

chelation through a carboxylic acid group. Further stabilization was achieved through intermolecular disulfide cross-linking.

Ponder et al. (2000) synthesized supported Fe-nanoparticles using polymeric resin, silica gel or sand as a support material (Ponder et al., 2000). They studied the rates of remediation of Cr(VI) and Pb(II) using both the modified and unmodified NZVI. Their modified particles showed high reactivity for a longer time compared to unmodified NZVI. Colloidal stability of the modified nanoparticles was not reported.

Wu et al. (2005) used cellulose acetate to coat NZVI. The goal was to preserve the chemical nature of NZVI by inhibiting iron oxidation by non-target compounds until the particles are in contact with the chlorinated contaminant stream. The nanoparticles were mixed with a cellulose acetate-acetone solution and then formed into a ~100 μm thick porous membrane by phase inversion. The membranes contained ~6.3 wt% NZVI. The nanoparticles existed in the membrane as dispersed agglomerated clusters allowing good access to NZVI surfaces by the target contaminant. The polymer supported nanoparticles resulted better dechlorination compared to bare nanoparticles. The researchers explored an interesting possibility of synergy in the form of contaminant pre-concentration in the polymer due to organic partitioning. This concept was important because successful pre-concentration and subsequent contaminant degradation would enable NZVI treatment for low concentration contaminant situations.

Mohapatra et al. (2006) synthesized superparamagnetic nanosized magnetite particles by controlled coprecipitation of Fe^{2+} and Fe^{3+} in the presence of highly hydrophilic poly(vinylalcohol phosphate) (PVAP). They found that polymer concentration

affected the particle size, size distribution, and colloidal stability. The aqueous suspension of magnetite, prepared using a 1% PVAP solution, was stable for 4 weeks at pH 5-8.

Iron oxide nanoparticles were surface modified by Somaskandan et al. (2008) with hydrophilic ligands. The ligands facilitated excellent stability of the nanoparticles (for several weeks) in water and different buffer solutions. The surface modified iron oxide nanoparticles also showed excellent solubility in polar solvents. Based on previous work, hydrophilic dopamine hydrochloride and dopamine-PEG were used to modify the NZVI.

Tiraferri et al. (2008) studied the colloidal stability of NZVI modified by the biodegradable polymers alginate, potato starch and guar gum, and compared them with commercially-available unmodified and sodium polyaspartate-modified NZVI. They found good electrophoretic mobility of the guar gum coated particles at different pH while experiments with alginate and potato starch did not give good results. Colloidal stability with guar gum coated nanoparticles was observed for 20 min and it was found to be better than the bare nanoparticles. However, the coated particles settled much faster when the ionic strength of the aqueous medium was increased (Tiraferri et al., 2008). Guar gum is a naturally occurring water-soluble polysaccharide that consists of β-D-mannopyranose and α-D-galactopyranose units. Each unit contains nine hydroxyl groups which are available for the formation of hydrogen bonds with other molecules (Bradley et al., 1989). Guar gum was found to aid in lowering the hydrodynamic radius of nanoparticle aggregates from 300 nm to 200 nm as guar gum concentration was increased from 0.05 to 0.5 g/L. However, size reduction was not observed beyond 1 g/L. Guar gum is presentaly used as a dispersing and stabilizing agent for many industrial applications (Wang et al., 2000). It is also being investigated for use in stability enhancement experiments involving magnetorheological

fluids (Fang et al., 2005; Wu et al., 2006). Its low cost and "green" attributes are appealing for application as a nanoparticle dispersant (Tiraferri et al., 2008).

Polyacrylic acid (PAA) was used by Schrick et al (2004). to suspend zero-valent iron (ZVI) for the removal of chlorinated hydrocarbons. They found that the modified ZVI (400-500 nm) had lower aggregation and sticking coefficient as compared to unmodified metal particles. Polyethylene glycol (PEG) also increased dispersion stability of SiO_2 NPs through steric stabilization (Song et al., 2008). Franco et al. synthesized colloidal ZVI using carboxymethyl cellulose and used them for chromium(VI) remediation (Franco et al., 2009). Poly(maleic anhydride-co-methacrylic acid) [P(MAH-co-MAA)] modified Fe_3O_4 NPs demonstrated enhanced dispersibility and resistance to sedimentation. Comba and Sethi (2009) added xanthan gum (6 g/L) to nanoscale zero-valent iron (NZVI, 15 g/L) and achieved high colloidal stability in deionized water (DI) and in water with an ionic strength of $6x10^{-3}$-12 mM (Comba and Sethi, 2009).

Saleh et al. (2007) showed that amphiphilic triblock copolymers with an A-B-C triblock architecture enhanced colloidal stability and increased affinity of the coated NZVI towards a water/organic interface. The triblock, poly(methacrylic acid)-*b*-(methyl methacrylate)-*b*-(styrene sulfonate) (PMAA-PMMA-PSS), enhanced colloidal stability. However, a decreased trichloroethylene (TCE) degradation rate was observed with coated NZVI as compared to bare (i.e. unmodified) NZVI. The decrease in degradation rate was thought to have resulted from a reduction in the diffusion rate of the contaminant through the polymer onto the NZVI surface (Phenrat et al., 2009). The same research group also used polyelectrolytes [polyaspartate (PAP, MW= 2.5 kg/mol and 10 kg/mol), carboxymethyl celluloses (CMC, MW=90 kg/mol and 700 kg/mol), and polystyrene

sulfonates (PSS, MW=70 kg/mol and 1000 kg/mol) to coat NZVI (Saleh et al., 2008). Polyelectrolyte adsorption was confirmed by increases in NZVI electrophoretic mobility keeping the particles mobile even after 8 months. He et al. (2009) have used CMC to stabilized NZVI (CMC-Fe) for in-situ delivery in porous media. The attachment (to porous media) efficiency for CMC-Fe was found to be 1–2 orders of magnitude lower than that reported for NZVI stabilized with other commercial polymers (He et al., 2009). Simulation results showed that 99% of the CMC-Fe could be removed within the first 16 cm of soil matrix at a groundwater flow velocity of 0.1 m/day, but traveled over 146 m at a flow velocity of 61 m/day.

The environmental applications of surface modified NPs are interesting and endless. The widespread use of surface modified NPs in degradation and adsorption of pollutants results in less pollution and benign products. Until now, numerous surface modified NPs are available for environmental purpose with high efficiency and low cost. However, further insights into the interplay between the surface modified NPs and the entrapped NPs are still required. For example, how does the polymer chemistry affect the dispersion and distribution of NPs? Can the surface modified NPs and entrapped NPs enhance interaction between NPs and targeted pollutants?

CHAPTER 3. ENTRAPMENT OF IRON NANOPARTICLES IN CALCIUM ALGINATE BEADS FOR NITRATE REMOVAL

3.1. Introduction

In recent years, NZVI have been used for the removal of various groundwater contaminants including chlorinated compounds (Lui et al., 2006; Cheng et al., 2007), pesticides (Feitz et al., 2005; Joo et al., 2008; Thompson et al., 2008), heavy metals (Blowes et al., 1997; Alowitz et al., 2002), and explosive materials (Gregory et al., 2004; Oh et al., 2005). Advantages of NZVI over other zero-valent iron (ZVI) such as microparticles (MZVI) and iron filings include higher reactive surface area (25-54 $m^2g^{-1}$for NZVI, Chen et al., 2004; Li et al., 2006), faster and more complete reactions, and injectability into aquifer (Cantrell et al., 1995; Wang and Zhang, 1997). Due to their small particle size (< 100 nm, Wang and Zhang, 1997) and high reactivity, NZVI has also been proposed to be used in the remediation of contaminated soils (Martin et al., 2008), sediments (Zhang et al., 2006), and biosolids (Li et al., 2007). For groundwater remediation using NZVI effectiveness will depend on the ability to deliver the NZVI to the contaminants. NZVI tend to agglomerate due to magnetic and van der Waals forces. Agglomeration increases the effective particle size resulting in precipitation (Krajangpan et al., 2008). To overcome the problems, NZVI can be entrapped in a porous polymeric hydrogel and the entrapped particles can then be used effectively.

Entrapment within calcium (Ca) alginate beads is one of the most common methods for immobilizing living cells in food and beverage industries (Kobaslija and McQuade, 2006; Olivas and Barbosa-Canovas, 2008). Ca-alginate has also been used to prepare alginate hydrogels and microbeads for drug delivery (Morch et al., 2006). In addition,

calcium alginate entrapped bacterial cells have been used in environmental remediation (Fundueanu, et al., 1999; Mishra, et al. 2004; Zala et al., 2004; Pongjanyakul and Puttipipatkhachorn, 2007; Hill and Khan, 2008). Alginate is a white to yellowish brown filamentous, grainy, granular or powdered forms of polysaccharide and soluble in water. Alginates are unbranched binary copolymers of 1-4-linked β-D-mannuronic acid (M) and α-L-guluronic acid (G) residues. The number and sequence of the mannuronate and glucuronate residues vary among alginates. When alginate is coordinated to sodium, it forms a very flexible chain. The molecular formula and weight of sodium alginate are $(C_6H_7O_6Na)_n$ and 198.11, respectively. The melting, boiling and flash points of sodium alginate are >300°C, 495.2°C (at 760 mm Hg) and 211.1°C, respectively. During cell entrapment, sodium is replaced by calcium, and each calcium ion coordinates with two alginate chains and become less flexible (Smidsrød and Skjåk-Braek, 1990). The chemical structure of sodium alginate and calcium alginate are shown in Figures 3.1 and 3.2.

Immobilization of cells in calcium alginate is a simple and cost effective technique (Zala et al., 2004). The porosity in calcium alginate allows solutes (contaminants and substrate) to diffuse through the beads and come in contact with the entrapped cells (Huang and Zhihui, 2002). Moreover, alginate is nontoxic, biodegradable, and nonimmunogenic. Because of the divalent calcium ions alginate produces thermally irreversible gels that are insoluble in water (Vold et al., 2006). Alginate and calcium crosslinking has been described in details elsewhere (Velings and Mestdagh, 1995).

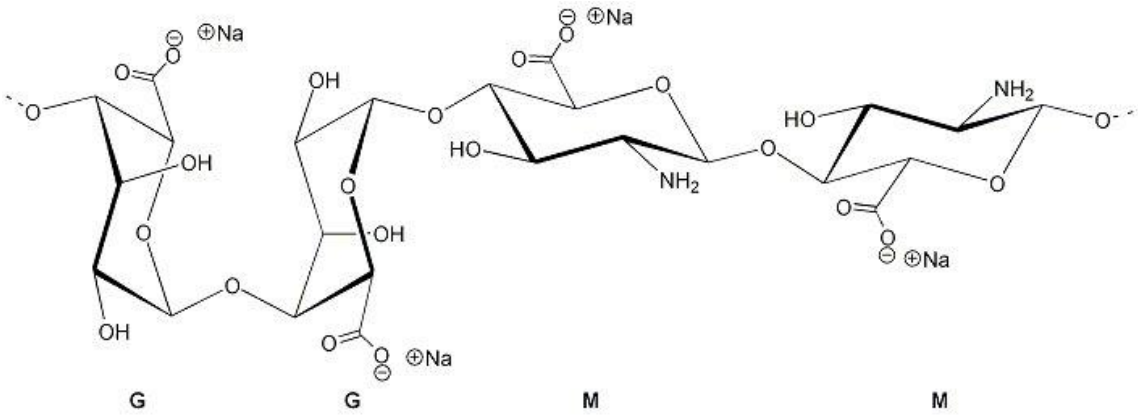

Figure 3.1. Structure of sodium alginate (Smidsrød and Skjåk-Braek, 1990)

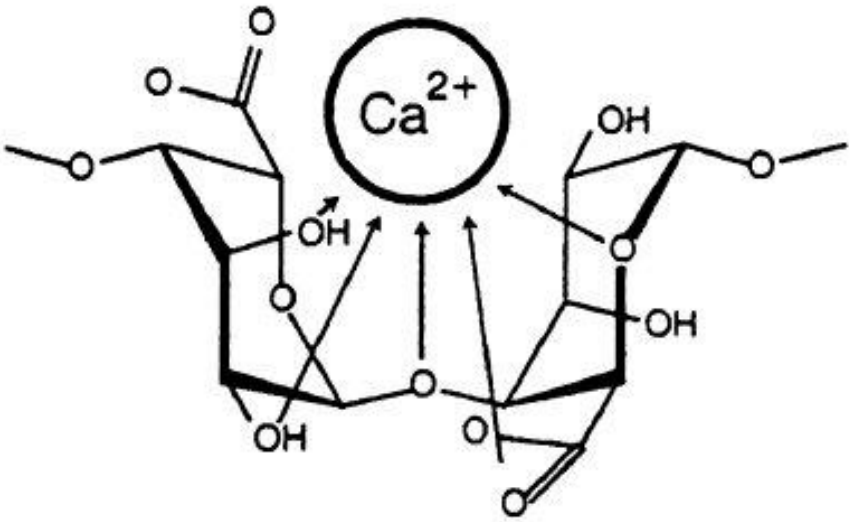

Figure 3.2. Structure of calcium alginate (Smidsrød and Skjåk-Braek, 1990)

The objective of work described in this chapter is to demonstrate that iron nanoparticles can be effectively entrapped in a biopolymer matrix without significant reduction in their reactivity. The study described in this paper targeted at retaining NZVI within alginate beads to increase dispersibility of NZVI and, thus, increase NZVI contact time with target contaminant to ensure better contaminant removal. Nitrate was used as a test contaminant to examine the effectiveness of the entrapped nanoparticles in degrading environmental contaminants. Nitrate was selected because of simplicity of analysis and availability of literature on nitrate degradation using ZVI (Siantar, et al., 1996; Cheng, et al., 1997; Huang, et al., 1998; Westerhoff and James, 2003; Choe, et al., 2004; Su and Puls, 2004). In addition, groundwater contamination by nitrate remains an ongoing problem of concern (Kapoor and Viraraghavan, 1997; Alowitz et al., 2002; Schnobrich et al., 2007). The major sources of nitrate pollution in groundwater are the use of nitrogen fertilizers and nitrogen pesticides, animal wastes, and drainage of domestic wastewater (Su and Puls, 2004). Chemical reduction of nitrate by ZVI is a highly energetic reaction. It has long been known as a potential technology to remove nitrate from water (Siantar, et al., 1996; Huang, et al., 1998; Huang and Zhang, 2006). ZVI has been used for nitrate removal from groundwater under different experimental conditions (Yang et al., 2005). Bare NZVI has been used in remediating nitrate under different environmental conditions (Chen et al., 2004; Li et al., 2006; Liu et al., 2006; Sohn et al., 2006).

3.2. Experimental section

3.2.1. Chemicals

Iron(II) sulfate heptahydrate ($FeSO_4 \cdot 7H_2O$, 99%, Alfa Aesar), sodium borohydride ($NaBH_4$, 98%, Aldrich), iron powder (<10 μm, 99.9%, Aldrich), calcium chloride ($CaCl_2$,

ACS grade, BDH), sodium alginate (production grade, PFALTZ&BAUER), methanol (production grade, BDH), and ethanol (ACS grade, Mallinckrodt Chemicals) were purchased from VWR (West Chester, PA) and were used as received unless otherwise specified.

3.2.2. Synthesis of NZVI

Iron nanoparticles were synthesized by borohydride reduction of ferrous ion in $FeSO_4.7H_2O$ in an aqueous phase (Lui et al., 2005; Bezbaruah et al., 2009; Bezbaruah et al., 2011). The use of this method is well documented (Li et al., 2006). The method is inexpensive and requires no specialized equipment. Additionally, the nanoparticles synthesized by this method have shown both high reactivity and durability (Lui et al., 2006). The reaction scheme for the synthesis is as follows:

$$2\ Fe^{2+} + BH_4^- + 3H_2O \rightarrow 2Fe^0\downarrow + H_2BO_3^- + 4H^+ + 2H_2 \qquad (3\text{-}1)$$

The NZVI obtained was dried in a vacuum oven for ~6 h and allowed to stand at ambient conditions overnight to passivate the iron (Bezbaruah et al., 2009; Bezbaruah et al., 2011). Similar passivation techniques were employed by Sohn et al. (2006) for increased stability of NZVI. The dried NZVI was ground in a ceramic mortar and pestle and stored in a dry nitrogen atmosphere. Transmission electron microscopy (TEM, JEOL JEM-100CX II) images were used to determine particle size distribution. Scanning electron microscopy along with energy dispersive spectroscopy (SEM/EDS, JEOL JSM-6300) was used to observe surface morphology and characterize the elemental composition of NZVI. X-ray diffraction (XRD) was used to identify the chemical composition of the NZVI.

3.2.3. Entrapment of NZVI

The method developed by Aksu et al. (1998) for cell entrapment in alginate was modified for NZVI entrapment in the present study. One gram of sodium alginate was dissolved in 50 mL deionized deoxygenated water (DDW) at room temperature (22±2^{o}C). The deionized water was deoxygenated by purging it with nitrogen gas (ultra high purity grade) for about 15 minutes to remove dissolved oxygen (DO). DO removal was necessary to ensure that NZVI is not oxidized during entrapment. The alginate-water mixture was stirred until complete dissolution was achieved (~20-30 minutes). Then, the mixture was left at room temperature for 30 minutes to allow the air/gas bubbles generated from the mixing to escape. This step is necessary to ensure that the alginate beads do not float on the aqueous solution. The alginate solution (2% w/v) was gently mixed with 1 g of NZVI. The mixture was promptly dropped into a 3.5% (v/v) deoxygenated aqueous solution of $CaCl_2$ at room temperature (22±2^{o}C) using a peristaltic pump (Masterflex, Cole Parmer Instrument, with 0.5 mm internal diameter tubing at 2.5 mL min^{-1} flow rate). As soon as the drops came in direct contact with the $CaCl_2$ solution, calcium alginate gel beads were formed. The gel beads were retained in the deoxygenated solution of $CaCl_2$ for 9 h for hardening and then washed with DDW. A minimum of 6 h hardening ensures that beads allow optimal diffusion of substrates into and out of them (Aksu et al., 1998; Garbayo et al., 2002).

3.2.4. Nitrate degradation kinetics experiments

Nitrate degradation experiments were conducted through a series of batch trials. The experiments were performed in anaerobic batch reactors made of 500 mL commercial grade polyethylene terephthalate bottles with sleeve type silicone septum seal. Four

hundred fifty milliliters of DDW were spiked with a stock nitrate solution to obtain initial concentrations of 20, 60, and 100 mg NO^-_3-N/L. Alginate entrapped NZVI (1.0 g) were added to each reactor. The reactors were rotated end-over-end at 28 rpm in a custom made shaker. Aliquots were withdrawn periodically (at 0, 10, 15, 30, 45, 60, 90, and 120 minutes) and analyzed for nitrate and pH. Reactors with nitrate in DDW but no NZVI were run as controls. Similar experiments were conducted with bare NZVI. All experiments were conducted in triplicates.

3.2.5. NZVI characterization and analytical methods

The particle sizes of NZVI were analyzed through transmission electron microscopy (TEM, JEOL JEM-100CX II). The scanning electron microscopy with x-ray microanalysis (SEM/EDX, JEOL JSM-6300) was used to observe surface morphology and to analyze percent mass element composition of NZVI. X-ray diffraction (XRD, Philips X'Pert MPD with Cu Kα X-ray source, PANalytical) was carried out at 40 kV and 30 mA with a scan range from 20˚ to 80˚ to identify the chemical composition of the NZVI. A Micromeritics analyzer (ASAP 2000, GA) with Brunauer–Emmett–Teller (BET) gas adsorption was used to measure specific surface area of the particles.

The specific surface area of the synthesized NZVI was measured with micromeritics analyzer (ASAP 2000, GA) using Brunauer–Emmett–Teller (BET) gas adsorption with N_2. Nitrate and pH were determined according to *Standard Methods* (APHA et al., 1998). The concentration of NO_3^--N was measured with a nitrate electrode and a Ag/AgCl reference electrode (both SympHony, VWR). The pH was measured using a pH electrode (Orion $250A^+$ ORION 91-07).

For TEM and SEM/EDX analyses, the NZVI was stored in ethanol. A 200 mesh copper grid coated with carbon was carefully dipped into the mixture to adsorb NZVI from ethanol which was later dried under ambient temperature. The adsorbed NZVI was used for TEM analyses. The sample preparation for TEM and SEM/EDX was done under atmospheric and under high vacuum conditions, respectively. The entrapped NZVI particles were collected and stored in a 0.1 M $CaCl_2$ solution at 4°C before SEM analysis and prepared in accordance with Hill and Khan (2008). The samples were attached to aluminum mounts by silver paint and coated with gold/palladium using a Balzers SCD 030 sputter coater. Images were obtained by SEM under high vacuum condition.

3.3. Results and discussion

3.3.1. Characteristics of bare NZVI

Analysis of TEM image (Figure 3.3) indicates that NZVI particle size ranged from 10 to 90 nm with an average size of 35 nm (Figure 3.4). Figure 3.3 shows a cluster of NZVI. The particle agglomerated because of strong magnetic interaction between them. This agglomeration limits the availability of surface area on the particle, and hence, the available reactive surface area for contaminant degradation (Schlicker et al., 2003).

A higher magnification TEM image showed a ~2.5 nm of passivating oxide shell around the NZVI core (inset of Figure 3.3). An oxide shell, possibly of amorphous FeOOH, is clearly visible around the nanoparticles (NPs) (Cao et al., 2008; Martin et al., 2008). The shell was formed during the passivation process of NZVI (Section 3.2.2). Similar NZVI core/shell geometry has been reported earlier (Nurmi et al., 2005; Li et al., 2006). The oxide shell protects the NPs from rapid oxidation, yet allows contaminants access to NZVI (Li et al., 2006). XRD spectrum showed only Fe^0 in the synthesized NZVI (Figure 3.5).

TEM, BET, and SEM/EDX results of NZVI compared with MZVI are summarized in Table 3.1.

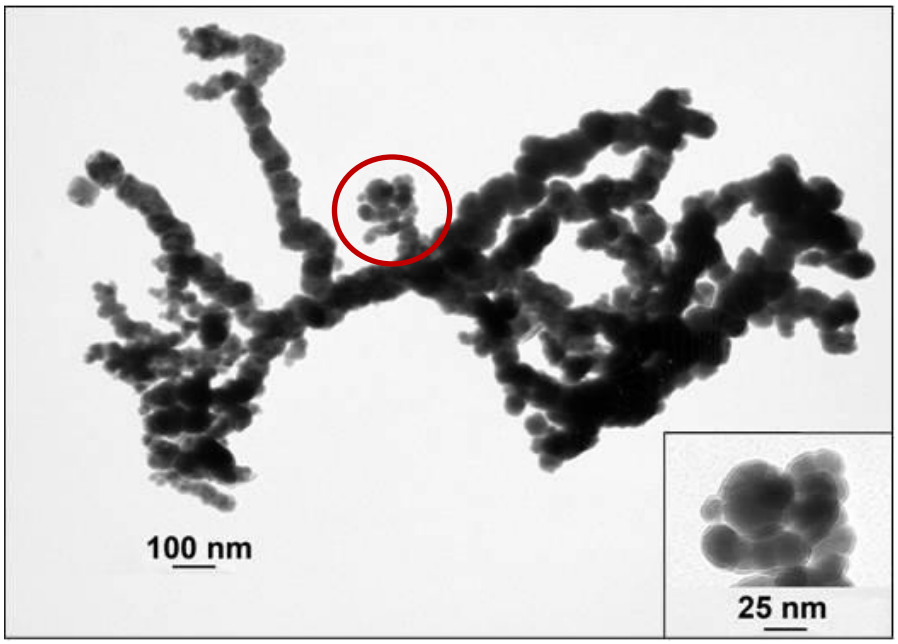

Figure 3.3. TEM images of bare NZVI (reproduced after Bezbaruah et al., 2009)

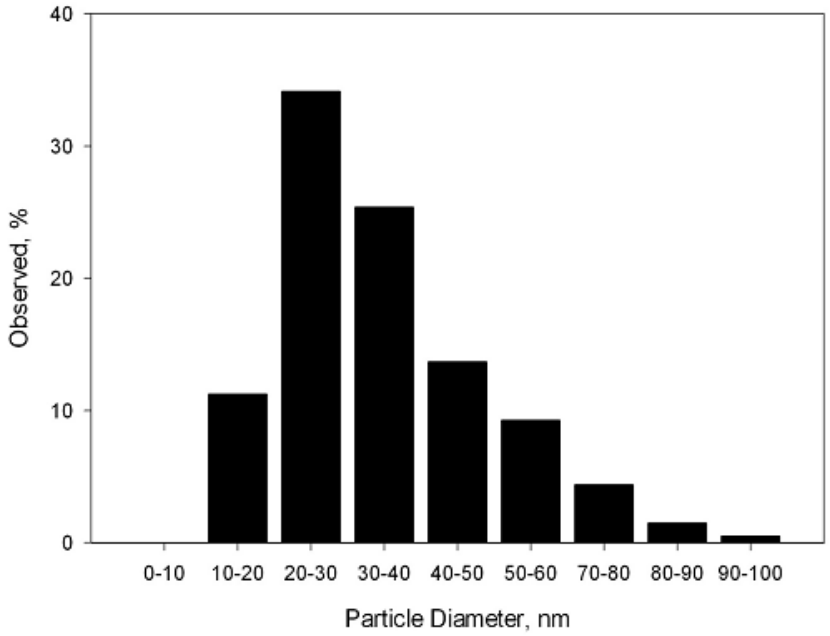

Figure 3.4. Particle size distribution of NZVI (n = 205) (reproduced after Bezbaruah et al., 2009)

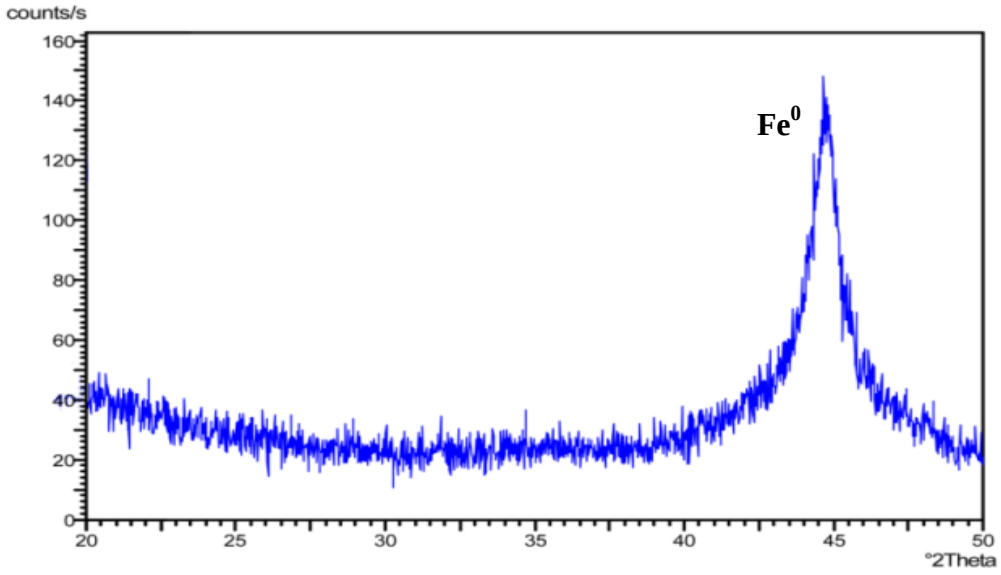

Figure 3.5. XRD spectrum of synthesized iron NPs showed only Fe^0; (c) EDX spectrum of freshly synthesized NZVI in the laboratory. The results indicate 84.34% iron and 15.66% oxygen in the NZVI (reproduced after Bezbaruah et al., 2009)

Table 3.1. The characteristics of the synthesized NZVI and the commercial grade MZVI

Parameter	NZVI	MZVI*
Particle size	35 nm	10 µm**
BET specific surface area	25 m^2g^{-1}	1 m^2 g^{-1}**
% Fe	84.34	99.6
% O	15.66***	0.4***

* MZVI was not used in this study but shown in this table for comparison purposes only
**Reported by Sigma-Aldrich
***The relative higher percentage of oxygen in NZVI seems to be because of it higher surface area as compared to MZVI

3.3.2. Characteristics of entrapped NZVI

NZVI entrapped alginate beads were analyzed with SEM (Figures 3.6-3.8) and TEM (Figures 3.9 and 3.10). The images are used to qualitatively understand the morphology inside the alginate beads. The dispersibility and location of NZVI inside the alginate bead were also investigated from these images. The images show that pore size of alginate beads is not identical because crosslinking between Ca and alginate is not uniform

throughout the bead. In some parts, Ca-alginate formed densely and entrapped more nanoparticles. In higher density areas there is a possibility of NZVI agglomeration and hence reduction in their reactive surface area.

The higher magnification TEM images (Figures 3.9 and 3.10) confirm high agglomeration of NZVI in parts of the beads. Further, SEM analysis revealed that the bead surface has undulations, folds, and pores (also reported by Benerjee et al., 2007). Benerjee et al. (2007) reported the pore size in similar alginate beads to be 3.17-5.07 nm. Reported small pore size ensures retention of NZVI used in this study.

3.3.3. Kinetics of nitrate degradation

Kinetic studies were conducted to find out the effectiveness of bare NZVI and entrapped NZVI on nitrate removal at three initial concentrations without any pH adjustment (Figures 3.11-3.13). With bare NZVI, the NO_3^--N concentration decreased from 100 mg/L, 60 mg/L, and 20 mg/L to 27 mg/L, 23 mg/L, 9 mg/L, respectively, over a 2 h period.

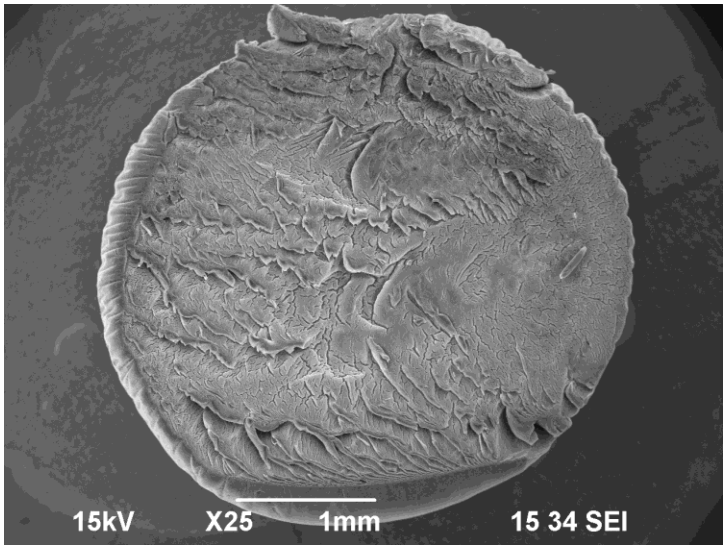

Figure 3.6. SEM image of a section through of an alginate bead (reproduced after Bezbaruah et al., 2009)

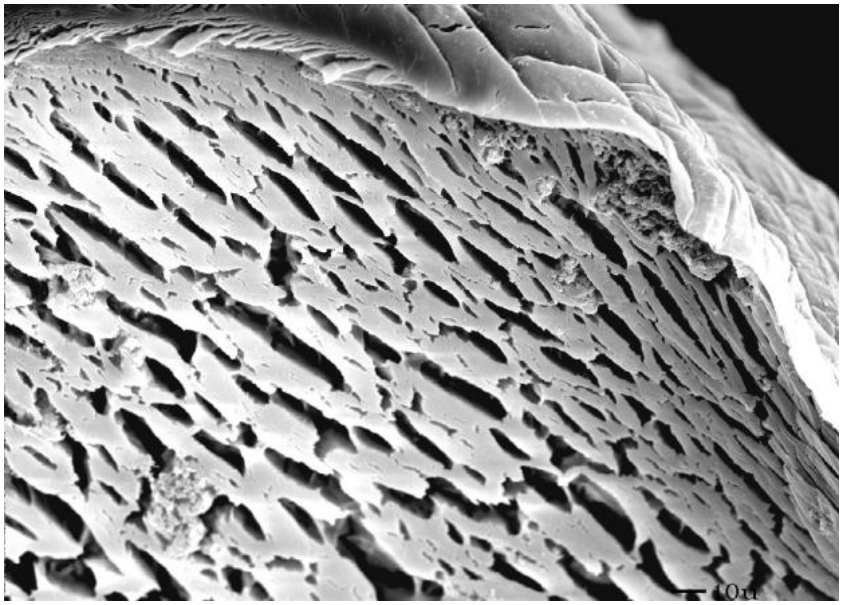

Figure 3.7. SEM image of alginate bead surface after NZVI entrapment (reproduced after Bezbaruah et al., 2009)

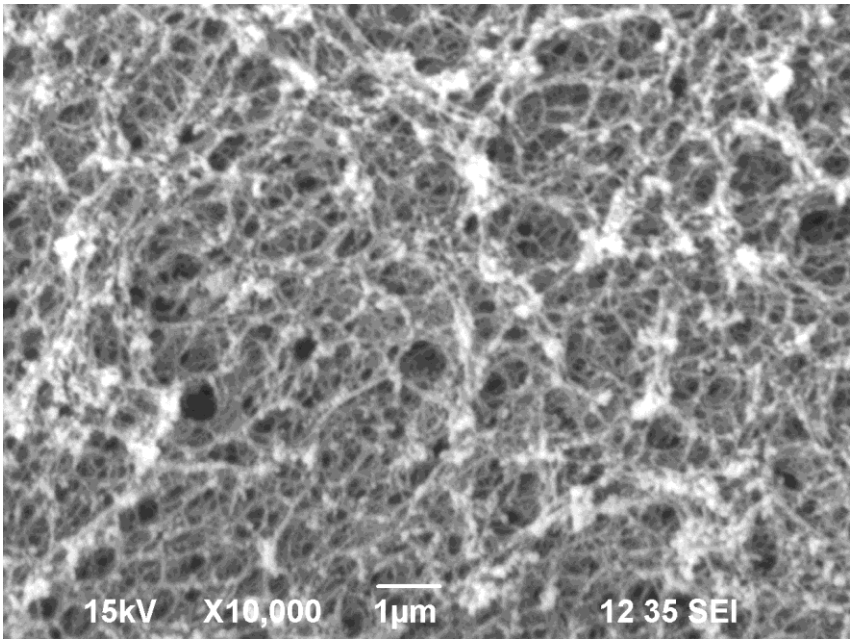

Figure 3.8. SEM image of alginate bead surface after NZVI entrapment (magnified) (reproduced after Bezbaruah et al., 2009)

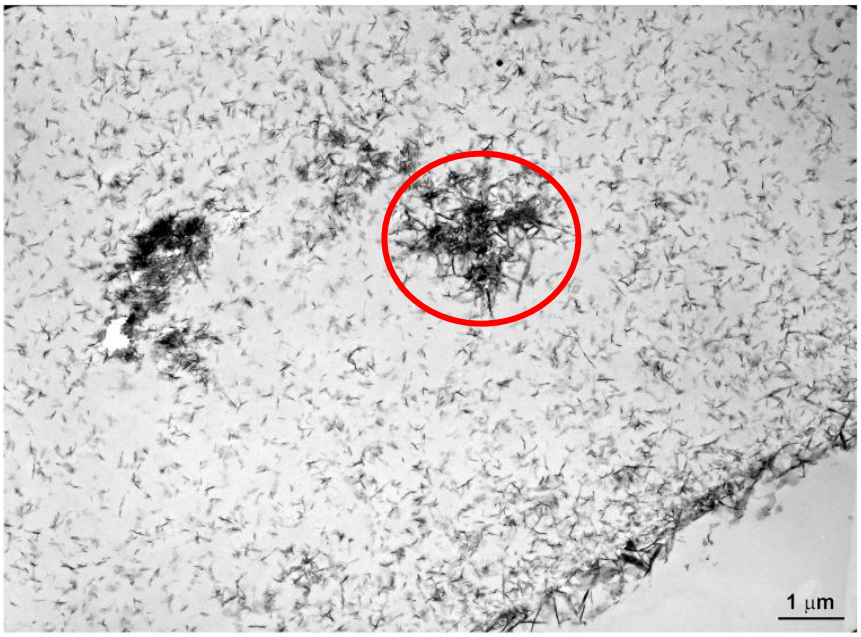

Figure 3.9. TEM image of Ca-alginate bead section shown in Figure 3.8 (reproduced after Bezbaruah et al., 2009)

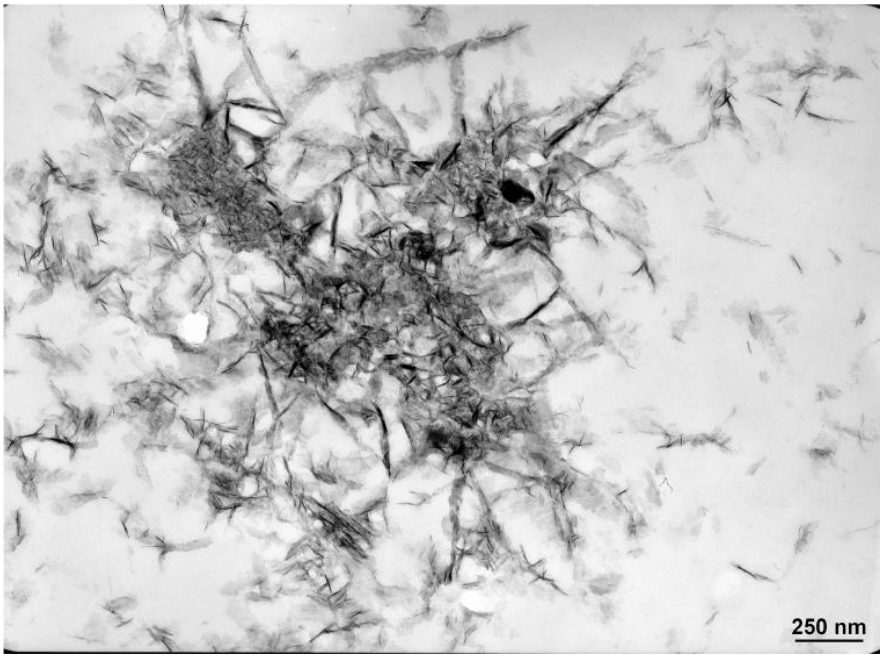

Figure 3.10. Blow-up image of the area circled in Figure 3.9. Nanoparticles are agglomerated/concentrated more in certain area rather than being uniformly distributed throughout the bead (reproduced after Bezbaruah et al., 2009)

The batch studies were continued for 24 h. However, only the results for the initial 2 h period were reported as the degradation curve leveled off beyond that time and no significant NO_3^--N reduction was observed. The slightly lower or similar NO_3^--N reductions were observed with entrapped NZVI than with bare NZVI for the same initial concentrations and the same reaction time. The initial NO_3^--N of 100, 60, and 20 mg/L reduced to 27 mg/L, 26 mg/L, 10 mg/L, respectively, with entrapped NZVI. Nitrate degradation by bare NZVI and entrapped NZVI followed first order reaction for all concentrations. The reaction rate constants (k) and the coefficient of determination (R^2) of the fit are summarized in Table 3.2.

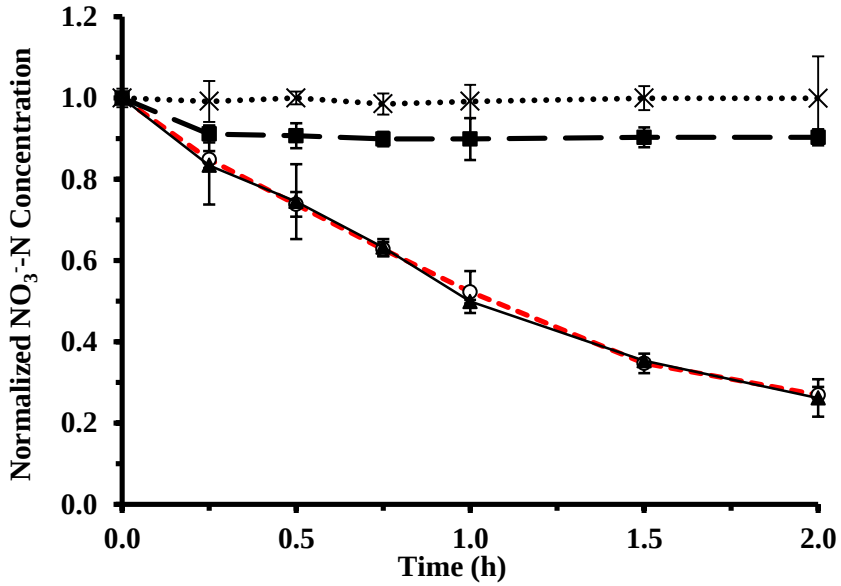

Figure 3.11. Reduction of NO_3^--N by bare NZVI and Ca-alginate entrapped NZVI over time with 100 mg/L initial NO_3^--N concentration (--○-- bare NZVI, —▲— entrapped NZVI, —■— control, ···×··· blank). The data points are connected with straight lines for ease of reading only and they do not represent trendlines. The vertical error bars indicate ± standard deviations. Blank (only NO_3^--N with no NZVI and alginate) did not show any change in concentration over (see Appendix C for raw data) (reproduced after Bezbaruah et al., 2009)

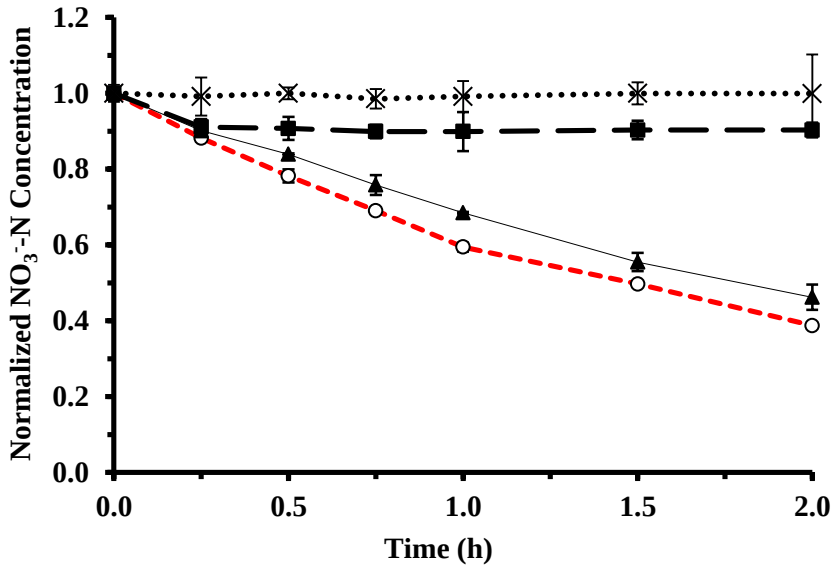

Figure 3.12. Reduction of NO_3^--N by bare NZVI and Ca-alginate entrapped NZVI over time with 60 mg/L initial NO_3^--N concentration (--○-- bare NZVI, —▲— entrapped NZVI, —■— control, ···×··· blank). The data points are connected with straight lines for ease of reading only and they do not represent trendlines. The vertical error bars indicate ± standard deviations. Blank (only NO_3^--N with no NZVI and alginate) did not show any change in concentration over (see Appendix C for raw data) (reproduced after Bezbaruah et al., 2009)

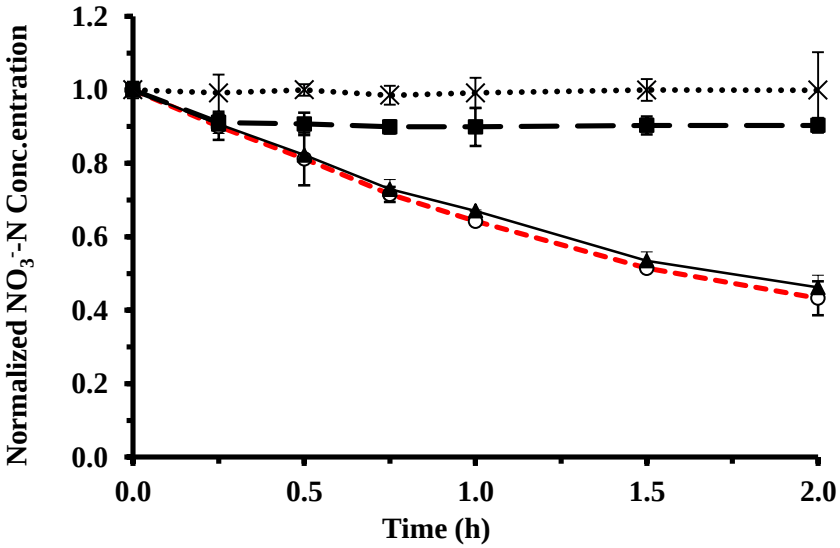

Figure 3.13. Reduction of NO_3^--N by bare NZVI and Ca-alginate entrapped NZVI over time with 20 mg/L initial NO_3^--N concentration (--○-- bare NZVI, —▲— entrapped NZVI, —■— control, ···×··· blank). The data points are connected with straight lines for ease of reading only and they do not represent trendlines. The vertical error bars indicate ± standard deviations. Blank (only NO_3^--N with no NZVI and alginate) did not show any change in concentration over (see Appendix C for raw data) (reproduced after Bezbaruah et al., 2009)

Table 3.2. First-order rate constants for NO_3^--N reduction by NZVI

Iron Type	Initial NO_3^--N Concentration (mg/L)	Reaction Rate Constant (h^{-1})	R^2
Bare NZVI	100	0.6547	0.9994
	60	0.4769	0.9966
	20	0.3990	0.9964
Entrapped NZVI	100	0.6465	0.9988
	60	0.4268	0.9986
	20	0.3716	0.9912

For entrapped NZVI, a marked drop in nitrate concentration during the first fifteen minutes was observed in the control (calcium alginate beads only). This initial drop in nitrate in the entrapped systems was a mere physical phenomenon. The initial drop in nitrate can be attributed to sorption into the calcium alginate bead due to the NO_3^--N gradient that existed between the aqueous (bulk) solution and the beads. Similar substrate sorption by Ca-alginate beads were reported by Hill and Khan (2008) in experiments involving cell entrapment.

The NO_3^--N reduction by entrapped NZVI was observed to be slightly lower compared to bare NZVI in some cases (Figure. 3.11-3.13). However, two-way ANOVA test on the reaction rate data indicates that there is no significant difference between the reaction rates of bare NZVI and entrapped NZVI ($\alpha = 0.05 <$ p-value $= 0.142$). There could be expected some reduction in degradation rate due to the presence of alginate coating on the NZVI due to diffusion limitations. It seems that there was no degradation reduction due to diffusion limitation. Nitrate diffusion in alginate beads is non-Fickian in nature and depends on the concentration of alginate and extent of crosslinking of calcium (Garbayo et al., 2002). The alginate beads used in this experiment were gelled for more than 6 h. Therefore, they should have reached optimal nitrate diffusion characteristics (Aksu et al.,

1998) and did not restrict substrate (nitrate here) diffusion through them (Garbayo et al., 2002).

The results from this study clearly indicate that the reactivity of entrapped NZVI was comparable to bare NZVI. Reduced mobility of iron nanoparticles can be achieved through entrapment in Ca-alginate. However, entrapement has not achieved dispersibility of the nanoparticles and they are still found to remain partially agglomerated within the alginate bead (Figures 3.9 and 3.10). With further improvement in dispersibility of the NZVI within the beads, the alginate entrapment technique may possibly offer a way to effectively use NZVI in permeable reactive barriers. The entrapped NZVI will have the advantage of being stationary in the aquifer under dynamic groundwater conditions as compared to the bare particles.

3.4. Summary

The results from this study indicate that NZVI entrapment in a biopolymer may increase the overall efficacy of permeable reactive barriers for groundwater remediation. The authors (2012) have shown for the first time that NZVI can be effectively entrapped in Ca-alginate beads and comparable reactivity of NZVI toward a model contaminant (nitrate here) was observed after the entrapment. The reduction in nitrate concentration using bare NZVI and entrapped NZVI were 55-73% and 50-73%, respectively, over a 2 h period. The two-way ANOVA test indicates that there was no significant difference between bare NZVI and entrapped NZVI reactivity. Calcium alginate entrapped NZVI would be a good alternative for in-situ remediation of nitrate and other contaminants in groundwater. Ca-alginate can be used as the entrapment media for NZVI to make the nanoparticles relatively stationary as compared to bare NZVI. Bare NZVI either migrate with groundwater flow or

settle into soil pore and, hence become unavailable for contaminant degradation. The entrapped NZVI can possibly be used in permeable reactive barriers. Further work needs to be conducted to investigate surface chemistry of the entrapped iron particle. Clogging due to iron corrosion byproducts was not examined in this study and is recommended for future research.

CHAPTER 4. DESIGN, PREPARATION, CHARACTERIZATION OF AMPHIPHILIC POLYSILOXANE GRAFT COPOLYMER COATED IRON NANOPARTICLES

4.1. Introduction

The effectiveness of NPs for groundwater remediation depends on their ability to access and interact with contaminants (Buffle et al., 1998; Schrick et al., 2004; He and Zhao, 2005). Two other important characteristics required of NPs for use in groundwater remediation are their dispersion and suspension in aqueous media (Schrick et al., 2004; Logan, 1999). It has been demonstrated that NP dispersibility is quite limited without appropriate particle surface modification (Saleh et al., 2007; Krajangpan et al., 2008). In the previous chapter (Chapter 3), the effect of entrapment of NZVI in a biopolymer matrix has been discussed. While there was no loss of reactivity of the entrapped NZVI as compared to bare NZVI, there was no improvement in dispersibility of the entrapped NZVI. NZVI particles were found to agglomerate or cluster together within the alginate beads (Figures 3.8 and 3.9). It is therefore necessary that the NZVI particles should be coated or surface modified individually to achieve proper dispersion.

This chapter reports a study involving the synthesis of novel amphiphilic graft copolymers (APGCs) and their use to coat NZVI for contaminant remediation. The graft copolymers were designed to resist NZVI agglomeration and sedimentation in aqueous solution. The new graft copolymers consisted of a polysiloxane backbone, PEG grafts, and pendent carboxylic acids as anchoring groups. As illustrated in Figure 4.1, it was hypothesized that a polysiloxane polymer backbone possessing pendent carboxylic acid would enable efficient adsorption of the polymer to NZVI surfaces because of the affinity

of carboxylic acid groups for NZVI and the low surface tension of polysiloxanes. The water-soluble PEG grafts would serve to provide dispersibility and colloidal stability of coated particles in the aqueous media. The polysiloxane, being non-polar and possessing a very low glass-transition temperature, was expected to readily allow permeation of contaminants through it onto NZVI surfaces.

4.2. Experimental section

4.2.1. Chemicals

Dichloromethane (purity 98%), PtO_2 (99.5+%), *tert*-butyl acrylate, toluene (HPLC grade), and trifluoroacetic acid (99.5%) were all obtained from Aldrich Chemical and used as received. $NaBH_4$ (ACS grade, Alfa Aesar), methanol (95+%, BDH), sodium hydroxide (ACS grade, BDH), sodium chloride (99%, Fisher Scientific). Poly(methylhydrosiloxane-dimethylsiloxane) (HMS-151, Gelest), polyethylene glycol allylmethyl ether (polyglykol AM 350, Clariant), and He and N_2 (both from Praxair) and all other chemicals were used as received unless otherwise specified.

4.2.2. NZVI synthesis

NZVI particles were prepared as described in Chapter 3 (Section 3.2.2).

4.2.3. APGC synthesis

APGCs were synthesized using a three-step process (Figure 4.2). In step 1, 10 g of poly(methylhydrosiloxane-dimethylsiloxane) (PDMS, MW 1950, 20.4 mmol hydride) and 3.57 g polyethylene glycol allylmethyl ethers (PEG, MW 350, 10.2 mmol) were dissolved in 30 mL of toluene. A catalytic amount of PtO_2 was added, and the mixture heated at 90°C for ~5 h (Sabourault et al., 2002).

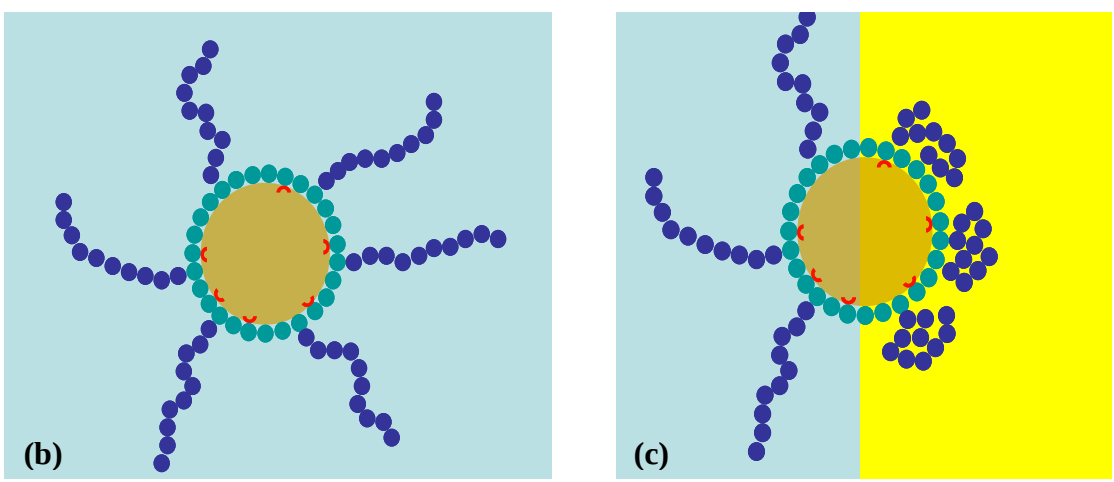

Figure 4.1. A schematic representation of APGC proposed within this research. (a) APGC adsorbed onto NZVI surface; (b) CNZVI dispersed in aqueous phase; (c) CNZVI at aqueous/organic interface. Aqueous phase is represented in blue and organic phase is represented in yellow

Upon completion of the hydrosilylation reaction (confirmed through proton nuclear magnetic resonance (^{1}H NMR) spectroscopy (JEOL ECA 400 MHz, JOEL Ltd.)), 1.31 g *tert*-butylacrylate (tBA, MW 128.17, 10.2 mmol) was added to the product and heated at 90°C for ~5 h (Step 2). Upon completion of the second hydrosilylation reaction, the reaction mixture was cooled to room temperature (22±2^{o}C). Platinum oxide was removed by filtration through a series of $NaHCO_3$ columns, and the copolymer (PDMS/PEG/tBA) was isolated by vacuum stripping the toluene. Step 3 was performed to generate the carboxylic acid (AA) anchoring groups by hydrolyzing the *tert*-butyl ester groups of the graft copolymers. The PDMS/PEG/tBA (10 g of the product synthesized in Step 2) was dissolved in 25 mL of dichloromethane in a 100 mL round bottom flask. Trifluoroacetic acid (TFA, 2.52 mL) was added to the solution, and the mixture was stirred for ~6 h at room temperature to complete the reaction.

The synthesized APGC was isolated by vacuum stripping the dichloromethane, TFA, and *tert*-butanol (a tBA hydrolysis product). Carbon nuclear magnetic resonance (^{13}C NMR, JEOL ECA 400 MHz, JOEL Ltd.) spectroscopy and Fourier transform infrared spectroscopy (FTIR, Nicolet 8700, Thermo Scientific) were used to confirm the completion of hydrolysis. The APGC was either immediately used to coat NZVI or stored in a refrigerator (4^{o}C) by dissolving it in toluene. The stored APGC was used to coat NZVI after evaporating toluene by passing N_2 gas through the solution. The complete removal of toluene was checked using ^{1}H NMR. Five different APGCs were synthesized each varying from the other in terms of the content (weight fraction) of the three different repeat units (Table 4.1). Glass transition temperature (T_g) of the APGC was measured using differential scanning calorimetry (DSC, DSC Q 1000, TA Instruments Inc.).

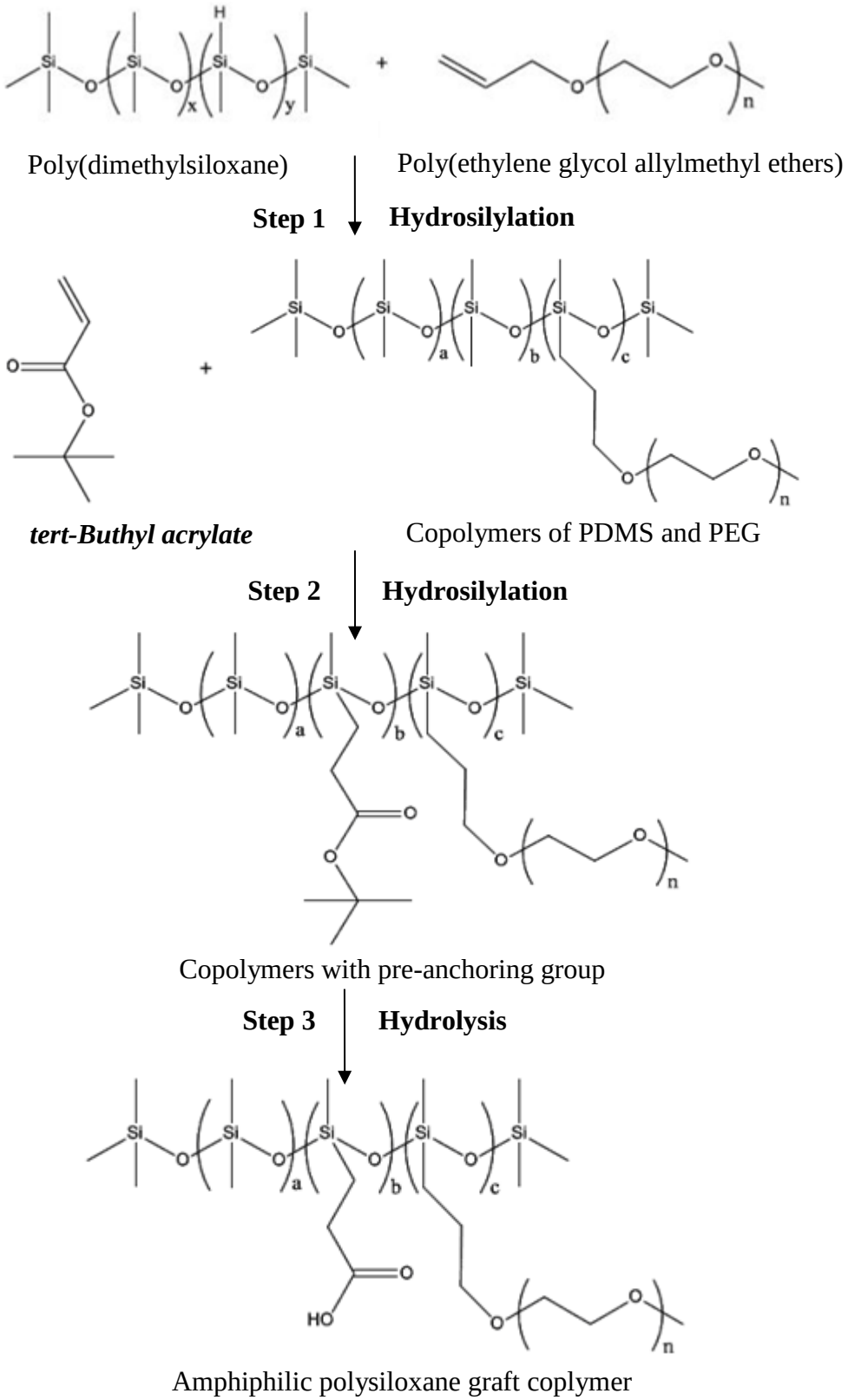

Figure 4.2. The APGC synthesis process. Patent filed (Krajangpan et al., 2010)

Table 4.1. Weight fractions of the three different repeat units of APGC used to optimize the APGC composition

Sample*	% Weight fractions		
	PDMS	**PEG**	**AA**
70/25/5	70	25	5
62/36/2	62	36	2
72.5/21/6.5	72.5	21	6.5
67/29/4	67	29	4
65/32/3	65	32	3

APGC concentration used was 15 g/L
*Weight fraction was decided based on mole fraction needed for reactions to take place

4.2.4. APGC coated NZVI preparation

NZVI particles (60 mg) were combined with 20 mL of APGC of various concentrations (2 g/L, 10 g/L and 15 g/L APGC in DDW). The mixtures were sonicated for 30 min to prevent agglomeration of NZVI and rotated in a custom-made end-over-end shaker (28 rpm) for 72 h to allow the APGC to adsorb (i.e. coat) onto the NZVI surface. The CNZVI suspension was stored in borosilicate glass bottles at room temperature. FTIR spectra were obtained with a Nicolet 6700 FTIR Spectrometer operated with OMNIC software. The spectra were obtained from 400 to 4000 cm^{-1}. The solid samples (NZVI and CNZVI) were dried in a vacuum oven for two days before analysis. The dried samples were then mixed with KBr corresponding to an approximate mass ratio of 1:10 (sample: KBr) for pellet preparation. The liquid samples (PDMS/PEG/tBA and APGC) were prepared by adding the samples as droplets to KBr pellet. The spectra were recorded at a resolution of 4 cm^{-1} with each spectrum corresponding to the co-addition of 64 scans. The background collected from KBr was automatically subtracted from the sample spectra. Bright field images of CNZVI were obtained by using high-resolution transmission

electron microscopy (HRTEM) (JEOL JEM-2100 LaB_6, JOEL Ltd.) attached with GATAN Orius SC1000 CCD camera.

4.2.5. Colloidal stability studies

The colloidal stability of the CNZVI was evaluated by measuring sedimentation rates of suspensions. A 20 mL suspension of CNZVI (3 g/L of NZVI) in a 20 mL vial was centrifuged (1800 rpm, Heraeus Labofuge 400R Centrifuge, Thermo Electron Corporation) and washed three times with copious amounts of DDW to remove any excess, non-adsorbed APGC. Fresh DDW (20 mL) was added to the CNZVI. The mixture in the vial was shaken well, and 2 mL of CNZVI suspension in water was withdrawn to a glass cuvette. The sedimentation behavior of the CNZVI was interpreted from the change of light intensity at the wave length of 508 nm over time (2 h) using a UV spectrophotometer (Cary 5000, Varian). The same evaluation was done for a control using 3 g/L bare NZVI in DI water.

4.2.6. Shelf-life studies

Many batches of CNZVI (60 mg of iron per each batch) were prepared and stored in a cabinet at room temperature and their colloidal stability investigated every month over a 12-month period.

4.3. Results and discussion

4.3.1. NZVI characterization

NZVI characterization data are already presented in Chapter 3 (Section 3.3.1).

4.3.2. APGC synthesis

^{1}H-NMR and ^{13}C NMR were used to monitor hydrosilylation and hydrolysis reactions (Figure 4.3-4.10). During the first hydrosilylation step, PEG was added into

PDMS solution. The proton peaks at δ 5.2-5.4 and δ 5.9 ppm corresponding to the double bond of allyl PEG (Figure 4.4) disappeared (Figure 4.5), and the hydride peak in PDMS (HMS-151) at δ 4.8 ppm (Figure 4.3) decreased by about half and the new Si-CH_2-CH_2 peaks were visible at δ 0.6 and δ 1.7 ppm in the PDMS/PEG graft copolymer (Figure 4.5) indicating complete of hydrosilylation of PDMS and allyl PEG. For further confirmation ^{13}C NMR was run. In ^{13}C NMR, the double bond carbon peak of starting material PEG at δ 110-130 ppm was not observed after hydrosilylation. The methylene peak for the PDMS/PEG copolymer at δ 13 and δ 23 ppm (Figure 4.6) indicated that the reaction between PEG and PDMS had taken place.

After adding tBA to the PDMS/PEG graft copolymer, the proton peaks at δ 5.2-5.4 and δ 5.9 ppm corresponding to double bond peak of tBA disappeared. The hydride proton peak at δ 4.8 ppm also disappeared completely due to successful hydrosilylation of tBA to the PDMS/PEG graft copolymer producing PDMS/PEG/tBA graft copolymer. The peaks for the PDMS/PEG/tBA graft copolymer at δ 0.4-0.5 and δ 1.4-1.6 ppm in the ^{1}H NMR spectrum correspond to methylene protons (Figure 4.7). ^{13}C NMR spectrum also show the disappearance of the double bond carbon peak of starting material tBA at δ 110-130 ppm. The new carbon peaks from grafted tBA were visible at δ -0.4 ppm, δ 23ppm, δ 29 ppm, and δ 85.7 ppm. The carbonyl carbon peak was visible at δ 150 ppm as a result of successful hydrosilylation of tBA (Figure 4.8).After hydrolysis was completed, the methyl proton peaks associated with the *t*-butyl ester group were absent indicating complete hydrolysis (Figure 4.7 and Figure 4.9). The ^{13}C NMR spectrum (Figure 4.10) also confirmed complete hydrolysis by the absence of the *t*-butyl methyl carbon peak at δ 29 ppm and a down-field shift of the carbonyl carbon peak.

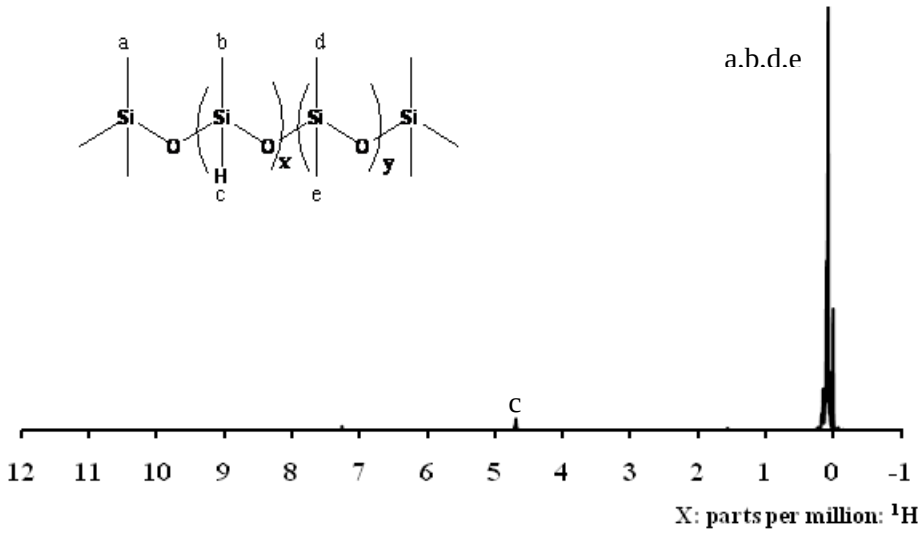

Figure 4.3. ^{1}H NMR of PDMS. PDMS is one of the raw materials used in the synthesis of APGC. The methyl group peaks are identified as a,b,d, and e, and hydride group is identified as c. The hydride group was hypothesized to react with PEG and tBA to form the copolymer (APGC)

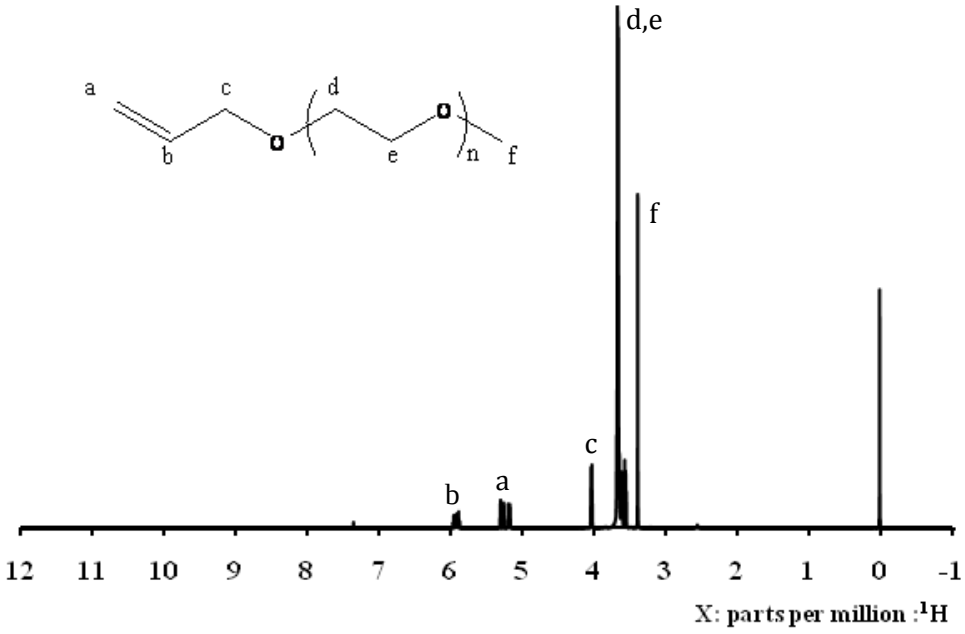

Figure 4.4. ^{1}H NMR of PEG. PEG is one of the raw materials used in the synthesis of APGC. Here a and b are double bond from allyl PEG, c, d, e, and f represent the methylene (CH_2) groups. The double bond present here was expected to react with the hydride groups from PDMS

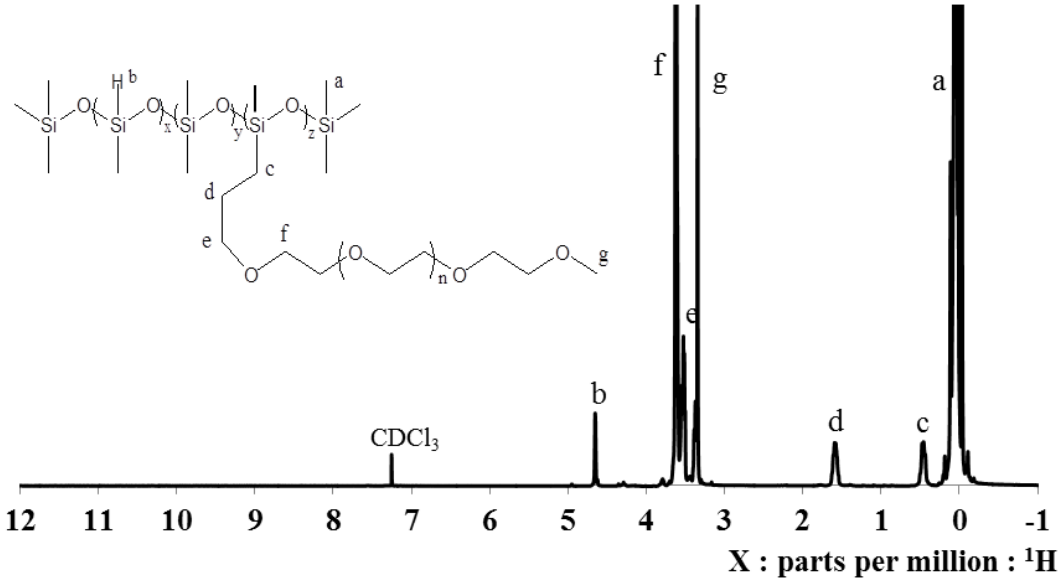

Figure 4.5. ^{1}H NMR of the hydrosilylation product of PDMS and PEG. Here b is the hydride group remaining after hydrosilylation which was expect to later react with the double bond group from tBA. The peaks at δ 5.2-5.4 corresponding to allyl peaks in PEG disappeared Figure 4.4 peak a and b. The peaks at a, and g represent methyl group, c, d, e, and f are methylene groups

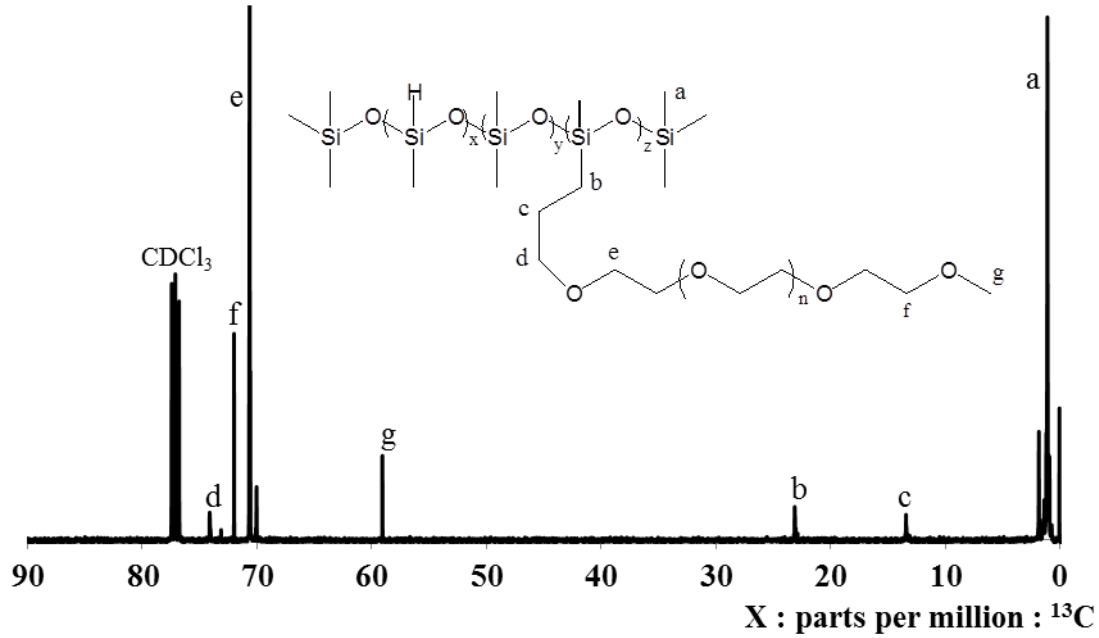

Figure 4.6. ^{13}C NMR of the hydrosilylation product of PDMS and PEG. The double bond carbon peak of starting material PEG at δ 110-130 ppm was gone. The new methylene peaks at b and c indicate that the reaction between PEG and PDMS has taken place. The peaks at a and g are methyl groups, and the peaks at d, e, and f represent -OCH_2

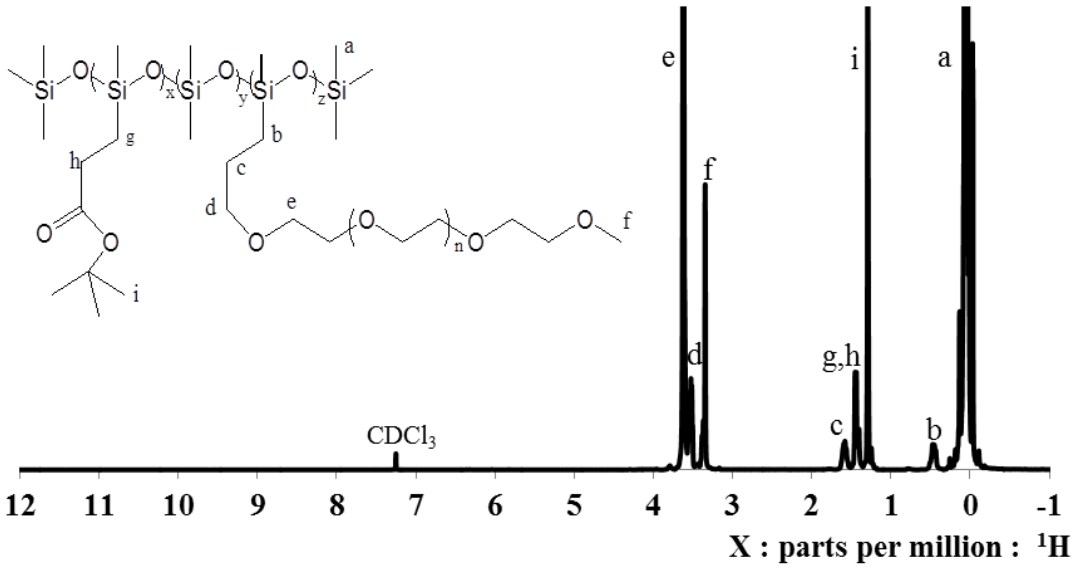

Figure 4.7. ^{1}H NMR of the hydrosilylation product of PDMS-graft-PEG and tBA. This is the precursor to APGC. The absence of a hydride peak at δ 4.8 ppm indicated the completion of the hydrosilylation reaction. This PDMS/PEG/tBA was hydrolyzed to get APGC. The peaks at a, f, and i represent methyl groups. The peaks at b, c, d, e, g, and h represent methylene groups

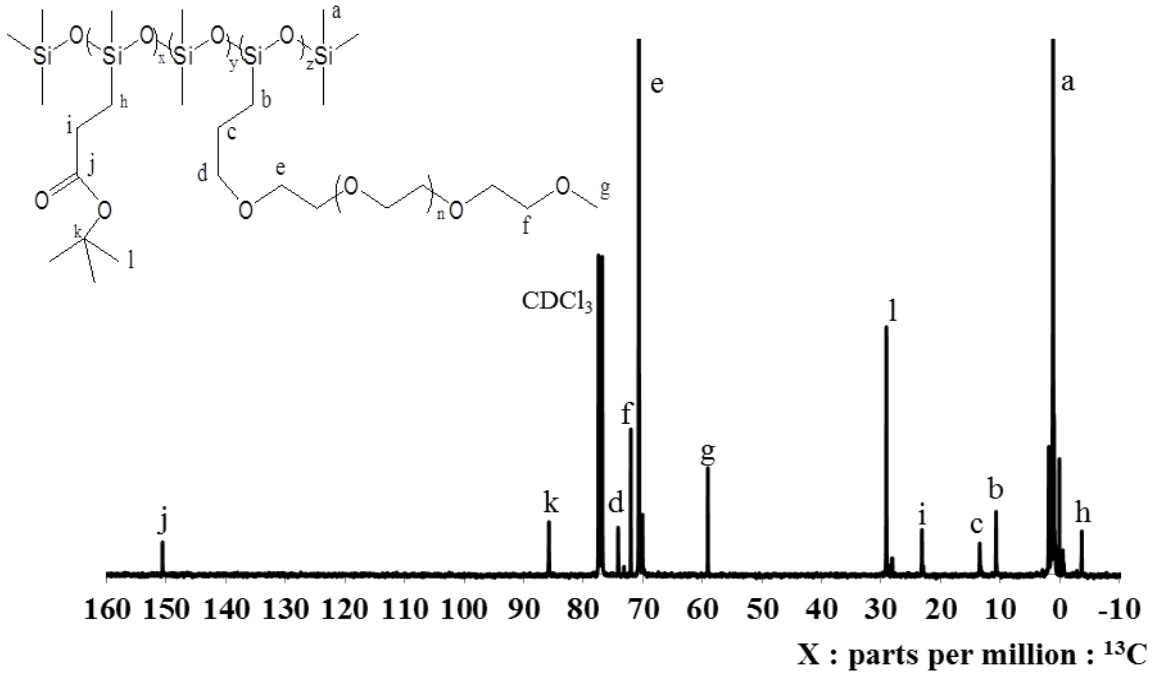

Figure 4.8. ^{13}C NMR of the hydrosilylation product of PDMS-graft-PEG and tBA. The double bond carbon peak of starting material tBA at δ 110-130 ppm disappeared. The peaks at h, i, l, and k are new carbon peaks from grafted tBA. The peak at j represents the carbonyl group from acrylate

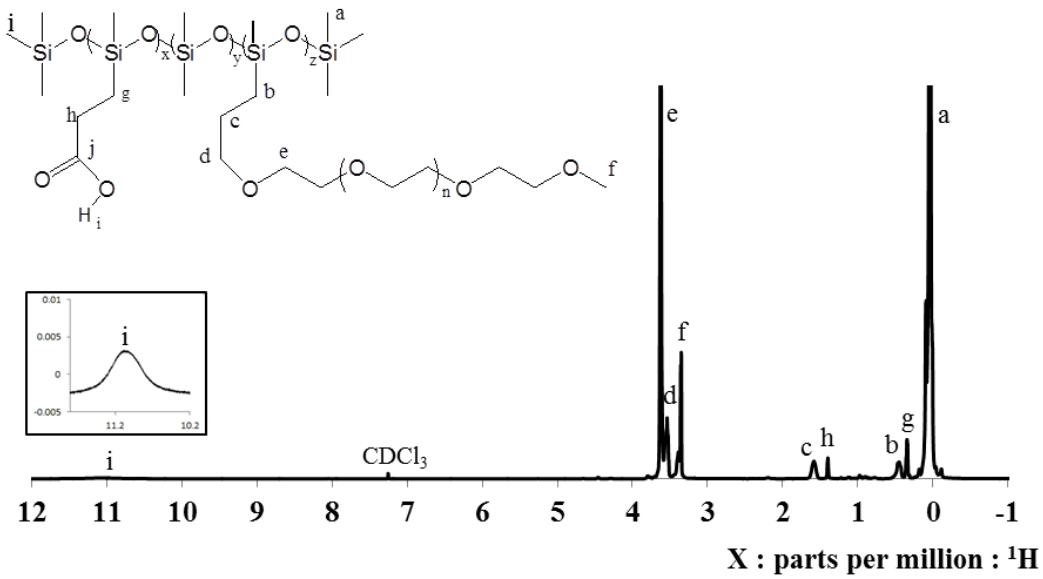

Figure 4.9. ^{1}H NMR of the final product (APGC). The carboxylic acid proton peak can be observed at i. The enlargement of peak i was shown in the small box. The peaks at a and f represent methylene groups. The peaks at b, c, d, e, h, and g represent methyl groups

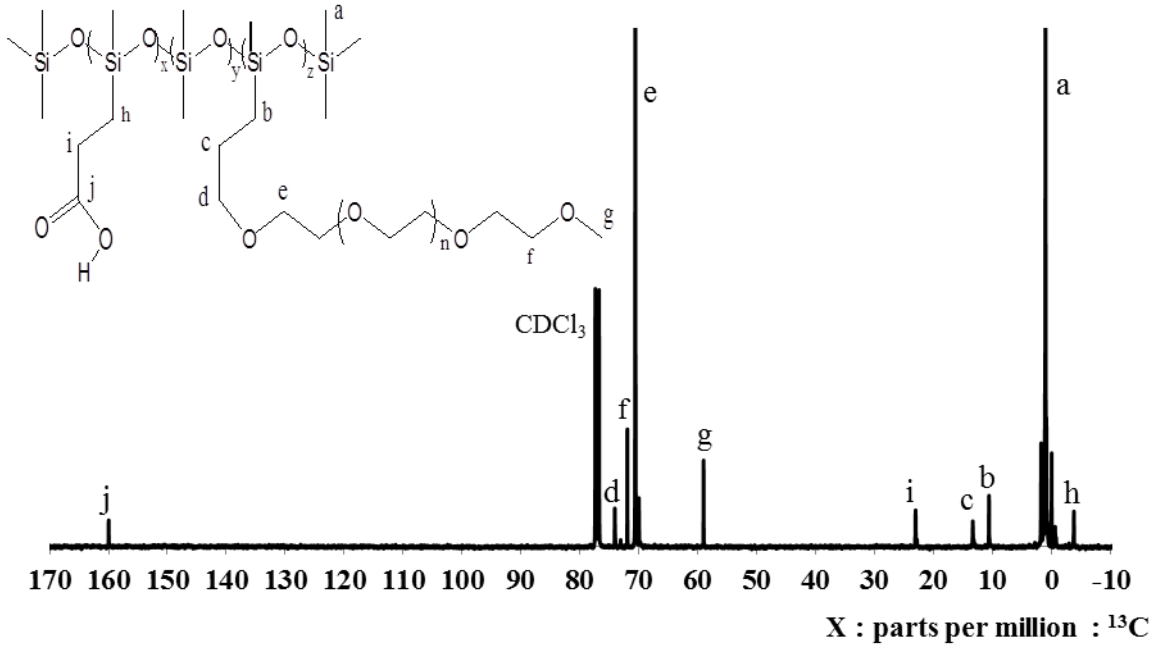

Figure 4.10. ^{13}C NMR spectrum of APGC (after hydrolysis). This ^{13}C NMR was done to verify the results obtained with ^{1}H NMR (Figure 4.9). The tert-butyl CH_3 peak at δ 29.0 ppm and the tertiary carbon from acrylate at δ 85.7 ppm disappeared. The tert butanol group was hydrolyzed and the singlet carbonyl group at j could be seen indicating the completion of hydrolysis forming APGCs with carboxylic acid anchoring groups. The anchoring groups were expected to attach to the NZVI surface

FTIR spectroscopy was also used to examine the polymers before and after hydrolysis (i.e., PDMS/PEG/tBA, Figure 4.11a and PDMS/PEG/AA, Figure 4.11b). The spectra showed a noticeable shift of the position of the carbonyl peak from 1732 cm^{-1} to 1712 cm^{-1}. The appearance of hydroxyl peak from 3000 cm^{-1} to 3500 cm^{-1} due to $\nu(O\text{-}H)_{COOH}$ indicates complete hydrolysis (Figure 4.11b) (Kataby et al., 1999). Table 4.2 shows the peak assignments and wave numbers for FTIR spectra of polymer before hydrolysis (PDMS/PEG/tBA), polymer after hydrolysis (PDMS/PEG/AA), and CNZVI.

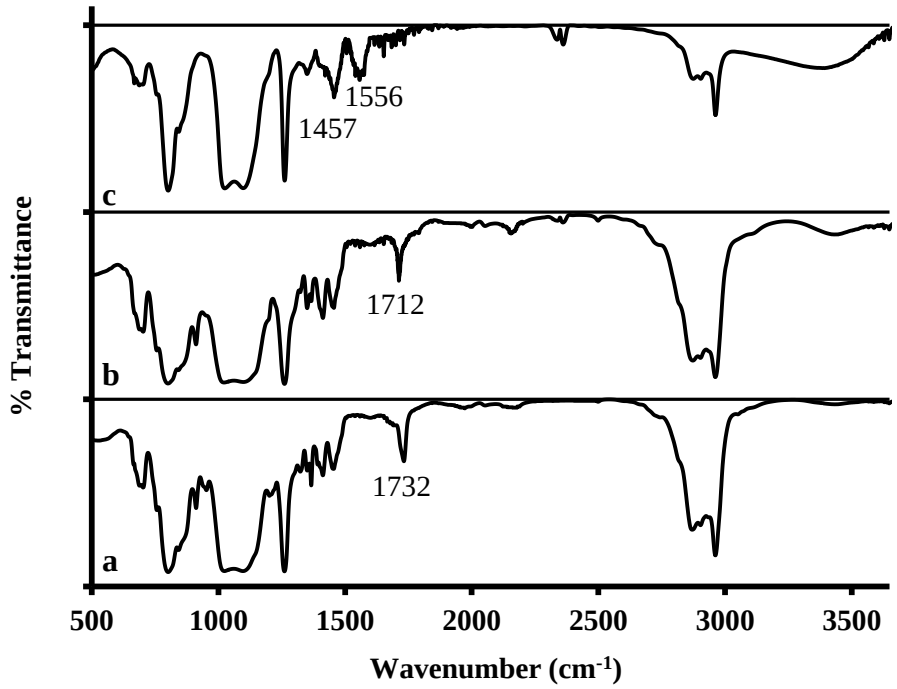

Figure 4.11. (a) FT-IR spectrum of APGC before hydrolysis; (b) FT-IR spectrum after hydrolysis; (c) FT-IR spectrum of CNZVI

Table 4.2. Peak assignments and wave numbers for FTIR spectra of polymer before hydrolysis (PDMS/PEG/tBA), polymer after hydrolysis (PDMS/PEG/AA), and CNZVI

Peak Assignment	PDMS/PEG/tBA (cm^{-1})	PDMS/PEG/AA (cm^{-1})	CNZVI (cm^{-1})
O-H stretch	-	3200-3500	3050-3550
$-CH_2$ (asymmetric)	2957	2960	2962
$-CH_3$ stretch	2900	2898	2879
$-CH_2$ (symmetric)	2861	2868	2869
C=O stretch	1732	1712	-
-COO stretch (asymmetric)	-	-	1556
-COO stretch (symmetric)	-	-	1456
C-O-C stretch	1256	-	-
$(C\text{-}O)_{COOH}$ stretch	-	1260	1261
C-O-C (broad)	1010-1093	1015-1105	1016-1085

DSC was used to determine the influence of pendant group grafting on thermal properties (Figures 4.12-4.14). As shown in Figure 4.12, the PDMS starting material exhibits a T_g at -130°C and no melting transition. After grafting PEG side chains to the PDMS (Figure 4.13), a broad melting transition over the temperature range of approximately -70°C to 0°C was observed which was attributed to PEG side-chain crystallization. Incorporating carboxylic acid groups into the PDMS-PEG graft copolymer produced an amorphous copolymer exhibiting a single T_g at -94°C (Figure 4.14). This result indicates that the APGC produced was a single phase, amorphous material with a very low T_g which was expected to readily enable diffusion of groundwater contaminants to the particle surface.

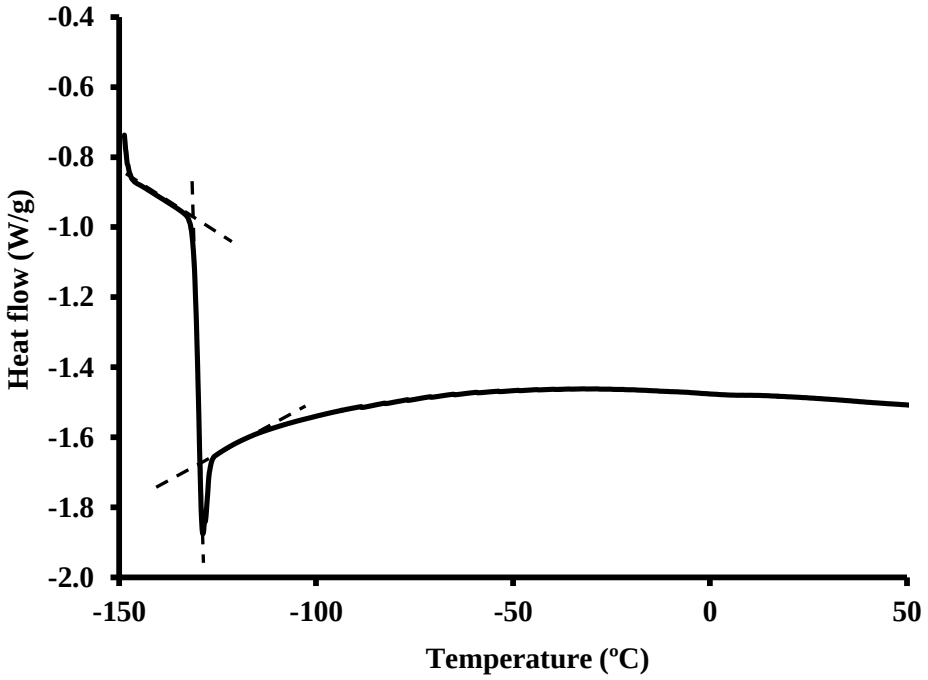

Figure 4.12. DSC thermogram of PDMS

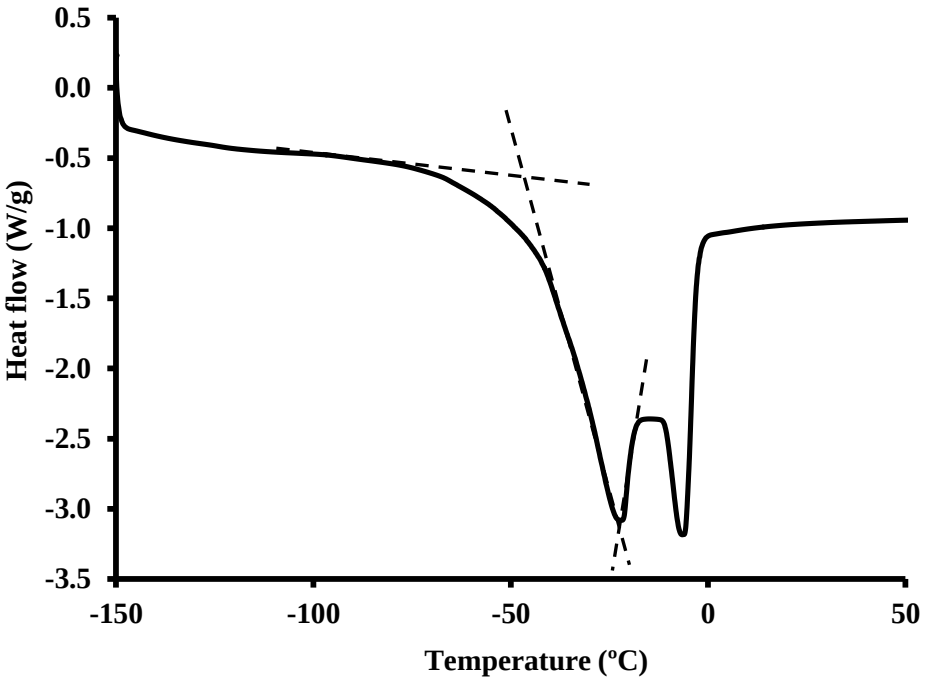

Figure 4.13. DSC thermogram of PEG

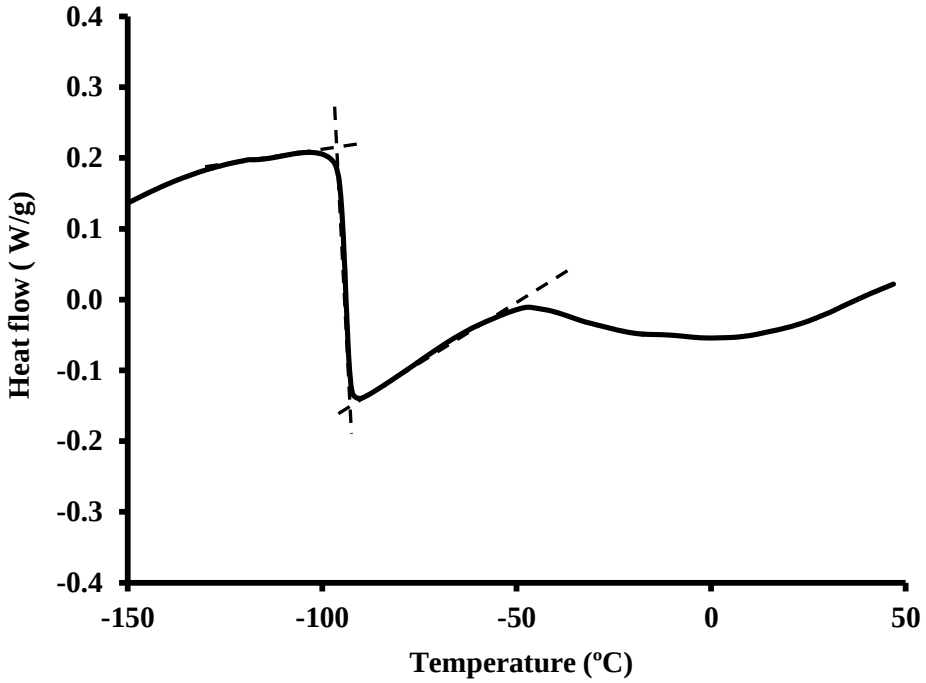

Figure 4.14. DSC thermogram of APGC

4.3.3. CNZVI preparation

FTIR spectra of NZVI and CNZVI confirm that APGC were coated onto NZVI surface (Figure 4.11c). The FTIR spectra for bare NZVI did not show any significant peaks while the spectra for CNZVI showed the formation of chemical bonds (C=O stretching) between carboxylic groups and amorphous surface of NZVI. The C=O peak of carboxylic groups originally at 1712 cm^{-1} (Figure 4.11b) disappeared (Figure 4.11c), while the peaks at 1556 cm^{-1} and 1457 cm^{-1} were observed after the NZVI particles were coated with APGC. Kataby et al. (1999) observed similar peak shift while coating carboxylic acid onto amorphous iron nanoparticles. High resolution TEM images showed that NZVI particles were effectively coated by APGC (Figure 4.15).

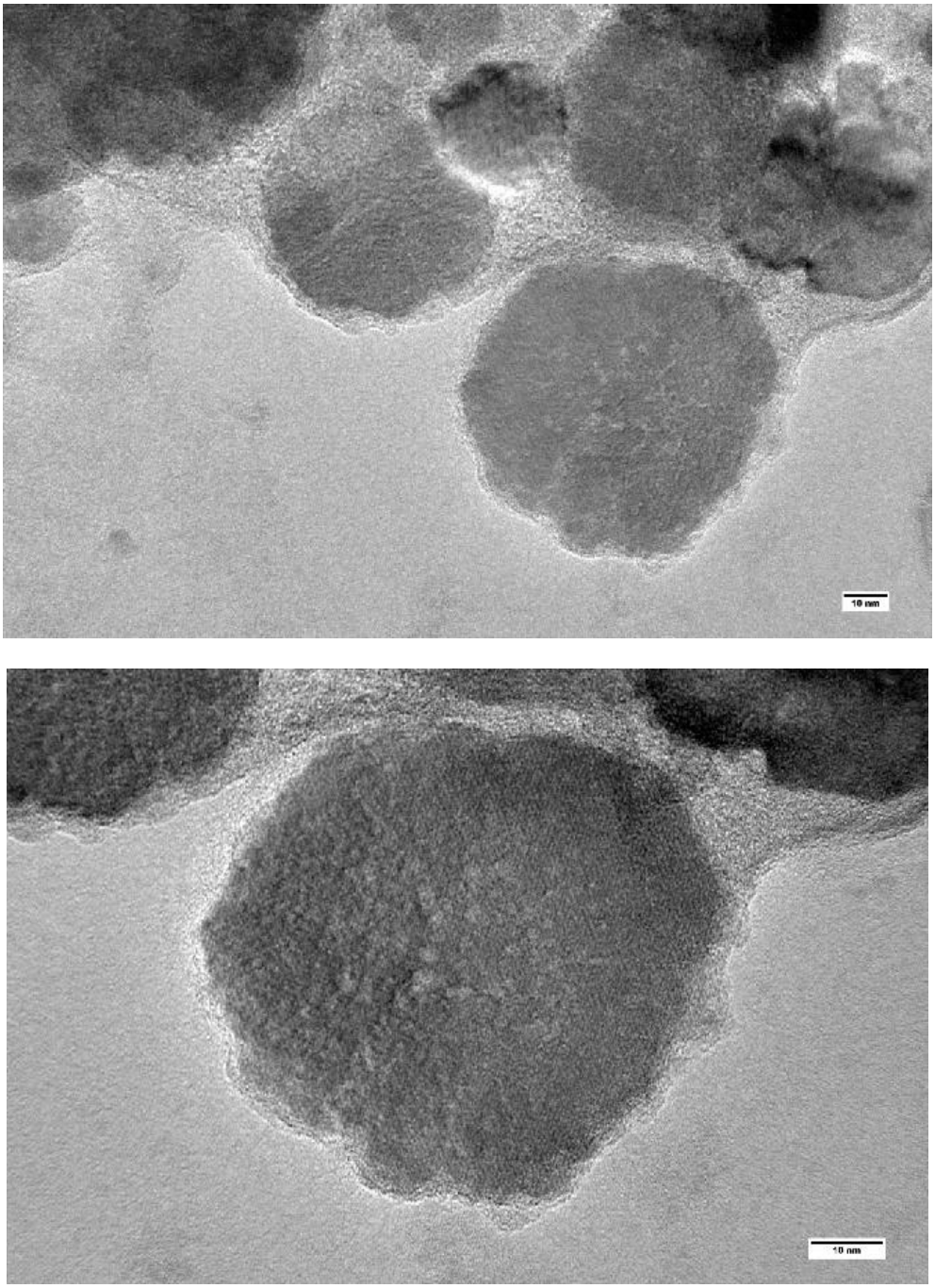

Figure 4.15. HRTEM images showed that NZVI particles were effectively coated by APGC

4.3.4. Colloidal stability studies

NZVI coated with three APGC concentrations (i.e. 2, 10, and 15 g/L) were used in sedimentation studies, and the NZVI coated with 15 g/L APGC formed the most stable suspension as compared to the lower APGC concentrations and bare NZVI (Figure 4.16). White gel like precipitates were formed at APGC concentrations >15 g/L and were considered unsuitable for coating NZVI. All further analyses were conducted with CNZVI coated with 15 g/L APGC.

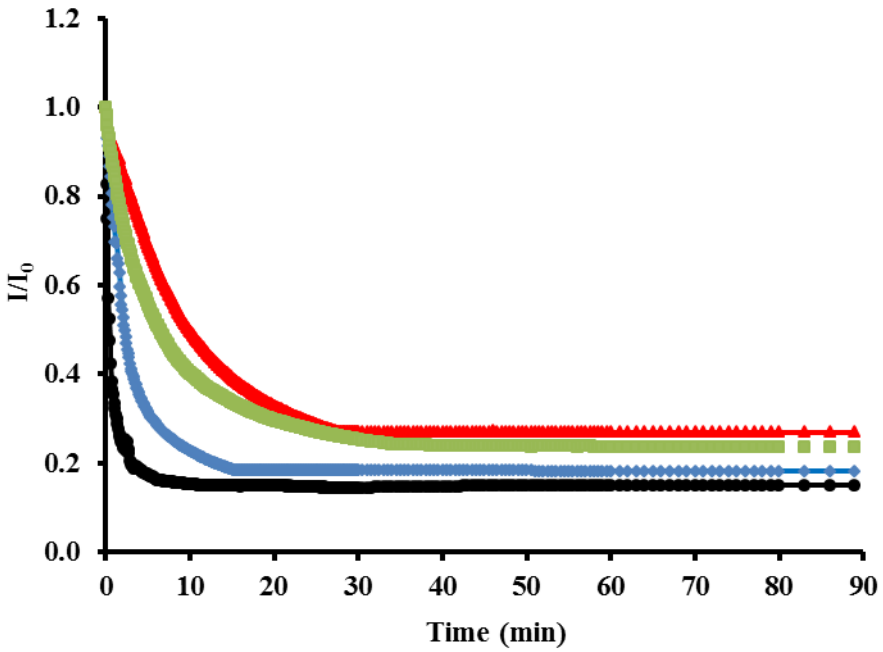

Figure 4.16. Sedimentation characteristics of bare NZVI and CNZVI with different concentration of APGC (• Bare NZVI, ◆ 2 g/L APGC, ■ 10 g/L APGC, and ▲ 15 g/L APGC). The amount of NZVI used was 3 g/L (both bare and coated). The NZVI coated with 15 g APGC L^{-1} had shown the best colloidal stability. Higher concentration (> 15 g/L) of polymer led to gel formation and the polymer could not be used for coating the NZVI particles. (I = measured light intensity, I_0 = initial light intensity)

To determine the effect of the functional groups on sedimentation characteristics of CNZVI, the percent weight fraction of PDMS, PEG, and AA was changed systematically (Table 4.1). The change in PEG/AA ratio had a profound effect on colloidal stability of CNZVI. The APGC with the highest concentration of AA anchoring groups (72.5/21/6.5 : PDMS/PEG/AA) provided the highest colloidal stability (Figures 4.17 and 4.18) and was used for further experimentation. It is, however, important to note that colloidal stability of CNZVI was always better than bare NZVI irrespective of composition of the APGC used (Figure 4.17). The APGC absorbed onto NZVI surface attributed to increased steric hindrance and that might have improved the colloidal stability of NZVI suspensions and can be expected to decrease adhesion to soil surfaces (Stokes and Evans, 1997). Rahme et al. (2009) used di- and tri-block copolymers poly(ethylene oxide) and poly(propylene oxide) to stabilize gold nanoparticles (~12 nm) in aqueous media, and concluded that amphiphilic nature of the polymer contributed to colloidal stability. The present copolymer coating helped steric suspension of the particles.

It is worth mentioning that the sedimentation studies were conducted for all the nanoparticles without any presedimentation. This is in contrast to work reported by others where particles were presettled for 5-60 min to separate the larger (agglomerated) particles (Tiraferri et al., 2008; Phenrat et al., 2007).

4.3.5. Shelf-life studies

The CNZVI particles need to have long shelf-life to be commercially viable (storage and transportability requirements). The results showed that the colloidal stability of the CNZVI remained unchanged for 12 months (two-way ANOVA, $\alpha = 0.05 < \text{p-value}_{0 \text{ and } 1\text{month}} = 0.395$, $\text{p-value}_{0 \text{ and } 12 \text{ month}} = 0.245$, Figure 4.19).

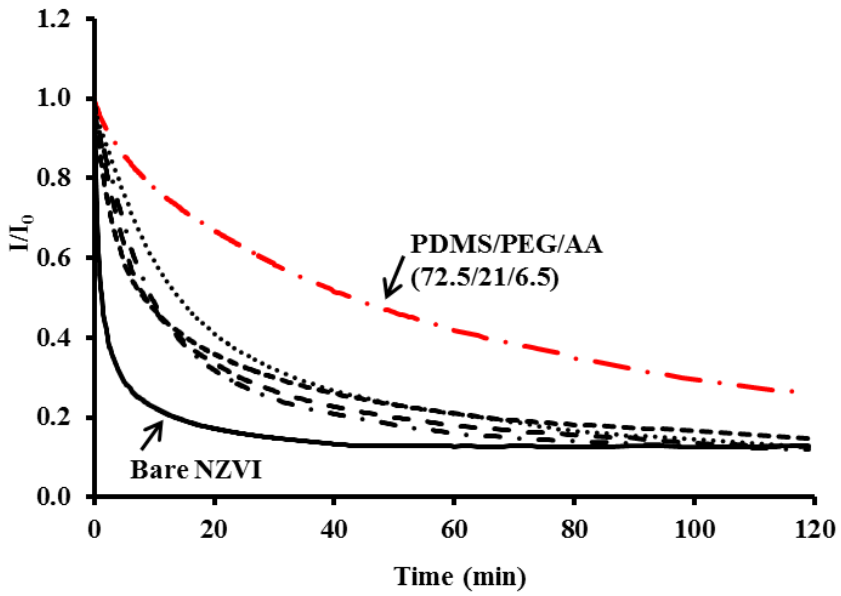

Figure 4.17. The APGC with the highest acrylic acid group (PDMS/PEG/AA (72.5/21/6.5)) showed the highest colloidal stability (– ·: (70/25/5); – – –: (62/36/2), —:(72.5/21/6.5), ····· : (67/29/4), – –: (65/32/3), ——: Bare NZVI) (I = measured light intensity, I_0 = initial light intensity)

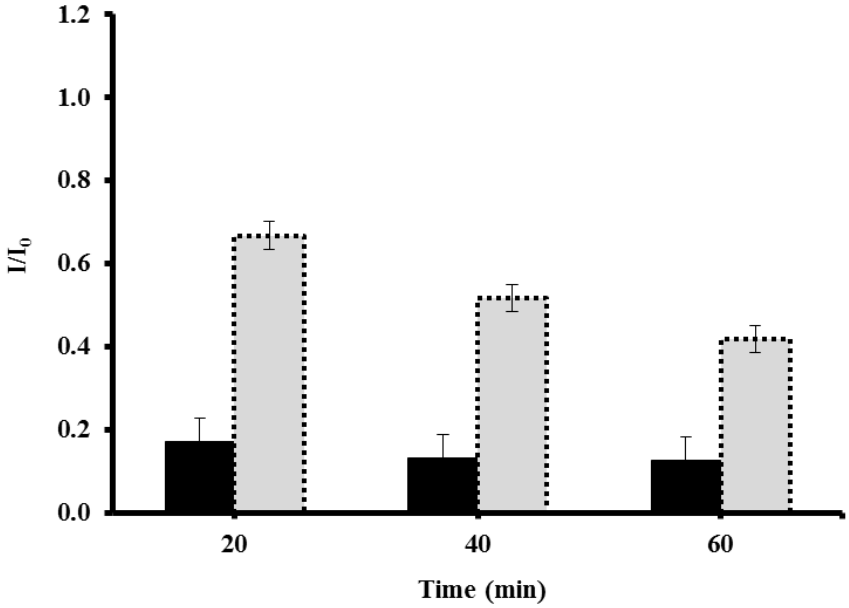

Figure 4.18. Comparison of sedimentation characteristics between NZVI coated with APGC having the optimal sedimentation characteristics [PDMS/PEG/AA (72.5/21/6.5) plot in Figure 4.17] and bare NZVI (■ Bare NZVI, ⬚ CNZVI). (I = measured light intensity, I_0 = initial light intensity)

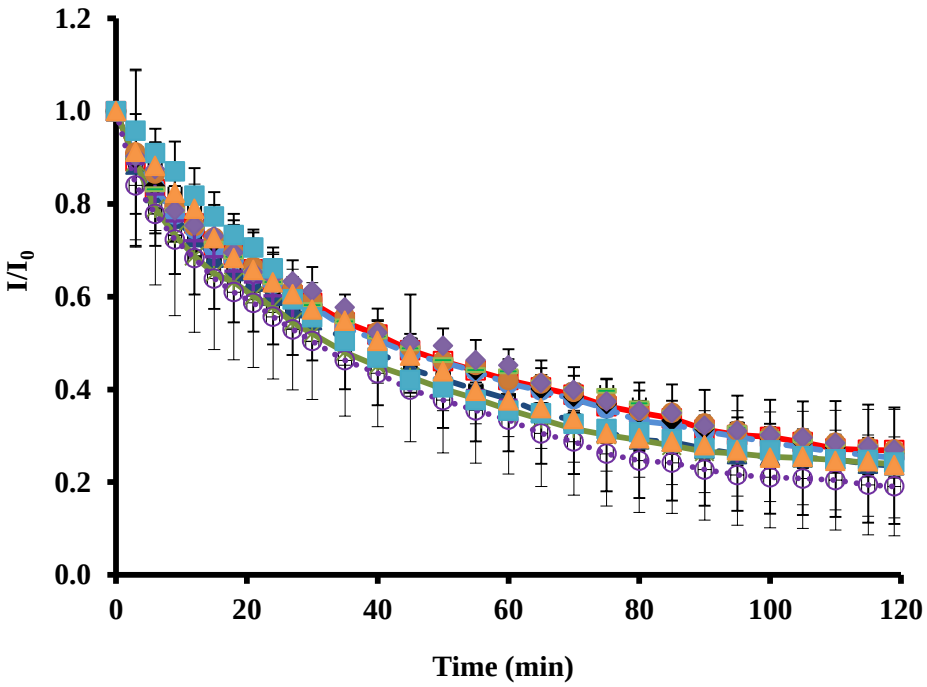

Figure 4.19. Sedimentation studies for CNZVI over a 12-month period for shelf-life evaluation. The data points are connected with straight lines for ease of reading only and they do not represent trendlines. The vertical error bars indicate ± standard deviations. (0 month 1 month, 2 month, 3 month, 4 month, 5.5 month, 6 month, 7 month, 8 month, 9 month, 10 month, 11 month, and 12 month). (I = measured light intensity, I_0 = initial light intensity)

4.3.6. Effect of ionic strength on colloidal stability

The variations in ionic strength due to mono-valent (5 and 10 mM NaCl) and divalent cationic (5 and 10 mM $CaCl_2$) salts did not affect sedimentation characteristics (Figure 4.20). In this study there was no difference in sedimentation behavior of the CNZVI at various ionic strengths because all carboxyl groups apparently chelated to the iron leaving no free carboxyl ion. Absence of carboxylic-carbonyl group in FTIR spectrum at 1712 cm^{-1} in CNZVI (Figure 4.11c) confirms that there was no unreacted/unattached carboxylic acid group left and justifies the assumption about possible complete chelation of the acid group to iron.

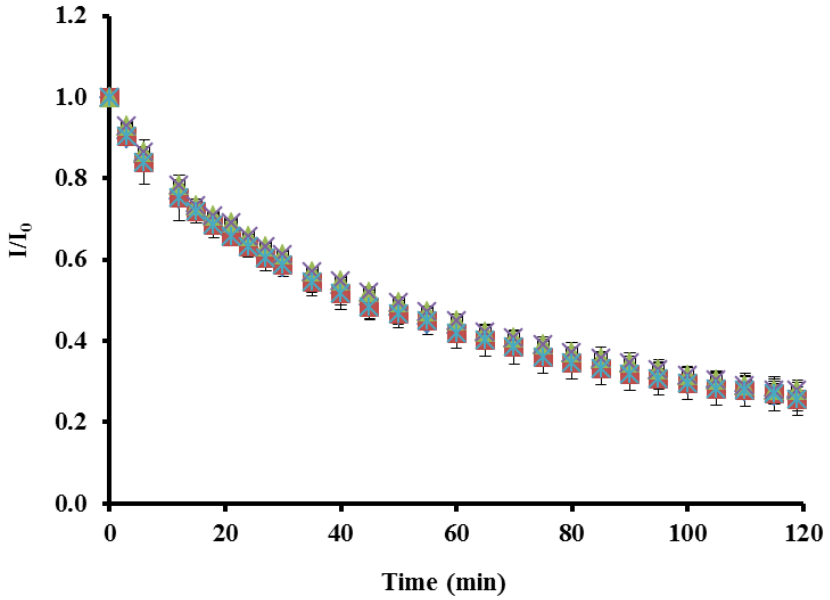

Figure 4.20. Sedimentation studies of CNZVI in water with different ionic strengths (DI water, 5 mM NaCl, 10 mM NaCl, 5 mM $CaCl_2$, 10 mM $CaCl_2$). The concentration of APGC used for coating was 15 mg/L and NZVI was 3 g/L. The data points are connected with straight lines for ease of reading only and they do not represent trendlines. The vertical error bars indicate ± standard deviations.

Saleh et al. (2008) conducted column studies to investigate the effects of Na^+ and Ca^{2+} on the mobility of surface modified NZVI in water. They found that the mobility of NZVI coated with surface modifiers having surface charges decreased with increasing salt concentration, and divalent cation (Ca^{2+}) had a greater effect than monovalent cation (Na^+) (Saleh et al., 2008). This is in contrast to the findings in this study. The triblock copolymers (analogous to the APGC designed within this research) used by Saleh et al. (2008) had a large number of charged sulfonate groups that apparently got distributed throughout an extended polymer layer on the nanoparticle surface. The surface modification of NZVI increased the negative surface potential of the particles and affected dispersibility of CNZVI under high ionic conditions. The triblock copolymer on the NZVI offered electrosteric stabilization of the particles and provided the greatest resistance to adverse

effects (mobility reduction) under low salt concentration conditions but was ineffective at Ca^{2+} > 2 mM (Saleh et al., 2008). The present APGC coated NZVI particles were not affected by high Ca^{2+} concentration (10 mM) as the coated particles had no charges and their stability was steric in nature. It is expected that sticking coefficient of APGC coated NZI will be negligible and the CNZVI can be injected into the aquifer easily and a large zone of influence can be achieved.

4.4. Summary

A series of novel APGC was successfully synthesized using a process that consisted of hydrosilylation of PDMS, PEG, and tBA, and subsequent hydrolysis of tBA to AA. Coating of NZVI particles with APGC was found to enhance their colloidal stability in water and the magnitude of the enhancement was a function of APGC chemical composition. The APGC possessing the highest concentration of carboxylic acid anchoring group (AA) provided the highest colloidal stability. It was also found that the colloidal stability of the APGC coated NZVI remain effectively unchanged up to 12 months. Such a long shelf-life is desired for storage and transportability of coated NZVI, and will make it a commercial viable product. Moreover, different concentrations of NaCl and $CaCl_2$ representing groundwater ionic strengths had no impact on sedimentation behavior of the APGC coated NZVI possibly because of steric nature of stabilization. The new copolymer dispersion technique can possibly be used for other NPs for environmental, biomedical, and other applications.

CHAPTER 5. TRICHOLROETHYLENE TREATABILITY STUDY USING AMPHIPHILIC POLYSILOXANE GRAFT COPOLYMER COATED IRON NANOPARTICLES

5.1. Introduction

Trichloroethylene (TCE) represents one of the most problematic classes of volatile organic compounds found in groundwater (Wu and Schaum, 2000). A number of studies have demonstrated that the widespread presence of TCE in groundwater is a serious public concern due to the hazardous nature of this contaminant (Ellis and Rivett, 2007; Pant and Pant, 2010; Tsai et al., 2011). TCE is listed by the United States Environmental Protection Agency (USEPA, 1992) as a Class A hazardous waste, believed to be a carcinogen and a mutagen. Improper storage and disposal of chlorinated degreasing solvents has resulted in a number of cases of TCE contamination of groundwater. TCE may ultimately found their way to the local and regional aquifers. Spills can result in extremely high concentrations (approaching TCE solubility limits) which would call for remedial action. TCE solubility limit in groundwater is 1000 mg/L (Wu and Schaum, 2000). The maximum contaminant level (MCL) for TCE in drinking water is 5 μg/L or parts per billion (ppb) (USEPA, 1992).

TCE is a dense non-aqueous-phase liquid (DNAPL), and has the ability to penetrate deep into the aquifer much below the water table. Once in the aquifer, TCE gets dissolved in water to form plumes and may remain in the aquifer over several decades depending on the concentration. The size of these plumes may even be a few kilometers depending on the sorption capacity of aquifer materials and their reactivity with TCE (Jackson, 1998; Rivett et al., 2001). The USEPA has reported a number of National Priority List (NPL) Sites that

are contaminated with TCE and require immediate attention under the Comprehensive Environmental Response, Compensation, and Liability Act (CERCLA).

Surface modified NZVI have been used by others for TCE degradation (Saleh et al., 2008; Kim et al., 2010; Bezbaruah et al., 2011). The researchers used polymer matrix (e.g. Ca-alginate) for NZVI entrapment (Kim et al., 2010) and encapsulation (Bezbaruah et al., 2011), however, the there was no or only marginal improvement in TCE degradation by entrapped or encapsulated NZVI compared to bare NZVI. Polymer coated NZVI was studied by Saleh et al. (2008) and Phenrat et al. (2009) to enhance colloidal stability of the particles, hence, increase reactivity of TCE degradation. They used triblock poly(methacrylic acid)-*b*-(methyl methacrylate)-*b*-(styrene sulfonate) (PMAA-PMMA-PSS) coated NZVI to treat TCE (Saleh et al., 2008). They, however, observed a decreased TCE degradation rate using the triblock copolymers coated NZVI compared to bare (i.e., unmodified) NZVI. The decrease in degradation rate was thought to have resulted from a reduction in the diffusion rate of the contaminant through the polymer onto the NZVI surface (Phenrat et al., 2009). This chapter describes the investigations of the degradation behaviors of TCE using APGC coated NZVI (CNZVI, the new polymer described in Chapter 4), and shelf-life of the CNZVI after TCE degradation.

5.2. Experimental section

5.2.1. Coated NZVI synthesis

Coated NZVI(CNZVI) were synthesized as described in Chapter 4 (Section 4.2.4). APGC used has a PDMS/PEG/AA percent weight composition of 72.5/21/6.6. APGC (15 g/L) was used to coat 3 g/L NZVI and used in this study.

5.2.2. TCE degradation batch studies

Batch experiments were conducted in 20 mL amber glass bottles fitted with Teflon septa stoppers. TCE (1, 15, and 30 mg/L initial concentrations) was used as the test contaminant. TCE solutions were prepared with deoxygenated DI water. Bare NZVI (1.5 g/L) or CNZVI (1.5 g/L of NZVI) were added into 20 mL TCE solution. Controls with only APGC (no NZVI) in TCE solution and blank with only TCE solution were run and analyzed simultaneously following the same procedure as bare NZVI and CNZVI batch studies. The reactors were rotated end-over-end at 28 rpm in a custom-made shaker to reduce mass transfer resistance. Aliquots were withdrawn from sacrificial batch reactors at pre-determined time intervals (30, 60, 120, 180, and 360 min), and analyzed using GC/MS (Model 5975, Agilent). The temperatures for GC/MS analyses were as follows: column, injector 200°C, and detector 360°C. Helium was used as the carrier gas at 30 mL/min. Samples were heated at 110°C in an autosampler chamber for 30 min before being vented into the GC. Each sample was run for 8 min. The detection limit of GC/MS for TCE was 1 µg/L.

5.2.3. Shelf-life studies

Several batches of CNZVI (60 mg of iron per each batch) were prepared and stored in a cabinet at room temperature. TCE degradation studies were conducted every month over a 6-month period.

5.2.4. Quality control and statistical analysis

All experiments were conducted in triplicates and average values reported along with standard deviations. Two-way ANOVA analysis was used to find statistical significance comparing between TCE degradation by fresh CNZVI and aged CNZVI.

5.3. Results and discussion

5.3.1. TCE degradation studies

The results from degradation batch studies indicate effective removal of TCE by CNZVI. After 5 h, the TCE concentration decreased from the initial 30 mg/L to 5.64 mg/L (84% removal) and 2.38 mg/L (90% removal) for bare NZVI and CNZVI, respectively (Figure 5.1). No significant decrease of TCE was observed for either the control or the blank. A two-way ANOVA analysis of variance test on the degradation data indicated that there was a significant difference between TCE degradation by bare NZVI and CNZVI ($\alpha = 0.05 >$ p-value = 0.035).

Similar results were obtained in batch studies with initial TCE concentrations of 15 and 1 mg/L (Figures 5.2 and 5.3). For 15 mg/L TCE concentration, removal efficiencies were 76% and 83% for NZVI and CNZVI, respectively (Figure 5.2). With 1 mg/L initial concentration removal were 75% and 78% for NZVI and CNZVI, respectively (Figure 5.3).

The TCE degradation reaction was found to follow psuedo first-order kinetics which is common for the dehalogenation of organic compounds by NZVI (Johnson et al., 1996; Nurmi et al., 2005). The classical first-order rate reaction is expressed as in Eq. 5-1.

$$\frac{dC}{dt} = k_{obs}C \tag{5-1}$$

where,

C = TCE concentration (mg/L)

k_{obs} = the observed rate constant (h^{-1})

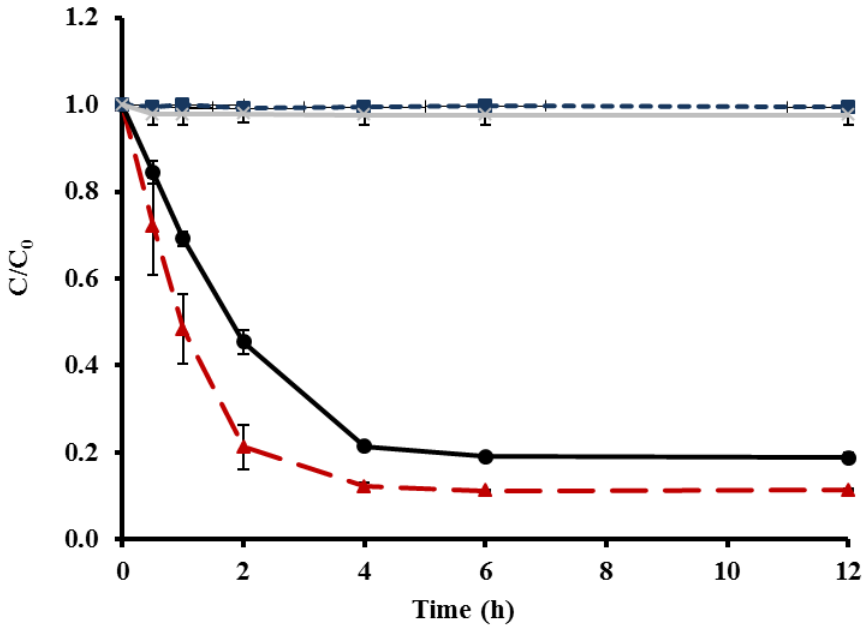

Figure 5.1. Dechlorination of TCE by bare NZVI and CNZVI with 30 mg/L initial TCE concentration (CNZVI, Bare NZVI, Blank, Control). The data points are connected with straight lines for ease of reading only and they do not represent trendlines. The vertical error bars indicate ± standard deviations

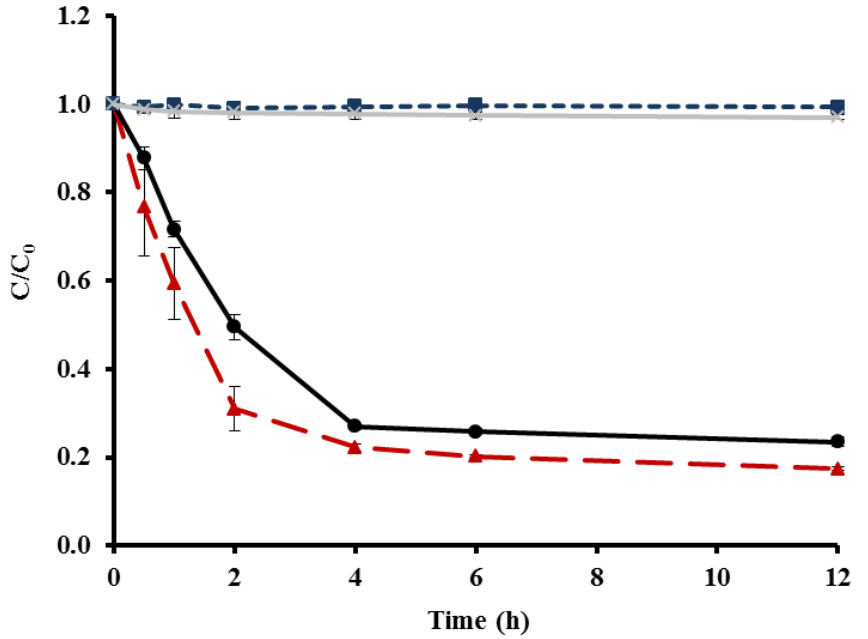

Figure 5.2. Dechlorination of TCE by bare NZVI and CNZVI with 15 mg/L initial TCE concentration. (CNZVI, Bare NZVI, Blank, Control). The data points are connected with straight lines for ease of reading only and they do not represent trendlines. The vertical error bars indicate ± standard deviations

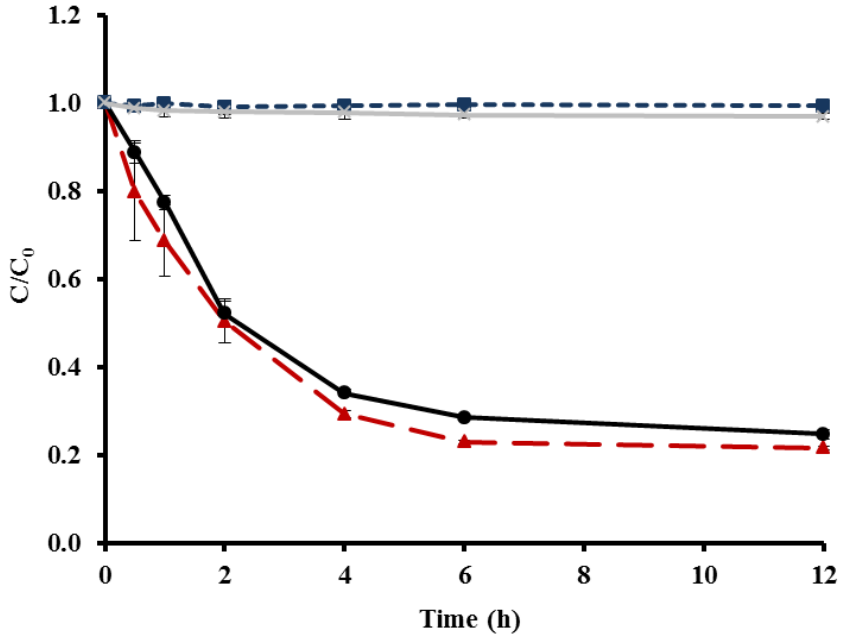

Figure 5.3. Dechlorination of TCE by bare NZVI and CNZVI with 1 mg/L initial TCE concentration. (CNZVI, Bare NZVI, Blank, Control). The data points are connected with straight lines for ease of reading only and they do not represent trendlines. The vertical error bars indicate ± standard deviations

In the case of heterogeneous reactions, such as NZVI-mediated dehalogenation, it is instructive to normalize k_{obs} with respect to (iron) surface area. It is believed that normalizing reaction rare with respect to surface area allows for more valid comparisons with different sized iron particles (Johnson et al., 1996; Nurmi et al., 2005; Thompson et al., 2010). Most researchers reported nanoscale iron reaction rate constants on a surface area normalized basis. Johnson et al. (1996) have presented the following surface area normalized first-order rate equation:

$$\frac{dC}{dt} = k_{SA}\rho_A C \quad (5\text{-}2)$$

where

k_{SA} = surface area normalized rate constant (L m^{-2} h^{-1})

ρ_A = iron surface area per solution volume (m^2 L^{-1})

Therefore,

$$k_{OBS} = k_{SA}\,\rho_A \quad (5\text{-}3)$$

Surface normalized reaction rate constants, k_{SA}, for TCE degradation ranged from 0.007-0.016 $Lm^{-2}h^{-1}$ to 0.008-0.024 $Lm^{-2}h^{-1}$ for bare NZVI and CNZVI (Table 5.1).

The results from the present study indicate no adverse effect of the polymer coating on NZVI reactively, rather the reactivity significantly increased when particles were coated with APGC. This is in contrast to findings by Lowry's research group (Phenrat et al., 2009). Lowry's group found that NZVI surface modification with poly(styrene sulfonate), carboxymethyl cellulose, and polyaspartate enhanced colloidal stability and subsurface mobility of the particles but the reactivity had gone down nonlinearly with the amount of surface modifier used. Blocking of reactive surface sites on the particles and partitioning of TCE to the surface modifiers was suggested as the possible reasons for the decrease in reactivity up to 24 times as compared bare NZVI (Phenrat et al., 2009). There was no loss of reactivity of NZVI due to coating in the present study possibly because of the nature of the constituent groups. PDMS used in this research to coat the NZVI is known to permeate organic contaminants without partitioning (Stokes, 1997). Statistical analysis of TCE degradation data indicated that there was no significant difference (two-way ANOVA, α =

0.05 < p-value = 0.245) between the blank (only TCE) and the control (APGC and TCE) validating the point that there was no partitioning of TCE into the copolymer.

Table 5.1. Summary of TCE degradation reaction rate constants with bare NZVI and CNZVI

	Observed Reaction Rate K_{obs} (h^{-1})	**Surface Normalized Reaction Rate k_{SA} ($L\ m^{-2}\ h^{-1}$)**	**Correlation Coefficient R^2**
Initial TCE = 30 mg/L			
Bare NZVI	0.389	0.016	0.999
CNZVI	0.90	0.024	0.987
Initial TCE = 15 mg/L			
Bare NZVI	0.332	0.008	0.997
CNZVI	0.424	0.011	0.902
Initial TCE = 1 mg/L			
Bare NZVI	0.278	0.007	0.985
CNZVI	0.317	0.008	0.986

Average NZVI particle diameter = 35 nm; NZVI surface area = 25 m^2g^{-1}; NZVI surface area concentration in test solution (ρ_A) = 37.5 m^2L^{-1}

5.3.2. Shelf-life studies

The CNZVI particles need to have long shelf-life to be commercially viable (storage and transportability requirements). The results showed that the TCE degradation rate remained more or less constant (k_{SA} = 0.023 – 0.024 $Lm^{-2}h^{-1}$) over a six-month period ($\alpha = 0.05 <$ p-$value_{0and1month}$=0.224, p-$value_{0and6month}$=0.103, Figure 5.4). Having such a long shelf life will make CNZVI more attractive to remidiation practioners. It is worth mentioning that self life of NZVI evaluated using sedimention behavior as the criterion (Chapter 4, Section 4.3.5) was found to be 12 months.

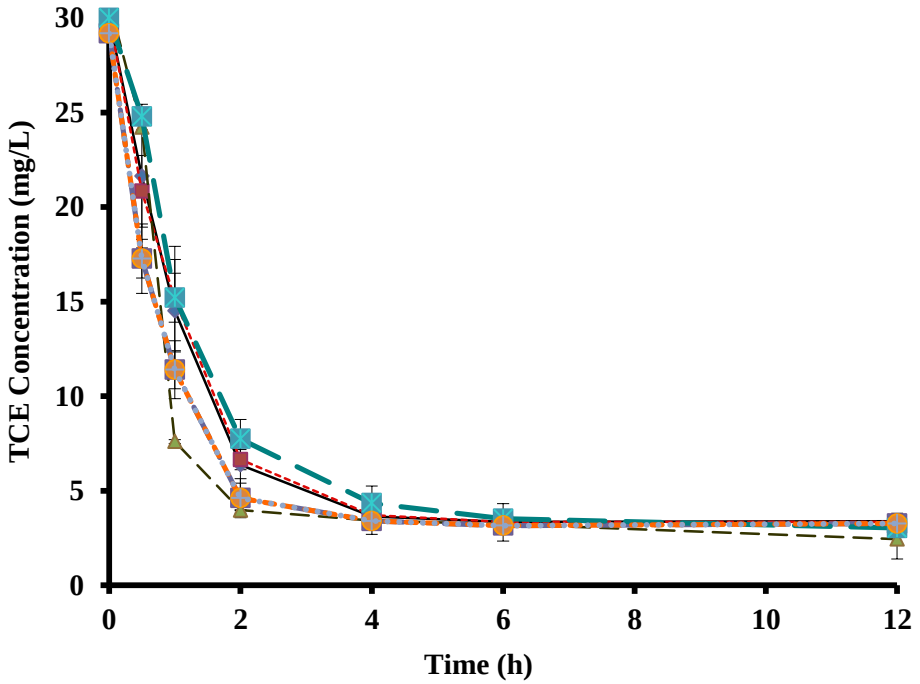

Figure 5.4. TCE degradation studies using CNZVI over a 6-month period (shelf-life evaluation) (—◆— 0 month, ---■--- 1 month, – –▲– – 2 months, —■— 3 months, —■— 4 months, - -●- - 5 months, ... 6 months). The data points are connected with straight lines for ease of reading only and they do not represent trendlines. The vertical error bars indicate ± standard deviations

5.4. Summary

APGC coated NZVI (CNZVI) was found to effectivily degrade TCE. The degradation rates of TCE using CNZVI were determined to be greater than using bare NZVI. The surface normalized degradation rate constants, k_{SA} ($Lm^{-2}\,h^{-1}$), for TCE removal by CNZVI and bare NZVI ranged from 0.008 to 0.024 and 0.007 to 0.016, respectively when the initial TCE concentration was from 1 to 30 mg/L. It was found that TCE degradation capacity of the APGC coated NZVI remain effectively unchanged up to 6 months. Such a long shelf-life is desired for storage and transportability of the particles, and will make it a commercial viable product.

CHAPTER 6. ARSENIC (V) TREATABILITY STUDY USING AMPHIPHILIC POLYSILOXANE GRAFT COPOLYMER COATED IRON NANOPARTICLES

6.1. Introduction

Arsenic (As) is a metalloid, that occurs in environment in different oxidation states, e.g., As as As(V), As(III), As(0) and As (-III) (Choong et al, 2007, Jain and Ali, 2000). Inorganic arsenic generally exists in two major oxidation states, arsenite [As(III)] and arsenate [As(V)] (Hussam and Munir, 2007).

The presence of inorganic arsenic compounds in groundwater, and eventually in drinking water, is a serious environmental problem (Jain and Ali, 2000; Smedley and Kinniburgh, 2002). Arsenic species present in water are pH dependent (Figure 6.1). At low pH (pH 2.0-6.9), $H_2AsO_4^-$ is dominant under oxidizing conditions while $HAsO_4^{2-}$ becomes dominant at higher pH. Under reducing conditions and at pH less than 9.2, the uncharged arsenite species H_3AsO_3 dominate (Smedley and Kinniburgh, 2002).

As(V) is stable under aerobic or oxidizing conditions, while As(III) is stable under anaerobic or mildly reducing conditions (Choong et al., 2007). Both As(III) and As(V) are toxic to human and plants. Arsenic is considered a potential carcinogen to human, and is linked to increased risk for cancer of the skin, lungs, urinary bladder, liver and kidney as well as higher stroke rates, pigmentation changes, skin thickening, neurological disorders, muscular weakness, loss of appetite, and nausea (Kiping 1997, Jain and Ali, 2000, Smedley and Kinniburgh, 2002, Akram et al., 2010, Lisabeth et al., 2010). Increased concentrations of arsenic in natural water have been reported in many areas all over the world including South East Asia (Bangladesh, Vietnam, India, Nepal, Cambodia, Mongolia, China, Thailand, Pakistan and Taiwan), Central and South America (Mexico, Chile and

Argentina), North America (USA and Canada), and Australia (Berg et al., 2001; Kanel et al., 2006; Hussam and Munir, 2007). Because of the risks posed by arsenic, the USEPA has lowered the maximum contaminant level (MCL) of arsenic in drinking water from 50 µg/L to 10 µg/L in 2006 (USEPA, 2001). The new MCL has technologically challenged many water utilities more particularly the utilities serving small communities (USEPA, 2011). Further, the cost of enhanced treatment has brought in addition economic burden on city governments and rural communities. The MCL of arsenic for drinkingwater in selected countries are shown in Table 6.1 (Mohan and Pittman Jr., 2007).

There are several treatment methods used for As removal from drinking water. These methods include membrane filtration, coagulation and flocculation, anion exchange, and adsorption. Nanofiltration (NF) is considered as one of the methods that can be used to meet regulations for lowered arsenic concentrations in drinking water (Urase et al., 1998). Saitua et al. (2011) used a negative charged NF membrane to removed over 95% of As(V) (409 to 16 µg/L). Oh et al. (2000) studied the feasibility of removing the arsenic with a low pressure (maximum pressure of 5.0 Mpa) NF system that can be used in rural areas with an inadequate electric power supply and reported over 95% arsenic removal from water with As(III) concentration of 0.2 mg/L to 0.02 mg/L and As(V) concentration of 1 mg/L to 0.01 mg/L. Sato et al. (2002) reported removal of >95% of As(V) and >75% of As(III) using NF. Reverse osmosis (RO) membranes have been identified as another alternative to remove arsenic in water.

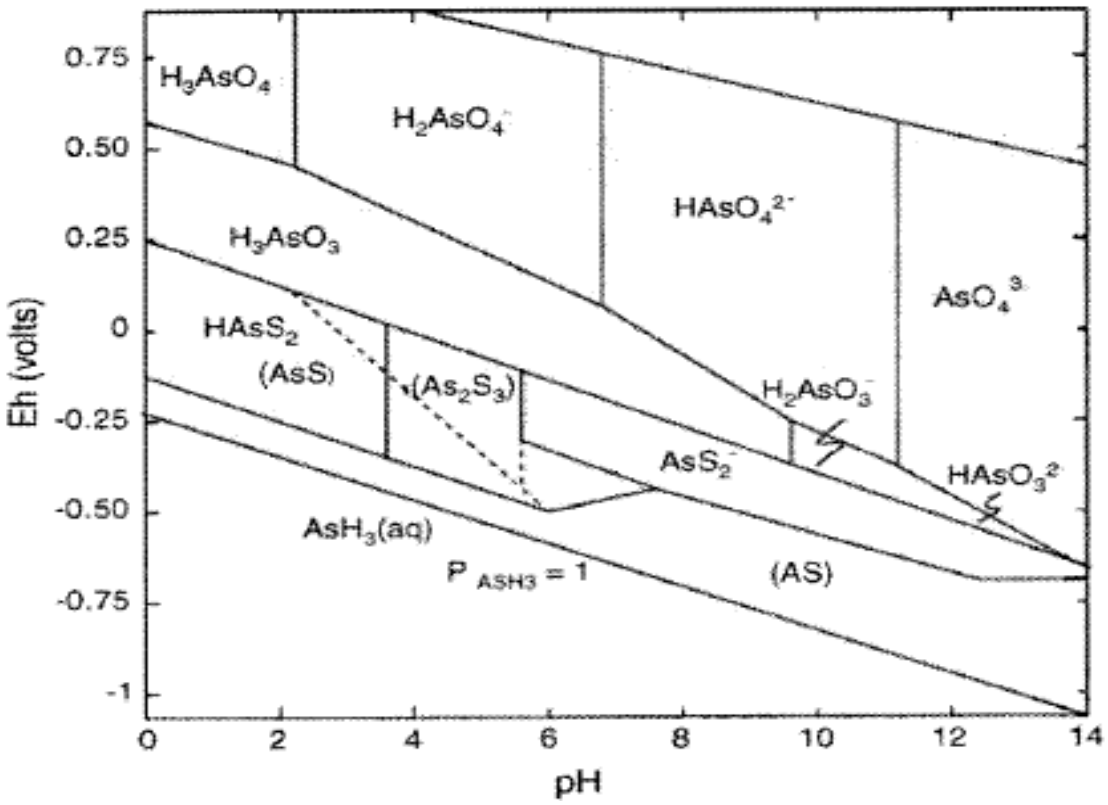

Figure 6.1. pH-Eh diagram for aqueous arsenic (Smedley and Kinniburgh, 2002)

Table 6.1. Maximum contaminant level (MCL) for arsenic in drinking water (Mohan and Pittman, 2007)

Country	MCL (µg/L)
Argentina	50
Bangladesh	50
China	50
Chile	50
India	10
Mexico	50
Nepal	50
New Zealand	10
USA	10
Vietnam	10

Kang et al. (2000) investigated arsenic removal by RO at the pH range of 3-10. They found that As(V) removal (95%) was higher than As(III) (43% removal) with the initial concentration As(III) and As(V) concentraton of 50 µg/L. They suggested that pH control for the membrane feed water is essential for the successful removal of arsenic compounds. However, the membrane technology will find limited use when arsenic is the only contaminant in the water. The membranes are justified when multiple contaminants such as sulfates, nitrates, carbonates require treatment. Coagulation just before membrane treatment increases membrane performance. The coagulant plays the role of adsorbent and the membrane acts as the physical separator (Choong et al., 2007). Curko et al. (2011) found that coagulation with $FeCl_3$ combined with microfiltration is very effective as it could remove As(V) from 100 to 3.4 µg/L (96.6% removal).

The most common method used for As removal is coagulation and flocculation. McNeill and Edwards (1995) used aluminium-based coagulation with disinfection by chlorination to decrease As(V) in water treatment process. They reported a wide range of removal (6-74%) in soluble As(V) in water. For effective arsenic removal with coagulation, sedimentation and filtration have to be followed (Mohan and Pittman, 2007).

Ion exchange is another very effective technique. It can separate different species of arsenic depending on pH (Guell et al., 2011). Ion exchange does not remove As(III) because it occurs predominantly as neutral complexes (H_3AsO_3) in water at pH values of less than 9.0. The predominant species of As(V) (H_2AsO_4 and $HAsO_4^{2-}$) are negatively charged, and, thus, are removable by ion exchange. If As(III) is present, it is necessary to oxidize As(III) to As(V) before removal (Eljamal et al., 2011). In small-scale systems and point-of-use systems (treating water as it enters the home or building) ion-exchange is

often used for arsenic removal because of ease of handling and sludge-free operation (Malik et al., 2009). However, treatment costs are relatively higher than for conventional treatment in large-scale systems.

ZVI is one of the emerging adsorbents for the rapid removal of As(III) and As(V) in the subsurface environment (Biterna et al., 2007; Ngai et al., 2007; Tyrovola et al., 2007; Su and Puls, 2008; Katsoyiannis et al., 2009). Arsenic removal by ZVI under aerobic conditions has been reported (Su and Puls, 2001 and Sun et al., 2006). Katsoyiannis et al. (2008) found that the reactive species produced during ZVI can oxidize As(III) at different pH (3-11) conditions under aerobic environment. Eljamal et al. (2011) investigated removal of As(III) by ZVI in aerated water. As(III) removal can be represented using the following equations (Eljamal et al., 2011):

$$H_2AsO_3^- + 2Fe^{3+} + 3OH^- \rightarrow 2Fe^{2+} + HAsO_4^{2-} \quad (6\text{-}1)$$

$$H_2AsO_3^- + Fe\text{-}OH = FeH_2AsO_3 + OH^- \quad (6\text{-}2)$$

As(V) removal by iron can be represented by using the following equation (Eljamal et al., 2011):

$$HAsO_4^{2-} + Fe\text{-}OH + H^+ = FeHAsO_4^- + H_2O \quad (6\text{-}3)$$

Sun et al. (2006) studied the kinetics of arsenic removal by ZVI powder. They found that both arsenate and arsenite compounds could be removed efficiently by ZVI under aerobic and relatively anaerobic conditions. Aerobic conditions were favorable to

arsenic removal especially for arsenate, while arsenite could be removed more rapidly than arsenate in anaerobic conditions.

ZVI reactions are known to be surface area dependent and the reactivity tend to increase with the increase in specific surface area (Thompson et al., 2010). While microscale ZVI (MZVI) particles have a surface of 1-2 m^2/g (Thompson et al., 2010), nanoscale ZVI (NZVI) particles have a surface of 25 to 54 m^2/g (Chen et al., 2004; Li et al., 2006; Bezbaruah et al., 2009). Further being nanosize, NZVI behaves differently than MZVI and has been reported to remediate a host of contaminants very efficiently including chlorinated compounds (Lowry and Liu, 2006; Cheng et al., 2007; Katsenovich and Miralles-Wilhelm, 2009; Bezbaruah et al., 2011), pesticides (Feitz et al., 2005; Joo et al., 2008; Thompson et al., 2010), heavy metals (Ponder et al., 2000; Alowitz and Scherer, 2005; Xi et al., 2010; Klimkova et al., 2011), and explosives (Gregory et al., 2004; Oh et al., 2005; Zhang et al., 2010) in water.

While NZVI particles are very effective in contaminant removal because of their high specific surface area, the particles agglomerate due to magnetic and van der Waals forces and form larger particles. (Krajangpan et al., 2008; Tiraferri et al., 2008). Once agglomerated the reactive surface area is reduced (Saleh et al., 2008; Phenrat et al., 2009). To make NZVI more effective for As removal, it is important to ensure that the particles remain unagglomerated. An amphiphilic polysiloxane graft copolymer (APGC) has been developed within this research to surface modify NZVI (Chapter 4) and higher dispersibility of the particles have been achieved (Krajangpan et al., 2008, Krajangpan et al., 2009).

The objective of this research was to test the effectiveness of APGC coated NZVI (CNZVI) for the removal of aqueous As(V). The experiments were conducted in aerobic and anaerobic conditions, and results were compared with As(V) removal efficiency of bare NZVI.

6.2. Experimental section

6.2.1. NZVI and CNZVI preparation and characterization

NZVI were prepared and characterized as described in Chapter 3 (Section 3.2.2). APGC synthesis and characterization were done as described in Chapter 4 (Section 4.2.3). CNZVI were prepared as described in Chapter 4 (Section 4.2.4).

6.2.2. Arsenic removal batch studies

Batch arsenic removal studies were performed under anaerobic and aerobic conditions in 40 mL commercial grade borosilicate glass reactors with silicone septum cap. A 100 mg/L As(V) stock solution was prepared using As_2O_5 and used to make the initial As(V) concentrations of 1, 5, and 10 mg/L. Bare NZVI and APGC coated NZVI (0.75 g/L NZVI concentration for both) were used in a 40 mL As(V) solution. Controls with polymer in the As(V) solution and blanks with only the As(V) solution were run simultaneously. All experiments were conducted in triplicate. To simulate anerobic conditions the As solutions in reactors were purged with N_2 gas. The reactors were rotated end-over-end at 28 rpm in a custom-made shaker. Aliquots were withdrawn at definite time intervals and filtered using a syringe filter (Whatman ANOTOP 25, 0.02 μm) to remove NZVI and CNZVI. Samples were preserved using nitric acid for As analysis using an inductively coupled plasma (ICP) spectrophotometer.

6.2.3. Effect of ionic strength

This study was conducted with 10 mM of NaCl and $CaCl_2$ under aerobic conditions in 40 mL reactors made of commercial grade borosilicate glass vials with silicone septum cap reactors. The initial As(V) concentration was 10 mg/L. The CNZVI concentration was the same as that used for arsenic removal batch studies (0.75 g/L NZVI, Section 6.2.2). Blank were run with only As(V) solution and control with CNZVI and As(V) solution but without any NaCl/$CaCl_2$ were run simultaneously. Sample collection, preparation, and analyses were performed as described in Section 6.2.2.

6.2.4. Analytical determination of arsenic (ICP analysis)

A Spectro Genesis ICP-OES (Crossflow nebulizer, SOP) was used to analyze As(V) concentration in test solutions. The software used for this analysis was SmartAnalyzer (version v. 3.013.0752). The plasma power, coolant flow, auxiliary flow, nebulizer flow were optimized to 1400, 13.5, 1.2, and 1.0 L/min, respectively, for this instrument. Five-point calibration was performd before testing. The arsenic standard and sample solutions were prepared in 5% HNO_3. The measurement time was 24 sec and pre-flush time was 60 sec. The results are mean concentrations (mg/L) of three replicate measurements.

6.3. Results and discussion

6.3.1. NZVI and CNZVI

NZVI and CNZVI characterization data are already discussed in Chapter 3 (Section 3.3.1) and Chapter 4 (Section 4.3.3), respectively.

6.3.2. As(V) removal batch studies

As(V) adsorption kinetics were investigated in batch at a contant NZVI and CNZVI mass (0.75 g/L) and varying As(V) initial concentrations (1, 5, and 10 mg/L; Figures 6.2-6.4). The results showed higher As(V) removal using CNZVI than bare NZVI in both aerobic and anaerobic condition, under anaerobic condition, As(V) removal of CNZVI and bare NZVI ranged from 83.4 to 90.6% and 79 to 94% after 2 h, respectively. Under aerobic condition, 99.6 to 100% of As(V) using CNZVI was removed while bare NZVI removed As(V) over 84.5 to 95.7% after 2 h.

Sun et al. (2006) also found that both arsenate and arsenite compounds could be removed efficiently by using ZVI under aerobic and relative anaerobic conditions. Aerobic conditions were favorable to arsenic removal especially for As (V), while As(III) could be removed more rapidly than As(V) in anaerobic condition. Water oxidizes iron (Fe^0) to Fe^{2+} in anaerobic (Eq. 6-4) and aerobic conditions (Eq. 6-5) (Tanboonchuy et al., 2011).

$$Fe^0 + 2H_2O \leftrightarrow Fe^{2+} + H_2 + 2OH^- \quad (6\text{-}4)$$

$$2Fe^0 + 2H_2O + O_2 \leftrightarrow 2Fe^{2+} + 4OH^- \quad (6\text{-}5)$$

Tanboonchuy et al. (2011) also found that 99% and 76% of As(V) were removed after 7 min of reaction with NZVI under oxic and deoxygenated conditions, respectively. This indicates that arsenic removal can be enhanced in the presence of oxygen because arsenic can form inner- and/or outer-sphere complexes with the oxygen-induced iron corrosion products such as iron (hydr)oxides (Bang et al., 2005; Mayo et al., 2007; Zhang

et al., 2004). The presence of DO in water will enhance the rate of iron corrosion and subsequently improve the arsenic removal (Tanboonchuy et al., 2011).

The removal of As(V) was found to follow pseudo-first-order reaction kinetics (Table 6.2). The same surface area normalized rate equation was used as discussed in Chapter 5 (Eq. 5-2). The surface normalized reduction rate constants of As(V) by CNZVI under aerobic conditions for all initial As(V) concentrations (1, 5, and 10 mg/L) were determined to be greater (k_{SA} = 0.308-0.376 $Lm^{-2}\,h^{-1}$) as compares to anaerobic conditions (k_{SA} = 0.152-0.258 $Lm^{-2}\,h^{-1}$), and bare NZVI under both aerobic (k_{SA} = 0.115-0.219 $Lm^{-2}\,h^{-1}$) and anaerobic conditions (k_{SA} = 0.102-0.193 $Lm^{-2}\,h^{-1}$). Interestingly, As(V) removal rate was decreased with increasing initial As (V) concentrations (1, 5,and 10 mg/L). Kanel et al. (2006) showed 100% removal of As(V) using bare NZVI and the reaction was found to follow the pseudo-first-order adsorption kinetic, with observed reaction constant (k_{obs}) of 1.2 to 42.6 h^{-1} and surface area normalized rate constant (k_{SA}) of 0.9 to 1.74 $Lm^2\,h^{-1}$. They also found that k_{SA} was increased with increasing NZVI concentration because of increase in reactive surface area concentration (Kanel et al., 2006).

CNZVI was found to remove As(V) better than NZVI. This was not expected as CNZVI was coated with APGC which has PDMS as the backbone. Arsenic should not have been removed by CNZVI as PDMS was supposed to permeate only organic contaminants through it. This because of an initial pH of the arsenic solution was found to be ~5.7 which is slightly acidic. In the pH range of 2-7, the dominant form of As(V) is $H_2AsO_4^-$ which is a negatively charged ion. In the contrast NZVI surface would be positively charged. The opposite charges of the ion and the sorbent surface will lead to arsenic removal through electrostatic attraction (Tanboonchuy et al. 2011). For the basic

pH condition (7-12), the dominant form of As(V) is $HAsO_4^{2-}$, whereas the adsorbent surface (NZVI) become negative charged. Thus, electrostatic repulsion force would result in decreased adsorption of As(V).

Table 6.2. Summary of arsenic removal rate constants with bare NZVI and CNZVI

	Observed Reaction Rate k_{obs} (h^{-1})	**Surface Normalized Reaction Rate k_{SA} (L m^{-2} h^{-1})**	**Correlation Coefficient R^2**
Initial As(V) = 10 mg/L			
Bare NZVI (aerobic)	2.168	0.115	0.912
Bare NZVI (anaerobic)	1.930	0.102	0.925
CNZVI (aerobic)	5.790	0.308	0.981
CNZVI (anaerobic)	2.857	0.152	0.847
Initial As(V) = 5 mg/L			
Bare NZVI (aerobic)	2.916	0.155	0.907
Bare NZVI (anaerobic)	2.798	0.149	0.930
CNZVI (aerobic)	5.900	0.315	0.893
CNZVI (anaerobic)	3.777	0.201	0.953
Initial As(V) = 1 mg/L			
Bare NZVI (aerobic)	4.111	0.219	0.962
Bare NZVI (anaerobic)	3.635	0.193	0.965
CNZVI (aerobic)	7.047	0.376	0.986
CNZVI (anaerobic)	4.855	0.258	0.917

Average NZVI particle diameter = 35 nm; NZVI surface area = 25 m^2g^{-1}; NZVI surface area concentration in test solution (ρ_A) = 18.75 m^2L^{-1}

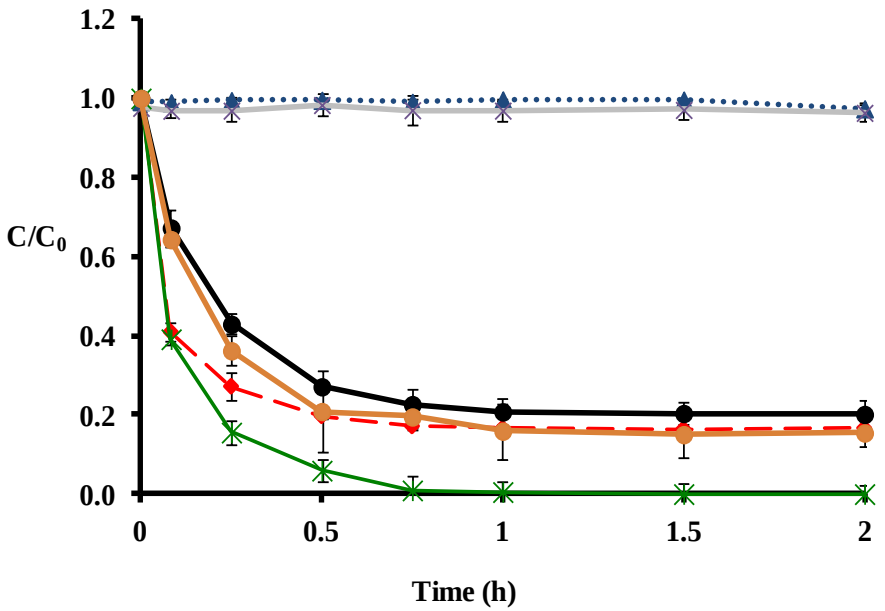

Figure 6.2. Normalized concentration of As (V) removal with initial concentration of 10 mg/L. [CNZVI (anaerobic), Bare NZVI (anaerobic), Bare NZVI (aerobic), CNZVI (aerobic), Blank, Control]. The data points are connected with straight lines for ease of reading only and they do not represent trendlines. The vertical error bars indicate ± standard deviations

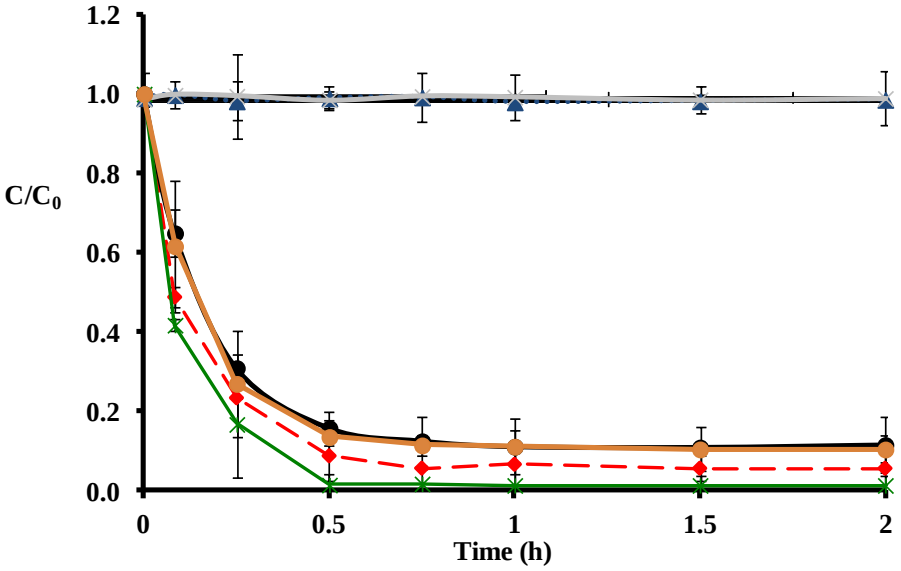

Figure 6.3. Normalized concentration of As (V) removal with initial concentration of 5 mg/L. [CNZVI (anaerobic), Bare NZVI (anaerobic), Bare NZVI (aerobic), CNZVI (aerobic), Blank, Control]. The data points are connected with straight lines for ease of reading only and they do not represent trendlines. The vertical error bars indicate ± standard deviations

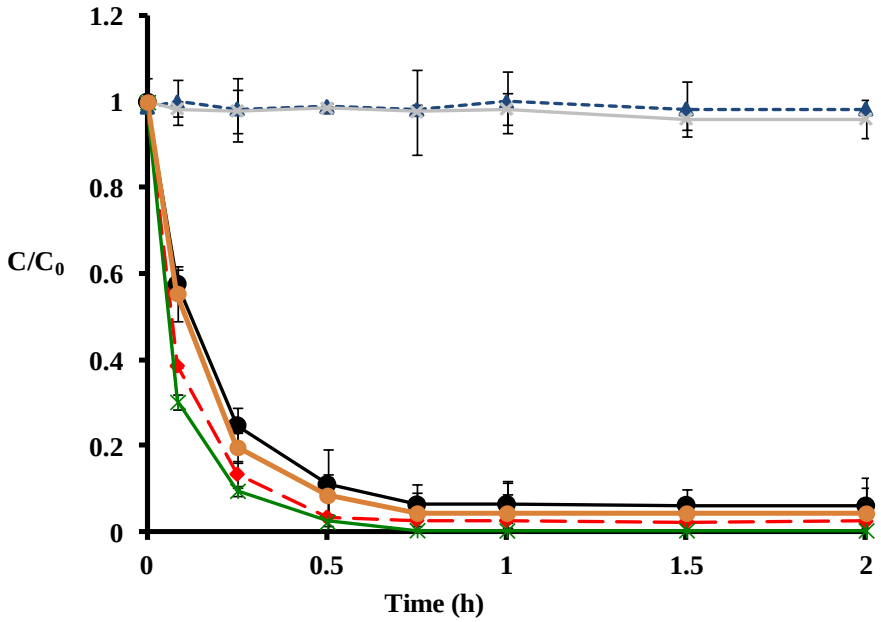

Figure 6.4. Normalized concentration of As (V) removal with initial concentration of 1 mg/L. [CNZVI (anaerobic), Bare NZVI (anaerobic), Bare NZVI (aerobic), CNZVI (aerobic), Blank, Control]. The data points are connected with straight lines for ease of reading only and they do not represent trendlines. The vertical error bars indicate ± standard deviations

6.3.3. Effect of ionic strength

Batch experiments were also conducted to investigate the efficiency of As(V) removal by CNZVI in ionic solutions. The results showed adverse effects of ionic strength due to 10 mM NaCl (~4%) and 10 mM $CaCl_2$ (~8%) on As(V) as compared to removal without $CaCl_2$/NaCl (Figure 6.5). Biterna et al. (2010) found decrease in arsenic removal (~7%) in the presence of chloride. The inhibiting effect of chloride has also been reported in the removal of perchlorate by ZVI and was attributed to the competition for sorption site on NZVI surface (Moore and Young, 2005). Triscz et al. (2009) also reported a slight decrease in the corrosion rates of ZVI in the presence of chloride, probably due to the ability of chloride to destabilize ferric oxides (Triscz et al., 2009).

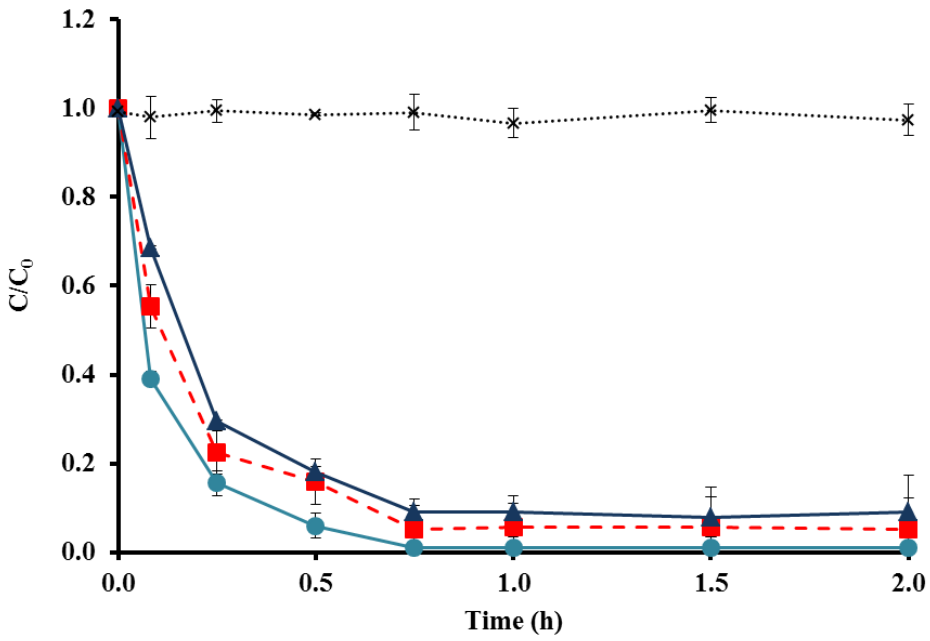

Figure 6.5. Arsenic removal by CNZVI in aerobic condition with and without ionic strengths (CNZVI+As (V); CNZVI+As (V) +10mM NaCl); CNZVI+As (V) + 10mM $CaCl_2$; Blank). The data points are connected with straight lines for ease of reading only and they do not represent trendlines. The vertical error bars indicate ± standard deviations

6.4. Summary

The efficiency of CNZVI for removaing arsenic from water was studied. Batch tests were conducted to investigate the efficiency of CNZVI in both aerobic and anaerobic conditions. Incraese arsenic removal efficiency was observed with CNZVI compared to bare NZVI in both aerobic and anaerobic conditions. The influence of ionic strengths for arsenic removal was also studied and ionic strength showed a slightly inhibiting effect on arsenic removal.

CHAPTER 7. CONCLUSIONS

The research presented in this dissertation targeted at improving the reactivity of NZVI for groundwater contaminant removal. The key to improving NZVI reactivity was to increase dispersibility of the nanoparticles. Zero-valent iron reactions are known to be surface area mediated and, hence, an increase in effective surface area due to dispersion was expected to improve NZVI reactivity. If not properly dispersed NZVI particles tend to agglomerate due to interparticulate magnetic and Van-der Waals attraction forces. Agglomerated particles are larger in size and specific reactive surface area is reduced.

A hydrogel matrix, Ca-alginate, was used to entrap and disperse NZVI. For the first time, NZVI was effectively entrapped in Ca-alginate beads without any loss of reactivity toward contaminants. The reduction in nitrate concentration using bare NZVI and entrapped NZVI were 55-73% and 50-73%, respectively, over a 2 h period. However, SEM and TEM images of NZVI entrapped in the alginate showed that NZVI still remained agglomerated inside the alginate beads.

A novel ampliphilic polysiloxane graft copolymer (APGC) was used to overcome the agglomeration problems. APGC was synthesized and coated onto NZVI particles to enhance their colloidal stability. Treatability studies were conducted for TCE and As (V).

APGC was successfully synthesized using a process that consisted of hydrosilylation of PDMS, PEG, and tBA, and subsequent hydrolysis of tBA to AA. Coating of NZVI particles with APGC was found to enhance their colloidal stability. The APGC possessing the highest concentration of carboxylic acid anchoring group provided the highest colloidal stability. It was also found that the colloidal stability of the APGC coated NZVI remained effectively unchanged up to 12 months. Moreover, different

concentrations of NaCl and $CaCl_2$ representing groundwater ionic strengths had no impact on sedimentation behavior of the APGC coated NZVI.

The results from TCE degradation batch studies with APGC coated NZVI (CNZVI) indicated effective removal of TCE. TCE degradation was found to be better with CNZVI compared to bare NZVI. The TCE concentration decreased from the initial 30 mg/L to 5.64 mg/L (84% removal) and 2.38 mg/L (90% removal) for bare NZVI and CNZVI, respectively. The surface normalized degradation rate constants, k_{SA} ($Lm^{-2}\,h^{-1}$), for TCE removal by CNZVI and bare NZVI ranged from 0.008-0.024 to 0.070-0.016, respectively when initial TCE concentration ranged from 1 to 30 mg/L. It was also found that TCE degradation capacity of the APGC coated NZVI remain effectively unchanged up to 6 months of storage.

As(V) removal using CNZVI was tried and the results showed higher As(V) removal using CNZVI than bare NZVI under both aerobic and anerobic conditions. Under anaerobic conditions, the As(V) removal by CNZVI and bare NZVI ranged from 83.4% to 90.6% and 79% to 94% in 2 h, respectively. Under aerobic conditions, the As(V) could be removed completely using CNZVI while bare NZVI also removed As(V) over 100% in 2 h. The surface normalized reduction rate constants of As(V) by CNZVI under aerobic conditions for all initial As(V) concentrations (1, 5, and 10 mg/L) were determined to be greater (k_{SA} = 0.308-0.376 $Lm^{-2}\,h^{-1}$) compared to anaerobic conditions (k_{SA} = 0.152-0.258 $Lm^{-2}\,h^{-1}$), and bare NZVI under both aerobic (k_{SA} = 0.115-0.219 $Lm^{-2}\,h^{-1}$) and anaerobic conditions (k_{SA} = 0.102-0.193 $Lm^{-2}\,h^{-1}$). The ionic strength (NaCl and $CaCl_2$) showed some inhibiting effects on arsenic removal.

With the observed improvement in dispersibility and treatability by NZVI when coated with APGC, it is safe to claim that CNZVI has potential for in-situ groundwater remediation applications. The long shelf-life (6-12 months) achieved for CNZVI is expected to make it a commercially viable product. The new copolymer can possibly be used for other NPs for environmental and other applications.

CHAPTER 8. RECOMMENDATIONS FOR FUTURE RESEARCH

Based on knowledge gained from this research, the following recommendations are made for future studies:

- Future research on NZVI entrapment in other polymer matrices including polyvinyl alcohol (PVA) and polyethylene glycol (PEG) to treat groundwater contaminants should be explored. These matrices may provide a better scope for scale-up of the production process.
- The composition of the copolymer used in coated NZVI (CNZVI) preparation process should be optimized for economic benefits. Structure-property relationships between the various components of the copolymer should be studied to know the optimal composition.
- Degradation of amphiphilic polysiloxane graft copolymer (APGC) should be studied to investigate the possible effect of CNZVI after its injection into the aquifer. This research did not scope degradation as a research objective.
- Biopolymers (e.g., guar gum, arabic gum, vegetable oil-based polymers) should be explored for use as surface modifiers. Such surface modifiers made from biopolymers are expected to be more environmental friendly.
- Contaminant degradation studies using CNZVI should be conducted in the presence of various ions such as HCO_3^-, NO_3^-, SO_4^{2-}. Results from such studies will help in designing more effective nanoparticles for environmental remediations.
- Regeneration of NZVI and CNZVI should be studied. Presently NZVI is very expensive and possible regeneration will cut down NZVI life-cycle cost.

- CNZVI should be tried for treating other contaminants.
- Column studies to simulate aquifer conditions should be conducted.
- Pilot studies should be conducted to examine the effectiveness of CNZVI under actual field conditions.
- Zeta potential should be investigated to confirm the dispersibility of particles. The zeta potential can be related to the stability of colloidal dispersions that can indicate the degree of repulsion between adjacent particles in dispersion. Colloids with high zeta potential are electrically stabilized while colloids with low zeta potentials tend to flocculate.
- Corrosion of NZVI should be studied. NZVI can be oxidized by non-target compounds in actual field conditions. For groundwater remediation, effectiveness will depend on the ability to deliver the NZVI to the contaminants without severe oxidation.
- Toxicity and biodegradability of APCG should be studied.

REFERENCES

Akram, Z.; Jalali, S.; Shami, S.A.; Ahmad, L.; Batool, S.; Kalsoom, O. (2010) Adverse effects of arsenic exposure on uterine function and structure in female rat. *Exp. Toxicol. Pathol.,* 62, 451-459.

Aksu, Z. ; E-retli, G. (1998) A comparative study of copper(II) biosorption on Ca-alginate, agarose and immobilized *C. vulgaris* in a packed-bed column. *Process Biochem*., 33, 393-400.

Alcala, M.D.; and Real, C. (2006) Synthesis based on the wet impregnation method and characterization of iron and iron oxide-silica nanocomposites. *Solid State Ionics*, 177, 955-960.

Alowitz, M.J.; Scherer, M.M. (2002) Kinetics of nitrate, nitrite, and Cr(VI) reduction by iron metal. *Environ. Sci. Technol.,* 36, 299-306.

APHA, AWWA, WEF (1998) Standard Methods for the Examination of Water and Wastewater, 20th ed. American Public Health Association, Washington, D.C.

Bang, S.; Johnson, M.D.; Korfiatis, G.P.; Meng, X. (2005) Chemical reactions between arsenic and zero-valent iron in water. *Water Res.,* 39, 763-770.

Benerjee, A.; Nayan, D.; Lahiri, S. (2007) A new method of synthesis of iron doped calcium alginate beads and determination of iron content by radiometric method. *Biochem. Eng. J*., 33, 260-262.

Berg, M.; Tran, H.C.; Nguyen, T.C.; Pham, H.V.; Schertenleib, R.; Giger, W. (2001) Arsenic contamination of groundwater and drinking water in Vietnam: A Human health threat. *Envi. Sci. Technol*., 35, 2621- 2626.

Bezbaruah, A.N.; Krajangpan, S.; Chisholm, B.J.; Khan, E.; Bermudez, J.J.E. (2009) Entrapment of iron nanoparticles in calcium alginate beads for groundwater remediation applications. *J. Hazard. Mater*., 166, 1339-1343.

Bezbaruah, A.N.; Shanbhougue, S.S.; Simsek, S.; Khan, E. (2011) Encapsulation of iron nanoparticles in alginate biopolymer for trichloroethylene remediation. *J. Nanopart. Res.*, 13, 6673-6681.

Biterna, M.; Arditsoglou, A.; Tsikouras, E.; Voutsa, D. (2007) Arsenate removal by zero valent iron: Batch and column tests. *J. Hazard. Mater*., 149, 548-552.

Blowes, D. W.; Ptacek, C. J.; Jambor, J. L. (1997) In-situ remediation of Cr(VI) contaminated groundwater using permeable reactive walls: laboratory studies" *Environ. Sci. Technol*., 31, 3348-3357.

Buffle, J.; Wilkinson, K.J.; Stoll, S.; Filella, M.; Zhang, J. (1998) A generalized description of aquatic colloidal interactions: the three-colloidal component approach. *Environ. Sci. Technol*., 32, 2887-2899.

Bradley, T.D.; Ball, A.; Harding, S.E.; Mitchell, J.R. (1989) Thermal degradation of guar gum. *Carbohydr. Polym.,* 10, 205-214.

Cantrell, K.L. ; Kaplan, D.I. ; Wietsma, T.W. (1995) Zero-valent iron for the in-situ remediation of selected metals in groundwater. *J. Hazard.Mater*., 42, 201-212.

Cao, J.; Li, X.; Tavakoli, J.; Zhang, W.-X. (2008) Temperature programmed reduction for measurement of oxygen content in nanoscale zero-valent iron. *Environ. Sci. Technol.*, 42, 3780-3785.

Chen, H.; Luo, H.; Lan, Y.; Dong, T.; Hu, B.; Wang, Y. (2011) Removal of tetracycline from aqueous solutions using polyvinylpyrrolidone (PVP-K30) modified nanoscale zero valent iron. *J. Hazard. Mater.,* 192, 44-53.

Chen, S.S.; Hsu, H.-D.; Li, C.-W. (2004) A new method to produce nanoscale iron for nitrate removal. *J. Nanopart. Res.*, 6, 639-647.

Chen, S-.S.; Huang,Y.-C.; Kuo, T.-Y. (2010) The remediation of perchloroethylene contaminated groundwater by nanoscale iron reactive barrier integrated with surfactant and electrokinetics. *Ground Water Monit. R.,* 30, 90–98.

Cheng, F. ; Muftikian, R. ; Fernando, Q. ; Korte, N. (1997) Reduction of nitrate to ammonia by zero-valent iron. *Chemosphere,* 35, 2689-2695.

Cheng, R.; Wang, J.-L.; Zhang, W.-X. (2007) Comparison of reductive dechlorination of *p*-chlorophenol using Fe-0 and nanosized Fe-0. *J. Hazard. Mater.,* 144, 334–339.

Choe, S.; Chang, Y.Y.; Hwang, K.-Y.; Khim, J. (2000) Kinetics of reductive denitrification by nanoscale zero-valent iron. *Chemosphere,* 41, 1307–1311.

Choe, S.; Liljestrand, H.M.; Khim, J. (2004) Nitrate reduction by zero-valent iron under different pH regimes. *Appl. Geochem*., 19, 335–342.

Comba, S.; Sethi, R. (2009) Stabilization of highly concentrated suspensions of iron nanoparticles using shear-thinning gels of xanthan gum. *Water. Res*., 43, 3717-3726.

Choong T.S.Y.; Chuah, T.G.; Robiah, F.L.; Koay, G.; Azni, I. (2007) Arsenic toxicity, health hazards and removal technique from water: an overview. *Desalination,* 217, 139–166.

Ćurko, J.; Mijatović, I.; Matošić, M.; Jakopović, H.K.; Bošnjak, M.U. (2011) As(V) removal from drinking water by coagulation and filtration through immersed membrane. *Desalination,* 279, 404–408.

Eljamal, O.; Sasaki, K.; Hirajima, T. (2011) Numerical simulation for reactive solute transport of arsenic in permeable reactive barrier column including zero-valent iron. *Appl. Math. Model*, 35, 5198-5207.

Ellis, P.A.; M.O. Rivett. (2007) Assessing the impact of VOC-contaminated groundwater on surface water at the city scale. *J. Contam. Hydrol.*, 91, 107-127.

Fang, C.; Zhao, B.Y.; Chen, L.; Wu, Q.; Liu, N.;Hu, K.A. (2005) The effect of the green additive guar gum on the properties of magnetorheological fluid. *Smart Mater. Struct.*, 14, N1–N5.

Feitz, A.J.; Joo, S.H.; Guan, J.; Sun, Q.; Sedlak, D.L.; Waite, T.D. (2005) Oxidative transformation of contaminants using colloidal zero-valent iron. *Colloid Surface A,* 265, 88-94.

Franco, D.V.; Silva, L.M.D.; Jardim, W.F. (2009) Reduction of hexavalent chromium in soil and ground water using zero-valent iron under batch and semi-batch conditions. *Water. Air. Soil. Pollut.*, 197, 49–60.

Fundueanu, G.; Nastruzzi, C.; Carpov, A.; Desbrieres, J.; Rinaudo, M. (1999) Physicochemical characterization of Ca-alginate beads microparticles produced with different methods. *Biomaterials,* 20, 1427-1435.

Garbayo, I.; Leon, R.; Vigara, J.; Vılchez, C. (2002) Diffusion characteristics of nitrate and glycerol in alginate. *Colloid Surface, B* 25, 1–9.

Gregory, K. B.; Larese-Casanova, P.; Parkin, G. F.; Scherer, M. M. (2004) Abiotic transformation of hexahydro-1,3,5-trinitro-1,3,5-triazine by FeII bound to magnetite. *Environ. Sci. Technol*., 38, 1408-1414.

Gu, S.; Onishi, J.; Kobayashi, Y.; Nagao, D.; Konno, M. (2005) Preparation and colloidal stability of monodisperse magnetic polymer particles. *J. Colloid. Interf. Sci.,* 289, 419–426.

Guell, R.; Fontas, C.; Antico, E.; Salvado, V.; Crespo, J.G. (2011) Transport and separation of arsenate and arsenite from aqueous media by supported liquid and anion-exchange membranes. *Sep. Purif. Technol.*, 80, 428-434.

Hara, J.; Ito, H.; Suto, K.; Inoue, C.; Chida, T. (2005) Kinetics of trichloroethene dechlorination with iron powder. *Wat. Res*., 39, 1165-1173.

He, F.; Zhang, M.; Qian, T.; Zhao, D. (2009) Transport of carboxymethyl cellulose stabilized iron nanoparticles in porous media: column experiments and modeling. *J. Colloid Interface Sci.,* 334, 96–102.

He, F.; Zhao, D. (2005) Preparation and characterization of new class of starch-stabilized bimetallic nanoparticles for degradation of chlorinated hydrocarbon in water. *Environ. Sci. Technol.,* 39, 3314-3320.

Hill, C. B.; Khan, E. (2008) A comparative study of immobilized nitrifying and co-immobilized nitrifying and denitrifying bacteria for ammonia removal from sludge digester supernatant. *Water Air Soil Poll*., 195, 23-33.

Huang, C. P. ; Wang, H. W. (1998) Nitrate reduction by metallic iron. *Water Res*., 32, 2257–2264.

Huang, G.-L.; Zhihui, S. (2002) Immobilization of s*pirulina subsalsa* for removal of triphenyltin from water. *Artif. Cell. Blood. Sub***.,** 30, 293–305.

Huang, Y.H.; Zhang, T.C. (2006) Nitrite reduction and formation of corrosion coatings in zerovalent iron systems. *Chemosphere,* 64, 937-943.

Hussam. A.; Munir, A.K.M. (2007) A simple and effective arsenic filter based on composite iron matrix: Development and deployment studies for groundwater of Bangladesh. *J. Environ. Sci. Heal. A,* 42, 1869–1878.

Jackson, R.E. (1998) The migration, dissolution, and fate of chlorinated solvents in the urbanized alluvial valleys of the southwestern USA. *Hydrogeol. J*.. 6, 144-155.

Jain, C.K.; Ali, I. (2000) Arsenic: Occurrence, toxicity and speciation techniques. *Wat. Res.,* 34, 4304-4312.

Johnson, T.L.; Scherer, M.M.; Tratnyek, P.G. (1996) Kinetics of halogenated organic compound degradation by iron metal. *Environ. Sci. Technol*., 30, 2634-2640.

Joo, S.H.; Zhao, D. (2008) Destruction of lindane and atrazine using stabilized iron nanoparticles under aerobic and anaerobic conditions: effects of catalyst and stabilizer. *Chemosphere*, 70, 418-425.

Jun, Y.W.; Huh, Y.M.; Choi, J.; Lee, J.H.; Song, H.T.; Kim, S.; Yoon, S.; Kim, K.S.; Shin, J.S.; Suh, J.S.; Cheon, J. (2005) Nanoscale size effect of magnetic nanocrystals and their utilization for cancer diagnosis via magnetic resonance imaging. *J. Am. Chem. Soc.*, 127, 5732-5733.

Kapoor, A.; Viraraghavan, T. (1997) Nitrate removal from drinking water - review. *J. Environ. Eng*., 123, 371–380.

Kanel, S.R.; Manning, B.; Chatlet, L.; Choi, H. (2005) Removal of arsenic (III) from groundwater by nanoscale zero-valent iron. *Environ. Sci. Technol.,* 39, 1291-1298.

Kanel, S.R.; Greneche, J.M.; Heechul, C. (2006) Arsenic (V) removal from groundwater using nano scale zero-valent iron as a colloidal reactive barrier material. *Environ. Sci. Technol.,* 40, 2045-2050.

Kang, M.; Kawasaki, M.; Tamada, S.; Kamei, T.; Magara, Y. (2000) Effect of pH on the removal of arsenic and antimony using reverse osmosis membranes. *Desalination,* 131, 293-298.

Kataby, G.; Cojocaru, M.; Prozorov, R.; Gedanken, A. (1999) Coating carboxylic acids on amorphous iron nanoparticles. *Langmuir,* 15, 1703-1708.

Katsenovich Y.P.; Miralles-Wilhelm, F.R. (2009) Evaluation of nanoscale zerovalent iron particles for trichloroethene degradation in clayey soils, *Sci. Total Environ.*, 407, 4986–4993.

Katsoyiannis, I.A.; Ruettimann, T.; Hug, S.J. (2008) pH dependence of fenton reagent generation and As(III) oxidation and removal by corrosion of zero valent iron in aerated water. *Environ. Sci. Technol.,* 42, 7424-7430.

Kim, D.K.; Zhang, Y.; Kehr, J.; Klason, T.; Bjelke, B.; Muhammed, M. (2001) Characterization and MRI study of surfactant-coated superparamagnetic nanoparticles administered into the rat brain. *J. Magn. Magn. Mater*., 225, 256-261.

Kim, E.H.; Lee, H.S.; Kwak, B.K.; Kim, B.-K. (2005) Synthesis of ferrofluid with magnetic nanoparticles by sonochemical method for MRI contrast agent. *J. Magn. Magn. Mater.,* 289, 328-330.

Kim, H.; Hong, H.-J.; Jung, J.; Kim, S.H.; Yang, J.-W. (2010) Degradation of trichloroethylene (TCE) by nanoscale zero-valent iron (NZVI) immobilized in alginate bead. *J. Hazard. Mater.,* 176, 1038-1043.

Kipling, M.D. (1977) Arsenic. In: The Chemical Environment (Eds. J. Lenihan and W.W.Fletcher). Glasgow, Blackie, 93–120.

Klimkova, S.; Cernik. M.; Lacinova, L.; Filip, J.; Jancik, D.; Zboril, R. (2011) Zero-valent iron nanoparticles in treatment of acid mine water from in situ uranium leaching. *Chemosphere,* 82, 1178–1184.

Kobaslija, M.; McQuade, D.T. (2006) Removable colored coatings based on calcium alginate hydrogels. *Biomacromolecules*, 7, 2357-2361.

Krajangpan, S., Chishlom, B., Bezbaruah, A., (2011) Patent application number: 20110042325, Polymeric Delivery Vehicle for Nanoparticles, Nationalized PCT Patent filed.

Krajangpan, S.; Chisholm, B.J.; Kalita, H.; and Bezbaruah, A.N. (2009) Challenges in groundwater remediation with iron nanoparticles: Enhancement colloidal stability (Chapter 8) in T. Zhang, R. Surampalli; K. Lai, Z. Hu, R. Tyagi, and I. Lo, Eds, Nanotechnologies for Water Environment Applications. Reston, VA: Environmental and Water Resources Institute/American Society for Civil Engineers, pp. 191-212.

Krajangpan, S.; Jarabek, L.; Jepperson, J.; Chisholm, B.; Bezbaruah, A. (2008) Polymer modified iron nanoparticles for environmental remediation. *Polymer Preprint*, 49, 921-922.

Kroll, E.; Winnik, F.M.; Ziolo, R.F (1996) In Situ Preparation of Nanocrystalline g-Fe_2O_3 in Iron(II) Cross-Linked Alginate Gels. *Chem. Mater.,* 8, 1594-1596.

Lee, K.M.; Kim, S.-G.; Kim, W.-S.; Kim, S.S. (2002) Properties of iron oxide particles prepared in the presence of dextran. *Korean J. Chem. Eng.*, 19, 480-485.

Lee, H.S.; Kim, E.H.; Shao, H.; Kwak, B.K. (2005) Synthesis of SPIO-chitosan microspheres for MRI-detectable embolotherapy. *J. Magn. Magn. Mater.*, 293, 102-105.

Li, L.; Fan, M.; Brown, R.C.; Van Leeuwen, J H.; Wang, J.; Wang, W.; Song, Y.; Zhang, Z. (2006) Synthesis, properties, and environmental applications of nanoscale iron-based materials: A review. *Crit. Rev. Env. Sci. Tec.*, 36, 405-431.

Li, X.-Q. ; Brown, D.G. ; Zhang, W.-X. (2007) Stabilization of biosolids with nanoscale zero-valent iron (NZVI). *J. Nanopart. Res*., 9, 233-243.

Lin, J.; Zhou, W.; Kumbhar, A.; Fang, J.; Carpenter, E.E.; O'Connor, C.J. (2001) Gold-coated iron (Fe-Au) nanoparticles: synthesis, characterization, and magnetic field-Induced self-assembly. *J. Solid State Chem.*, 159, 26-31.

Lin, Y.-H.; Tseng, H.-H.; Wey, M.-Y; Lin, M.-D. (2010) Characteristic of two types of stabilized nano zero-valent iron and transport in porous media. *Sci. Total. Environ*., 408, 2260-2267.

Lisabeth, L.D.; Hyeong, A.J.; Chen, J.J.; Shawnita, S.J.; Burke, J.F.; Meliker, J.R. (2010) Arsenic in drinking water and stroke hospitalizations in Michigan. *Stroke*, 41, 2499-2504.

Liu, Y.; Liu, Y.; Majetich, S.A.; Tilton, R.D.; Sholl, D.S.; Lowry, G.V. (2005) TCE dechlorination rates, pathways, and efficiency of nanoscale iron particles with different properties. *Environ. Sci. Technol*., 39, 1338-1345.

Liu, Y.; Majetich, S.A.; Tilton, R.D.; Sholl, D.S.; Lowry, G.V. (2005) TCE dechlorination rates, pathways, and efficiency of nanoscale iron particles with different properties. *Environ. Sci. Technol.,* 39, 1338-1345.

Liu, Y.Q.; Lowry, G.V. (2006) Effect of particle age (Fe-o content) and solution pH on NZVI reactivity: H-2 evolution and TCE dechlorination. *Environ. Sci. Technol*., 40, 6085-6090.

Logan, B. E. *Environmental Transport Processes*; John Wiley and Sons: New York, USA, 1999.

Lowry, G.V.; Liu, Y. (2006). Nanoiron: reactant or catalyst? In:Proceedings of the Division of Environmental Chemistry for the 232nd ACS National Meeting, San Francisco, CA, September 10–14.

Lu, A.H.; Salabas, E.L.; Schuth, F. (2007) Magnetic nanoparticles: Synthesis, protection, functionalization, and application. *Angew. Chem. Int. Edit.,* 46, 1222-1244.Lu, X.X.; Wilson, J.T.; Shen, H.; Henry, B.M.; Kampbell, D.H. (2008) Remediation of TCE-contaminated groundwater by a permeable reactive barrier filled with plant mulch (Biowall). *J. Environ. Sci. A.,* 43, 24-35.

Luepin, O.X.; Hug, S.J.; Badruzzaman, A.B.M. (2005) Arsenic removal from bangladesh tube well water with filter columns containing zerovalent iron filings and sand. *Environ. Sci. Technol*., 39, 8032-8037.

Lui, Y.; Lowry, G.V. (2006) Effect of particle age (Fe^0 content) and solution pH on NZVI reactivity: H_2 evolution and TCE dechlorination. *Environ. Sci. Technol.,* 40, 6085-6090.

Malik, A.H.; Khan, Z.M.; Mahmood, Q.; Nasreen, S.; Bhatti, Z.A. (2009) Perspectives of low cost arsenic remediation of drinking water in Pakistan and other countries. *J. Hazard. Mater.*, 168, 1-22.

Martin, J.E.; Herzing, A.A.; Yan, W.L.; Li, X.Q.; Koel, B.E.; Kiely, C.J.; Zhang, W.X. (2008) Determination of the oxide layer thickness in core-shell zerovalent iron nanoparticles. *Langmuir,* 24, 4329-4334.

Matheson, L.; Tratnyek, P. (1994) Reductive dehalogenation of chlorinated methanes by iron metal. *Environ. Sci. Technol*., 28, 2045-2053.

Mayo, J.T.; Yavuz, C.; Yean, S.; Cong, L.; Shipley, H.; Yu, W.; Falkner, J.; Kan, A.; Tomson, M.; Colvin V.L. (2007) The effect of nanocrystalline magnetite size on arsenic removal. *Sci. Technol. Adv. Mat.,* 8, 71-75.

McNeill, L.S.; Edwards, M. (1995) Soluble arsenic removal at water treatment plants. *J. Am. Water Works Assoc.,* 87, 105–113.

Milazzo, G.; Caroli, S.; Sharma, V.K. (1978) *Tables of Standard Electrode Potentials*. London, England: Wiley.

Mishra, S.; Bajpai, J. (2004) Evaluation of the water sorption and controlled-release potential of binary polymeric beads of starch and alginate loaded with potassium nitrate as an agrochemical. *J. Appl. Polym. Sci*., 94, 1815–1826.

Mohan, D.; Pittman, C.U. (2007) Arsenic removal from water/wastewater using adsorbents - a critical review. *J. Hazard. Mater.,* 142, 1-53.

Mohapatra, S.; Pramanik, N.; Ghosh, S.K.; Pramanik, P. (2006) Synthesis and characterization of ultrafine poly(vinylalcohol phosphate) coated magnetite nanoparticles. *J. Nanosci. Nanotechno.,* 6, 823-829.

Moore, A.M.; Young, T.M., (2005) Chloride interactions with ironsurfaces: implications for perchlorate and nitrate remediationusing permeable reactive barriers. *J. Environ. Eng.,* 131, 924–933.

Morch, Y.A.; Donati, I.; Strand, B.L.; Skjak-Bræk G. (2006) Effect of Ca^{2+}, Ba^{2+}, and Sr^{2+} on alginate microbeads. *Biomacromolecules,* 7, 1471-1480.

Mutin, P.H.; Guerrero, G.; Vioux, A.C.R. (2003) Organic-inorganic hybrid materials based on organophosphorus coupling molecules: from metal phosphonates to surface modification of oxides. *C. R. Chim.*, 6, 1153-1164

Ngai, K.K.T.; Shrestha, R.R.; Dangol, B.; Maharjan, M.; Murcott, S.E. (2007) Design for sustainable development—household drinking water filter for arsenic and pathogen treatment in Nepal. *J. Environ. Sci. Health, Part. A,* 42, 1879–1888.

Nishio, Y.; Yamada, A.; Ezaki, K.; Miyashita, Y.; Furukawa, H.; Horie, K. (2004) Preparation and magnetometric characterization of iron oxide-containing alginate/poly(vinyl alcohol) networks. *Polymer*, 45, 7129-7136.

Nurmi, J.T.; Tratnyek, P.G.; Sarathy, V.; Baer, D.R.; Amonette, J.E.; Pecher, K.; Wang, C.; Linehan, J.C.; Matson, D.W.; Penn, R.L.; Driessen, M.D. (2005) Characterization and properties of metallic iron nanoparticles: spectroscopy, electrochemistry, and kinetics. *Environ. Sci. Technol*., 39, 1221-1230.

Oh, S.-Y.; Chiu, P.C.; Kim, B.J.; Cha, D.K. (2005) Zero-valent iron pretreatment for enhancing the biodegradability of RDX. *Water Res.,* 39, 5027-5032.

Oh, J.I.; Yamamoto, K.; Kitawaki, H.; Nakao, S.; Sugawara, T.; Rahmar, M.M.; Rahman, M.H. (2000) Application of low-pressure nanofiltration coupled with a bicycle pump for the treatment of arsenic-contaminated groundwater. *Desalination,* 132, 307-314.

Olivas, G.I.; Barbosa-Canovas, G.V. (2008) Alginate-calcium films: water vapor permeability and mechanical properties as affected by plasticizer and relative humidity. *LWT-Food Sci. and Technol*., 41, 359-366.

Orth, W.S.; Gillham, R.W. (1996) Dechlorination of trichloroethene in aqueous solution using Fe^0. *Environ. Sci. Technol*., 30, 66-71.

Pant, P.; Pant, S. (2010) A review: Advances in microbial remediation of trichloroethylene (TCE). *J. Environ. Sci.-China,* 22, 116-126.

Papell, S.S. (1965) Low viscosity magnetic fluid obtained by the colloidal suspension of magnetic IC particles. U.S. Patent number 3, 215-572.

Paul, K.G.; Frigo, T.B.; Groman, J.Y.; Groman, E.V. (2004) Synthesis of ultrasmall superparamagnetic iron oxides using reduced polysaccharides. *Bioconjugate Chem.*, 15, 394-401.

Phenrat, T.; Liu, Y.; Tilton, R. D.; Lowry, G. V. (2009) Adsorbed polyelectrolyte coatings decrease Fe^0 nanoparticle reactivity with TCE in water: conceptual model and mechanism. *Environ. Sci. Technol.,* 43, 1507-1514.

Phenrat, T.; Long, T. C.; Lowry, G.V.; Veronesi, B. (2009) Partial Oxidation ("Aging") and Surface Modification Decrease the Toxicity of Nanosized Zerovalent Iron. *Environ. Sci. Technol.,* 43, 195-200.

Phenrat, T.; Saleh, N.; Sirk, K.; Tilton, R.D.; Lowry, G.V. (2007) Aggregation and sedimentation of aqueous nanoscale zerovalent iron dispersions. *Environ. Sci. Technol*., 41, 284-290.

Ponder, S.M.; Darab, J.G.; Mallouk T.E. (2000) Remediation of Cr(VI) and Pb(II) aqueous solutions using supported nanoscale zero-valent iron. *Environ. Sci. Technol.,* 34, 2564-2569.

Pongjanyakul, T.; Puttipipatkhachorn, S. (2007) Modulating drug release and matrix erosion of alginate matrix capsules by microenvironmental interaction with calcium ion. *Eur. J. Pharm. Biopharm*., 67, 187–195.

Portet, D.; Denizot, B.; Rump, E.; Hindre, F.; LeJeune, J.-J.; Jallet, P. (2001) Comparative biodistribution of thin-coated iron oxide nanoparticles TCION: effect of different bisphosphonate coatings. *Drug Dev. Res.*, 54, 173-181.

Powell, R.M.; Puls, R.W.; Blowes, D.W.; Vogan, J.L.; Gillham, R.W.; Schultz, D.; Sivavec, T.; Powell, P.D.; Landis, R. (1998) Permeable reactive barrier technologies for contaminant remediation. EPA-600-R-98-125.

Quinn, J.; Geiger, C.; Clausen, C.; Brooks, K.; Coon, C.; O'Hara, S.; Krug, T.; Major, D.; Yoon, W.S.; Gavaskar, A.; Holdsworth, T. (2005) Field demonstration of DNAPL dehalogenation using emulsified zero-valent iron. *Environ Sci Technol.,* 39, 1309–1318.

Rahme, K.; Vicendo, P.; Ayela, C.; Gaillard, C.; Payre, B.; Mingotaud, C.; Gauffre, F. (2009) A simple protocol to stabilize gold nanoparticles using amphiphilic block copolymers: stability studies and viable cellular uptake. *Chem. Eur. J.*, 15, 11151-11159.

Rivett, M.O.; Feenstra, S.; Cherry, J.A. (2001) A controlled field experiment on groundwater contamination by a multicomponent DNAPL: creation of the emplaced-source and overview of dissolved plume development. *J. Contam. Hydrol*., 49, 111-149.

Rock, M.L.; Kearney, P.C.; Helz, G.R. (1998) Innovative remediation technology. In P.C. Kearney., T. Roberts (Eds.) Pesticide Remediation in Soils and Water, West Sussex, England: Wiley, pp. 1-19.

Rosen, M.J. (2002). *Surfactants and Interfacial Phenomena,* 3rd. ed. Wiley Interscience: New York.

Sabourault, N.; Mignani, G.; Wagner, A.; Mioskowski, C. Platinum oxide (PtO_2): a potent hydrosilylation catalyst. *Org. Lett.* 2002, 4, 2117-2119.

Sahoo, Y.; Goodarzi. A.; Swihart, M.T.; Ohulchanskyy, T.Y.; Kaur, N.; Furlani, E.P.; Prasad, P.N. (2005) Aqueous ferrofluid of magnetite nanoparticles: fluorescence labeling and magnetophoretic control. *J. Phys. Chem. B*, 109, 3879-3885.

Saitua, H.; Gil, R.; Padilla, A.P. (2011) Experimental investigation on arsenic removal with a nanofiltration pilot plant from naturally contaminated groundwater. *Desalination,* 274, 1-6

Saleh, N.; Kim, H.-J.; Phenrat, T.; Matyjaszewski, K.; Tilton, R.D.; Lowry, G.V. (2008) Ionic strength and composition affect the mobility of surface-modified Fe^0 nanoparticles in water-saturated sand columns. *Environ. Sci. Technol.*, 42, 3349-3355.

Saleh, N.; Phenrat, T.; Sirk, K.; Dufour, B.; Ok, J.; Sarbu, T.; Matyjaszewski, K.; Tilton, R.D.; Lowry, G.V. (2005) Adsorbed triblock copolymers deliver reactive iron nanoparticles to the oil/water interface. *Nano. Lett.*, 5, 2489 -2494.

Saleh, N.; Sirk, K.; Liu, Y.; Phenrat, T.; Dufour, B.; Matyjaszewski, K.; Tilton, R. D.; Lowry, G. V. (2007) Surface modifications enhance nanoiron transport and NAPL targeting in saturated porous media. *Environ. Eng. Sci.*, 24, 45-57.

Sato, Y.; Kang, M.; Kamei, T.; Magara, Y. (2002) Performance of nanofiltration for arsenic removal. *Water Res.*, 36, 3371-3377.

Schlicker, O.; Ebert, M.; Firth, M.; Weidner, M.; Wust, W.; Dahmke, A. (2003) Degradation of TCE with iron: the role of competing chromate and nitrate reduction. *Ground Water*, 38, 403–409.

Schnobrich, M.R.; Chaplin, B.P.; Semmens, M.J.; Novak, P.J. (2007) Stimulating hydrogenotrophic denitrification in simulated groundwater containing high dissolved oxygen and nitrate concentrations. *Water Res.*, 41, 1869-1876.

Schrick, B.; Hydutsky, W.; Blough, J.L.; Mallouk, T.E. (2004) Delivery vehicles for zerovalent metal nanoparticles in soil and groundwater. *Chem. Mater.*, 16, 2187-2193.

Shultz, M.D.; Reveles, J.U.; Khanna, S. N.; Carpenter, E.E. (2007) Reactive nature of dopamine as a surface functionalization agent in iron oxide nanoparticles. *J. Am. Chem. Soc.*, 129, 2482-2487.

Siantar, D. P.; Schreier, C. G. (1996) Treatment of 1, 2-dibromo-3-chloropropane and nitrate-contaminated water either zero-valent iron or hydrogen/palladium catalysts. *Water Res.*, 30, 2315-2322.

Smedley, P.L.; Kinniburgh, D.G. (2002) A review of the source, behavior and distribution of arsenic in natural waters. *Appl. Geochem.*, 17, 517-568.

Smidsrød, O.; Skjåk-Braek, G. (1990) Alginate as immobilization matrix for cells. *Trands in Biotechnology*, 8, 71–78.

Sohn, K.; Kang, S.W.; Ahn, S.; Woo, M.; Yang, S.K. (2006) Fe(0) nanoparticles for nitrate reduction: stability, reactivity, and transformation. *Environ. Sci. Technol.*, 40, 5514-5519.

Somaskandan, K.; Veres, T.; Niewczas, M.; Simard, B. (2008) Surface protected and modified iron based core-shell nanoparticles for biological applications. *New J. Chem.*, 32, 201-209.

Song, X.; Jiang, N.; Li, Y.; Xu, D.; Qiu, G. (2008) Synthesis of CeO_2-coated SiO_2 nanoparticle and dispersion stability of its suspension. *Mater. Chem. Phys.*, 110, 128–135.

Steinwinder, T.R.; Zhao, D. (2007) Minimizing arsenic leaching from water treatment process residuals, Auburn University, in Proceeding of Water Environment Federation Conference, 2007.

Stokes, R. J.; Evans, D. F. (1997) *Fundamentals of interfacial engineering*, Wiley-VCN: Canada.

Su, C.; Puls, R.W. (2004) Nitrate reduction by zerovalent iron: effects of formate, oxalate, citrate, chloride, sulfate, borate, and phosphate. *Environ. Sci. Technol*., 38, 2715-2720.

Su, C.; Puls, R.W. (2001) Arsenate and arsenite removal by zerovalent iron: kinetics, redox transformation, and implications for in situ groundwater remediation. *Environ. Sci. Technol.*, 35, 1487-1492.

Su, C.; Puls, R.W. (2008) Arsenate and arsenite sorption on magnetite: relations to groundwater arsenic treatment using zerovalent iron and natural attenuation. *Water Air Soil Poll.*, 193, 65-78.

Sun, H.; Wang, L.; Zhang, R.; Sui, J.; Xu, G. (2006) Treatment of groundwater polluted by arsenic compounds by zero valent iron. *J. Hazard. Mater. B*, 129, 297–303.

Sun, Y.-P.; Li, X.-Q.; Zhang, W.-X.; Wang, H.P. (2007) A method for the preparation of stable dispersion of zero-valent iron nanoparticles. *Colloids and Surfaces A: Physicochem. Eng. Aspects*, 308, 60–66.

Tanboobchuy, V.; Hsu, J.C.; Grisdanurak, N.; Liao, C.H. (2011) Impact of selected solution factors on arsenate and arsenite removal by nano ironparticles. *Environ. Sci. Pollut. R.*, 18, 857-864.

Thompson, J.M.; Chisholm, B.J.; Bezbaruah, A.N. (2010) Reductive dechlorination of chloroacetanilide herbicide (alachlor) using zero-valent iron nanoparticles. *Environ. Eng. Sci.*, 27, 227-232.

Tiraferri, A.; Chen, K.; Sethi, R.; Elimelech, M. (2008) Reduce aggregation and sedimentation of zero-valent iron nanoparticles in the presence of guar gum. *J. Colloid Interface Sci.*, 324, 71-19.

Tiraferri, A.; Sethi, R. (2009) Enhanced transport of zerovalent iron nanoparticles in saturated porous media by guar gum. *J. Nanopart. Res.*, 11, 635–645.

Tratnyek, P.G.; Johnson, R.L. (2006) Nanotechnologies for environmental clean-up. *Nanotoday. 1*, 44-48.

Triszcza, J.M.; Portaa, A.; García Einschlag, F.S. (2009) Effect of operating conditions on iron corrosion rates in zero-valent iron systems for arsenic removal. *Chem. Eng. J.*, 150, 431-439.

Tsai, T.T.; Kao, C.M.; Wang, J.Y. (2011) Remediation of TCE-contaminated groundwater using acid/BOF slag enhanced chemical oxidation. *Chemosphere*., 83, 687-692.

Tyrovola, K.; Peroulaki, E.; Nikolaidis, N.P. (2007) Modeling of arsenic immobilization by zero valent iron. *Euro. J. Soil Bio.,* 43, 356-367.

USEPA. (1992) Measurement of purgable organic compounds in water by capillary column gas chromatography/mass spectrometry, Method 524.2, Environmental Monitoring Systems Laboratory, Office of Research and Development. United Stated Environmental Protection Agency, Ohio.

USEPA (2001) National primary drinking water regulations: arsenic and clarifications to compliance and new source contaminants monitoring: delay of effective date. *Federal Register,* 66, 28342-28346.

USEPA (2004) Capital Costs of Arsenic Removal Technologies U.S. EPA Arsenic removal technology Demonstration Program Round 1 (by Chen, A.S.C.; Wang, L.; Oxenham, J.L.; Condit, W.E.). EPA/600/R-04/201. Cincinnati, Ohio.

USEPA (2011) Basic Information About the Arsenic Rule. Available at http://water.epa.gov/lawsregs/rulesregs/sdwa/arsenic/Basic-Information.cfm. Accessed December, 2011.

Urase, T.; Oh, J.I.; Yamamoto, K. (1998) Effect of pH on rejection of different species of arsenic by nanofiltration. *Desalination,* 117, 11-18.

Velings, N.M.; Mestdagh, M.M. (1995) Physicochemical properties of alginate gel beads. *Polym. Gels Netw*., 3, 311-330.

Vold, I.M.N.; Kristiansen, K.A.; Christensen, B.E. (2006) A study of the chain stiffness and extension of alginates, in vitro epimerized alginates, and periodate-oxidized alginates using size-exclusion chromatography combined with light scattering and viscosity detectors. *Biomacromolecules*, 7, 2136-2146.

Wang, C.B.; Zhang, W.-X. (1997) Synthesizing nanoscale iron particles for rapid and complete dechlorination of TCE and PCBs. *Environ. Sci. Technol*., 31, 2154-2156.

Wang, Q.; Ellis, P.R.; Ross-Murphy, S.B. (2000) The stability of guar gum in an aqueous system under acidic conditions. *Food Hydrocolloid*, 14, 129-134.

Westerhoff, P.; James, J. (2003) Nitrate removal in zero-valent iron packed columns. *Water Res*., 37, 1818–1830.

Wu, C.; Schaum, J. (2000) Exposure assessment of trichloroethylene. *Environ. Health Persp.*, 108, 359-363.

Wu, L.; Shamsuzzoha, M.; Ritchie, S.M.C. (2005) Preparation of cellulose acetate supported zero-valent iron nanoparticles for the dechlorination of trichloroethylene in water. *J. Nanopart. Res.*, 7, 469–476.

Wu, W.P.; Zhao, B.Y.; Wu, Q.; Chen, L.S.; Hu, K.A. (2006) The strengthening effect of guar gum on the yield stress of magnetorheological fluid. *Smart Mater. Struct.*, 15, N94–N98.

Xi, Y.; Mallavarapu, M.; Naidu, R. (2010) Reduction and adsorption of Pb^{2+} in aqueous solution by nano-zero-valent iron—A SEM, TEM and XPS study. *Mater. Res. Bull.*, 45, 1361–1367.

Yang, G. C.; Lee, H.-L. (2005) Chemical reduction of nitrate by nanosized iron:kinetics and pathways. *Water Res*., 39, 884–894.

Zala, S.L.; Ayyer. J.; Desai, A.J. (2004) Nitrate removal from the effluent of a fertilizer industry using a bioreactor packed with immobilized cells of *Pseudomonas stutzeri* and *Comamonas testosterone*. *World J. Microb. Biot*., 20, 661–665.

Zhang, W. (2003) Nanoscale iron particles for environmental remediation: An overview. *J. Nanopart. Res*., 5, 323-332.

Zhang, W.; Singh, P.; Paling, E.; Delides, S. (2004) Arsenic removal from contaminated water by natural iron ores. *Miner. Eng.*,17, 517-524.

Zhang, X.; Lin, Y.-M.; Shan, X.-Q.; Chen, Z.-L. (2010) Degradation of 2,4,6-trinitrotoluene (TNT) from explosive wastewater using nanoscale zero-valent iron. *Chem. Eng. J.*, 158, 566–570.

Zhang, Y.Q.; Frankenberger, W.T. (2006) Removal of selenate in river and drainage waters by *Citrobacter braakii* enhanced with zero-valent iron. *J. Agr. Food Chem.*, 54, 152-156.

APPENDIX A. CHARACTERIZATION OF NZVI (CHAPTER 3)

X-ray diffraction (XRD, Philips X'Pert MPD with Cu Kα X-ray source, PANalytical) was carried out at 40 kV and 30 mA with a scan range from 20˚ to 80˚ to identify the chemical composition of the NZVI. An example data set is shown below.

Table A.1. An example of XRD data set of NZVI

°2Theta	Counts	°2Theta	Counts	°2Theta	Counts	°2Theta	Counts
10.01	120	11.01	95	12.01	89	13.01	83
10.03	110	11.03	104	12.03	99	13.03	72
10.05	117	11.05	103	12.05	81	13.05	72
10.07	113	11.07	118	12.07	81	13.07	79
10.09	123	11.09	101	12.09	88	13.09	76
10.11	123	11.11	107	12.11	93	13.11	77
10.13	112	11.13	99	12.13	89	13.13	86
10.15	135	11.15	96	12.15	105	13.15	76
10.17	99	11.17	107	12.17	85	13.17	71
10.19	115	11.19	96	12.19	99	13.19	76
10.21	121	11.21	104	12.21	81	13.21	89
10.23	111	11.23	101	12.23	89	13.23	79
10.25	115	11.25	98	12.25	82	13.25	84
10.27	112	11.27	104	12.27	87	13.27	72
10.29	108	11.29	94	12.29	80	13.29	77
10.31	106	11.31	96	12.31	84	13.31	68
10.33	118	11.33	106	12.33	98	13.33	65
10.35	96	11.35	105	12.35	97	13.35	83
10.37	109	11.37	100	12.37	81	13.37	81
10.39	116	11.39	95	12.39	81	13.39	75
10.41	109	11.41	94	12.41	86	13.41	83
10.43	92	11.43	97	12.43	83	13.43	74
10.45	105	11.45	83	12.45	83	13.45	82
10.47	110	11.47	107	12.47	88	13.47	78
10.49	111	11.49	96	12.49	88	13.49	70
10.51	117	11.51	101	12.51	95	13.51	74

APPENDIX B. CHARACTERIZATION OF NZVI (CHAPTER 3)

Analysis of TEM image indicated that NZVI particle size ranged from 10 to 90 nm with an average size of 35 nm. The data presented here were used in Figure 3.4.

Table B.1. Particle size distribution of NZVI

Diameter (nm)	Observed (Counts)	Observed (%)
0-10	0	0.00
10-20	23	11.22
20-30	70	34.15
30-40	52	25.37
40-50	28	13.66
50-60	19	9.27
60-70	9	4.39
70-80	3	1.46
90-100	1	0.49

APPENDIX C. NITRATE REMOVAL BY ENTRAPPED NZVI (CHAPTER 3)

Table C.1. Nitrate removal by entrapped and bare NZVI

	100 mg/L				60 mg/L			
	Bare NZVI		Entrapped NZVI		Bare NZVI		Entrapped NZVI	
Time (h)	Avg. C/C_0	SD	Avg. C/C_0	SD	Avg. C/C_0	SD	Avg. C/C_0	SD
0	1.0000	0.0000	1.0000	0.0000	1.0000	0.0001	0.9999	0.0000
0.25	0.8486	0.0029	0.8340	0.0209	0.8821	0.0097	0.9013	0.0254
0.5	0.7381	0.0257	0.7451	0.0304	0.7819	0.0175	0.8394	0.0026
0.75	0.6278	0.0220	0.6324	0.0179	0.6904	0.0019	0.7583	0.0261
1	0.5228	0.0160	0.4990	0.0515	0.5945	0.0118	0.6847	0.0021
1.5	0.3469	0.0325	0.3535	0.0243	0.4971	0.0013	0.5550	0.0243
2	0.2693	0.0079	0.2616	0.0196	0.3874	0.0039	0.4622	0.0333
4	0.1609	0.0424	0.2144	0.0174	0.3066	0.0182	0.3425	0.0492
8	0.1531	0.0259	0.1920	0.0042	0.2295	0.0808	0.2905	0.0000
12	0.1501	0.0226	0.1830	0.0195	0.2276	0.0814	0.2799	0.0079
16	0.1470	0.0145	0.1780	0.0217	0.2282	0.0886	0.2600	0.0220
20	0.1443	0.0115	0.1746	0.0289	0.2261	0.0876	0.2562	0.0256
24	0.1432	0.0092	0.1735	0.0292	0.2257	0.0901	0.2494	0.0250

Table C.1. Nitrate removal by entrapped and bare NZVI (continued)

	20 mg/L				Control		Blank	
	Bare NZVI		Entrapped NZVI					
Time (h)	Avg. C/C_0	SD	Avg. C/C_0	SD	Avg. C/C_0	SD	Avg. C/C_0	SD
0	1.0000	0.0000	1.0000	5.51E-10	1.0000	0.0000	1.000000	0.022614
0.25	0.9069	0.0254	0.9000	0.096393	0.9112	0.0209	0.991493	0.050265
0.5	0.8225	0.0026	0.8123	0.091935	0.9071	0.0304	1.000000	0.015802
0.75	0.7296	0.0261	0.7153	0.020587	0.8991	0.0179	0.985311	0.025802
1	0.6706	0.0021	0.6425	0.004122	0.8991	0.0515	0.991512	0.041046
1.5	0.5347	0.0243	0.5144	0.002257	0.9031	0.0243	0.999660	0.029286
2	0.4618	0.0333	0.4329	0.046143	0.9031	0.0196	0.999248	0.103103
4	0.2616	0.0492	0.4386	0.0254	0.8991	0.0174	1.000000	0.057821
8	0.1943	0.0000	0.3773	0.0026	0.9112	0.0042	0.999908	0.070507
12	0.1926	0.0079	0.3484	0.0261	0.9152	0.0195	0.984040	0.065757
16	0.1834	0.0220	0.2997	0.0021	0.9071	0.0217	0.992731	0.062737
20	0.1810	0.0256	0.2706	0.0243	0.9112	0.0289	0.991854	0.092354
24	0.1778	0.0250	0.2612	0.0333	0.9112	0.0292	0.999904	0.138354

APPENDIX D. COLLOIDAL STABILITY STUDIES (CHAPTER 4)

Table D.1. Comparison between sedimentation of bare NZVI and CNZVI at 20, 40, and 60 min. Light intensity (I) readings from UV-Vis spectrometric study

Time (min)	20	SD	40	SD	60	SD
Bare NZVI	0.171815	0.056286	0.132870	0.053700	0.127033	0.059014
CNZVI	0.667962	0.038502	0.516487	0.033222	0.419087	0.026805

Table D.2. Shelf-life study of CNZVI for 0-4 months. Light intensity (I) readings from UV-Vis spectrometric study

	0 month		1 month		2 month		3 month		4 month	
Time(min)	**Avg. I/I_0**	**SD**	**Avg. I/I_0**	**SD**	**Avg. I/I_0**	**SD**	**Avg. I/I_0**	**SD**	**Avg. I/I_0**	**SD**
0	1	0	1	0	1	0	1	0	1	0
3	0.885	0.008	0.897	0.19	0.891	0.017	0.885	0.008	0.899	0.002
6	0.823	0.012	0.838	0.095	0.831	0.053	0.823	0.012	0.834	0.001
9	0.768	0.015	0.79	0.068	0.786	0.064	0.768	0.015	0.777	0.001
12	0.728	0.016	0.75	0.054	0.758	0.06	0.728	0.016	0.746	0.002
15	0.684	0.012	0.717	0.046	0.711	0.053	0.684	0.012	0.703	0.002
18	0.655	0.01	0.687	0.041	0.69	0.046	0.655	0.01	0.679	0.007
21	0.632	0.007	0.659	0.038	0.659	0.04	0.632	0.007	0.648	0.004
24	0.602	0.005	0.633	0.036	0.634	0.034	0.602	0.005	0.628	0.005
27	0.574	0.002	0.608	0.035	0.603	0.03	0.574	0.002	0.598	0.006
30	0.549	0.001	0.582	0.034	0.587	0.026	0.549	0.001	0.58	0.008
35	0.508	0.002	0.548	0.034	0.545	0.02	0.508	0.002	0.533	0.007
40	0.48	0.004	0.516	0.033	0.518	0.015	0.48	0.004	0.506	0.01
45	0.445	0.006	0.489	0.031	0.484	0.013	0.445	0.006	0.477	0.01
50	0.422	0.007	0.464	0.031	0.461	0.014	0.422	0.007	0.458	0.007
55	0.4	0.009	0.441	0.027	0.44	0.014	0.4	0.009	0.439	0.005
60	0.379	0.01	0.419	0.027	0.42	0.017	0.379	0.01	0.413	0.006
65	0.35	0.012	0.401	0.031	0.404	0.015	0.35	0.012	0.397	0.008
70	0.332	0.015	0.384	0.029	0.388	0.015	0.332	0.015	0.379	0.009
80	0.291	0.024	0.348	0.028	0.35	0.012	0.291	0.024	0.332	0.009
85	0.287	0.025	0.332	0.026	0.338	0.009	0.287	0.025	0.325	0.004
90	0.272	0.025	0.316	0.024	0.313	0.009	0.272	0.025	0.309	0.003
95	0.26	0.024	0.307	0.023	0.302	0.008	0.26	0.024	0.298	0
100	0.256	0.023	0.292	0.022	0.297	0.009	0.256	0.023	0.285	0

Table D.2. Shelf-life study of CNZVI for 5.5-9 months. Light intensity (I) readings from UV-Vis spectrometric study (continued)

	5.5 month		6 month		7 month		8 month		9 month	
Time(min)	**Avg. I/I_0**	**SD**	**Avg. I/I_0**	**SD**	**Avg. I/I_0**	**SD**	**Avg. I/I_0**	**SD**	**Avg. I/I_0**	**SD**
0	1	0	1	0	1	0	1	0	1	0
3	0.890	0.005	0.911	0.005	0.886	0.108	0.840	0.117	0.900	0.190
6	0.789	0.002	0.865	0.004	0.821	0.112	0.778	0.153	0.832	0.095
9	0.732	0.001	0.796	0.005	0.763	0.115	0.723	0.164	0.786	0.068
12	0.687	0.001	0.752	0.006	0.720	0.116	0.683	0.160	0.752	0.054
15	0.650	0.002	0.727	0.009	0.685	0.112	0.639	0.153	0.714	0.046
18	0.631	0.003	0.697	0.012	0.655	0.110	0.610	0.146	0.686	0.041
21	0.601	0.008	0.664	0.013	0.632	0.107	0.587	0.140	0.652	0.038
24	0.578	0.012	0.642	0.012	0.601	0.105	0.557	0.134	0.632	0.036
27	0.545	0.013	0.618	0.014	0.576	0.102	0.529	0.130	0.607	0.035
30	0.520	0.017	0.594	0.013	0.563	0.101	0.504	0.126	0.581	0.034
35	0.480	0.028	0.557	0.012	0.502	0.102	0.463	0.120	0.547	0.034
40	0.450	0.037	0.524	0.013	0.470	0.104	0.435	0.115	0.514	0.033
45	0.426	0.041	0.491	0.015	0.499	0.106	0.400	0.113	0.489	0.031
50	0.401	0.047	0.461	0.015	0.424	0.107	0.377	0.114	0.463	0.031
55	0.380	0.054	0.452	0.015	0.397	0.109	0.355	0.114	0.442	0.397
60	0.357	0.058	0.420	0.014	0.377	0.110	0.334	0.117	0.439	0.377
65	0.335	0.062	0.412	0.015	0.351	0.112	0.305	0.115	0.415	0.351
70	0.315	0.071	0.395	0.014	0.333	0.115	0.287	0.115	0.400	0.333
75	0.302	0.078	0.378	0.014	0.301	0.121	0.261	0.113	0.396	0.301
80	0.291	0.080	0.354	0.013	0.290	0.124	0.246	0.112	0.370	0.290
85	0.279	0.084	0.350	0.012	0.285	0.125	0.242	0.109	0.350	0.285
90	0.266	0.089	0.327	0.013	0.274	0.125	0.227	0.109	0.320	0.274
95	0.262	0.092	0.311	0.011	0.262	0.124	0.215	0.108	0.317	0.262
100	0.255	0.097	0.300	0.011	0.255	0.123	0.211	0.109	0.304	0.255

Table D.2. Shelf-life study of CNZVI for 10-12 months. Light intensity (I) readings from UV-Vis spectrometric study (continued)

	10 month		11 month		12 month	
Time(min)	**Avg. I/I_0**	**SD**	**Avg. I/I_0**	**SD**	**Avg. I/I_0**	**SD**
0	1	0	1	0	1	0
3	0.902	0.017	0.957	0.017	0.912	0.008
6	0.875	0.053	0.910	0.053	0.882	0.012
9	0.786	0.064	0.870	0.064	0.824	0.015
12	0.753	0.060	0.818	0.060	0.790	0.016
15	0.731	0.053	0.773	0.053	0.726	0.012
18	0.695	0.046	0.733	0.046	0.683	0.010
21	0.653	0.040	0.705	0.040	0.657	0.007
24	0.642	0.034	0.661	0.034	0.631	0.005
27	0.632	0.030	0.594	0.030	0.605	0.002
30	0.612	0.026	0.555	0.026	0.572	0.001
35	0.577	0.020	0.504	0.020	0.548	0.002
40	0.522	0.015	0.468	0.015	0.504	0.004
45	0.500	0.013	0.420	0.013	0.473	0.006
50	0.494	0.014	0.404	0.014	0.439	0.007
55	0.463	0.014	0.376	0.014	0.397	0.009
60	0.452	0.017	0.354	0.017	0.376	0.010
65	0.414	0.015	0.348	0.015	0.360	0.012
70	0.399	0.015	0.326	0.015	0.336	0.015
80	0.374	0.013	0.314	0.013	0.305	0.021
85	0.353	0.012	0.307	0.012	0.295	0.024
90	0.349	0.009	0.292	0.009	0.287	0.025
95	0.322	0.009	0.273	0.009	0.279	0.025
100	0.310	0.008	0.269	0.008	0.268	0.024

Table D.3. Sedimentation study of CNZVI in NaCl and $CaCl_2$ solutions. Light intensity (I) readings from UV-Vis spectrometric study

Time	0 mM		10 mM NaCl		5 mM NaCl		5 mM CaCl2		10 mM CaCl2	
(min)	Avg.I/I_0	SD	Avg. I/I_0	SD	Avg. I/I_0	SD	Avg. I/I_0	SD	Avg. I/I_0	SD
0	1	0	1	0	1	0	1	0	1	0
3	0.897	0.190	0.928	0.008	0.904	0.006	0.928	0.006	0.904	0.006
6	0.838	0.095	0.865	0.012	0.840	0.054	0.865	0.002	0.840	0.010
12	0.750	0.054	0.782	0.016	0.753	0.056	0.782	0.004	0.753	0.013
15	0.717	0.046	0.733	0.012	0.720	0.030	0.733	0.005	0.720	0.013
18	0.687	0.041	0.706	0.010	0.684	0.029	0.706	0.007	0.684	0.012
21	0.659	0.038	0.690	0.007	0.657	0.022	0.690	0.006	0.657	0.013
24	0.633	0.036	0.658	0.005	0.632	0.025	0.658	0.005	0.632	0.017
27	0.608	0.035	0.632	0.002	0.603	0.029	0.632	0.007	0.603	0.020
30	0.582	0.034	0.611	0.001	0.586	0.027	0.611	0.009	0.586	0.023
35	0.548	0.034	0.571	0.002	0.544	0.032	0.571	0.011	0.544	0.025
40	0.516	0.033	0.547	0.004	0.516	0.039	0.547	0.012	0.516	0.027
45	0.489	0.031	0.518	0.006	0.482	0.026	0.518	0.014	0.482	0.030
50	0.464	0.031	0.493	0.007	0.466	0.024	0.493	0.014	0.466	0.033
55	0.441	0.027	0.470	0.009	0.450	0.021	0.470	0.016	0.450	0.034
60	0.419	0.027	0.449	0.010	0.420	0.010	0.449	0.016	0.420	0.037
65	0.401	0.031	0.421	0.012	0.402	0.017	0.421	0.016	0.402	0.039
70	0.384	0.029	0.408	0.015	0.386	0.014	0.408	0.016	0.386	0.042
75	0.368	0.027	0.389	0.021	0.361	0.011	0.389	0.014	0.361	0.039
80	0.348	0.028	0.370	0.024	0.346	0.018	0.370	0.015	0.346	0.039
85	0.332	0.026	0.358	0.025	0.331	0.001	0.358	0.016	0.331	0.038
90	0.324	0.025	0.344	0.026	0.319	0.014	0.344	0.018	0.319	0.040
95	0.307	0.023	0.329	0.024	0.306	0.026	0.329	0.019	0.306	0.040
100	0.292	0.022	0.315	0.023	0.294	0.015	0.315	0.019	0.294	0.039

APPENDIX E. TCE DEGRADATION BY CNZVI AND BARE NZVI (CHAPTER 5)

Table E.1. TCE degradation by CNZVI with C_0 = 30 mg/L (intial TCE concentration)

Time (h)	Conc.(1)	C/C_0 (1)	Conc. (2)	C/C_0 (2)	Conc. (3)	C/C_0 (3)	Avg. C/C_0	SD
0	30.864	1.000	29.185	1.000	29.834	1.000	1.000	0.000
0.5	24.220	0.785	17.273	0.592	23.403	0.784	0.720	0.111
1	16.374	0.531	11.398	0.391	15.780	0.529	0.483	0.080
2	6.826	0.221	4.609	0.158	7.672	0.257	0.212	0.050
4	4.072	0.132	3.399	0.116	3.465	0.116	0.122	0.009
6	3.458	0.112	3.156	0.108	3.432	0.115	0.112	0.003
12	3.415	0.111	3.268	0.112	3.465	0.116	0.113	0.003

Table E.2. TCE degradation by bare NZVI with C_0 = 30 mg/L (intial TCE concentration)

Time (h)	Conc.(1)	C/C_0 (1)	Conc. (2)	C/C_0 (2)	Conc. (3)	C/C_0 (3)	Avg. C/C_0	SD
0	29.997	1.000	30.426	1.000	29.732	1.000	1.000	0.000
0.5	24.790	0.826	25.283	0.831	25.974	0.874	0.844	0.026
1	20.209	0.674	21.491	0.706	20.623	0.694	0.691	0.016
2	12.742	0.425	14.645	0.481	13.522	0.455	0.454	0.028
4	6.343	0.211	6.362	0.209	6.655	0.224	0.215	0.008
6	5.521	0.184	5.774	0.190	5.874	0.198	0.190	0.007
12	5.304	0.177	5.711	0.188	5.918	0.199	0.188	0.011

Table E.3. TCE degradation without bare NZVI or CNZVI with C_0 = 30 mg/L (intial TCE concentration) Blank

Time (h)	Conc.(1)	C/C_0 (1)	Conc. (2)	C/C_0 (2)	Conc. (3)	C/C_0 (3)	Avg. C/C_0	SD
0	29.997	1.000	30.226	1.000	30.032	1.000	1.000	0.000
0.5	29.469	0.982	30.225	1.000	30.017	0.999	0.994	0.010
1	29.917	0.997	30.247	1.001	30.000	0.999	0.999	0.002
2	29.187	0.973	30.169	0.998	30.057	1.001	0.991	0.015
4	29.456	0.982	30.298	1.002	30.000	0.999	0.994	0.011
6	29.818	0.994	30.169	0.998	29.990	0.999	0.997	0.002
12	29.464	0.982	30.198	0.999	30.000	0.999	0.993	0.010

Table E.4. TCE degradation with only APGC and without any NZVI with C_0 = 30 mg/L (intial TCE concentration) Control

Time (h)	Conc.(1)	C/C_0 (1)	Conc. (2)	C/C_0 (2)	Conc. (3)	C/C_0 (3)	Avg. C/C_0	SD
0	30.051	1.000	30.000	1.000	30.132	1.000	1.000	0.000
0.5	29.532	0.983	29.549	0.985	30.045	0.997	0.988	0.008
1	29.022	0.966	29.655	0.989	30.002	0.996	0.983	0.016
2	29.001	0.965	29.420	0.981	30.000	0.996	0.980	0.015
4	29.000	0.965	29.332	0.978	29.922	0.993	0.979	0.014
6	29.056	0.967	29.156	0.972	29.616	0.983	0.974	0.008
12	29.026	0.966	29.055	0.969	29.420	0.976	0.970	0.005

Table E.5. TCE degradation by CNZVI with C_0 = 15 mg/L (intial TCE concentration)

Time (h)	Conc.(1)	C/C_0 (1)	Conc. (2)	C/C_0 (2)	Conc. (3)	C/C_0 (3)	Avg. C/C_0	SD
0	15.000	1.000	14.932	1.000	14.947	1.000	1.000	0.000
0.5	11.534	0.769	11.331	0.759	11.577	0.775	0.767	0.008
1	8.978	0.599	8.556	0.573	9.128	0.611	0.594	0.019
2	4.657	0.310	4.375	0.293	4.851	0.325	0.309	0.016
4	3.323	0.222	3.186	0.213	3.478	0.233	0.223	0.010
6	3.056	0.204	2.920	0.196	3.135	0.210	0.203	0.007
12	2.932	0.195	2.218	0.149	2.687	0.180	0.175	0.024

Table E.6. TCE degradation by bare NZVI with C_0 = 15 mg/L (intial TCE concentration)

Time (h)	Conc.(1)	C/C_0 (1)	Conc. (2)	C/C_0 (2)	Conc. (3)	C/C_0 (3)	Avg. C/C_0	SD
0	15.000	1.000	14.985	1.000	15.000	1.000	1.000	0.000
0.5	13.232	0.882	13.154	0.878	13.126	0.875	0.878	0.004
1	10.983	0.732	10.956	0.731	10.325	0.688	0.717	0.025
2	7.247	0.483	7.485	0.499	7.542	0.503	0.495	0.011
4	4.085	0.272	4.042	0.270	4.004	0.267	0.270	0.003
6	3.905	0.260	3.870	0.258	3.823	0.255	0.258	0.003
12	3.535	0.236	3.463	0.231	3.578	0.239	0.235	0.004

Table E.7. TCE degradation without bare NZVI or CNZVI with C_0 = 15 mg/L (intial TCE concentration) Blank

Time (h)	Conc.(1)	C/C_0 (1)	Conc. (2)	C/C_0 (2)	Conc. (3)	C/C_0 (3)	Avg. C/C_0	SD
0	14.686	0.989	14.190	0.980	14.557	1.000	0.990	0.010
0.5	14.844	1.000	14.451	0.998	14.474	0.994	0.997	0.003
1	14.463	0.974	14.174	0.979	14.433	0.991	0.981	0.009
2	14.704	0.991	14.190	0.980	14.520	0.997	0.989	0.009
4	14.547	0.980	14.485	1.000	14.472	0.994	0.991	0.010
6	14.435	0.972	14.168	0.978	14.361	0.987	0.979	0.007
12	14.521	0.978	14.156	0.977	14.406	0.990	0.982	0.007

Table E.8. TCE degradation with only APGC and without any NZVI with C_0 = 15 mg/L (intial TCE concentration) Control

Time (h)	Conc.(1)	C/C_0 (1)	Conc. (2)	C/C_0 (2)	Conc. (3)	C/C_0 (3)	Avg. C/C_0	SD
0	14.518	0.997	14.234	0.966	14.508	0.998	0.987	0.018
0.5	14.568	1.000	14.733	1.000	14.406	0.991	0.997	0.005
1	14.506	0.996	14.557	0.988	14.532	1.000	0.995	0.006
2	14.547	0.999	14.192	0.963	14.451	0.994	0.985	0.019
4	14.527	0.997	14.538	0.987	14.500	0.998	0.994	0.006
6	14.488	0.995	14.512	0.985	14.493	0.997	0.992	0.006
12	14.444	0.991	14.295	0.970	14.464	0.995	0.986	0.013

Table E.9. TCE degradation by CNZVI with C_0 = 1 mg/L (intial TCE concentration)

Time (h)	Conc.(1)	C/C_0 (1)	Conc. (2)	C/C_0 (2)	Conc. (3)	C/C_0 (3)	Avg. C/C_0	SD
0	1.003	1.000	0.996	1.000	0.989	1.000	1.000	0.000
0.5	0.812	0.810	0.763	0.766	0.811	0.820	0.799	0.029
1	0.695	0.693	0.674	0.677	0.685	0.693	0.687	0.009
2	0.491	0.490	0.507	0.509	0.512	0.518	0.505	0.014
4	0.300	0.299	0.295	0.296	0.284	0.287	0.294	0.006
6	0.222	0.221	0.231	0.232	0.236	0.239	0.231	0.009
12	0.200	0.199	0.210	0.211	0.238	0.241	0.217	0.021

Table E.10. TCE degradation by bare NZVI with C_0 = 1 mg/L (intial TCE concentration)

Time (h)	Conc.(1)	C/C_0 (1)	Conc. (2)	C/C_0 (2)	Conc. (3)	C/C_0 (3)	Avg. C/C_0	SD
0	1.028	1.000	1.025	1.000	1.000	1.000	1.000	0.000
0.5	0.925	0.900	0.910	0.888	0.880	0.880	0.889	0.010
1	0.832	0.809	0.780	0.761	0.755	0.755	0.775	0.030
2	0.567	0.552	0.505	0.493	0.523	0.523	0.522	0.029
4	0.377	0.367	0.354	0.345	0.312	0.312	0.341	0.028
6	0.288	0.280	0.297	0.290	0.289	0.289	0.286	0.005
12	0.245	0.238	0.260	0.254	0.252	0.252	0.248	0.008

Table E.11. TCE degradation without bare NZVI or CNZVI with C_0 = 1 mg/L (intial TCE concentration) Blank

Time (h)	Conc.(1)	C/C_0 (1)	Conc. (2)	C/C_0 (2)	Conc. (3)	C/C_0 (3)	Avg. C/C_0	SD
0	1.041	1.000	1.041	0.988	1.103	0.988	0.992	0.007
0.5	1.031	0.990	1.030	0.977	1.116	1.000	0.989	0.011
1	1.040	0.999	1.051	0.997	1.102	0.987	0.995	0.006
2	1.037	0.996	1.050	0.996	1.109	0.994	0.995	0.001
4	1.038	0.997	1.043	0.990	1.098	0.984	0.990	0.007
6	1.035	0.994	1.054	1.000	1.110	0.995	0.996	0.003
12	1.037	0.996	1.049	0.995	1.112	0.996	0.996	0.001

Table E.12. TCE degradation with only APGC and without any NZVI with C_0 = 1 mg/L (intial TCE concentration) Control

Time (h)	Conc.(1)	C/C_0 (1)	Conc. (2)	C/C_0 (2)	Conc. (3)	C/C_0 (3)	Avg. C/C_0	SD
0	14.518	0.997	14.234	0.966	14.508	0.998	0.987	0.018
0.5	14.568	1.000	14.733	1.000	14.406	0.991	0.997	0.005
1	14.506	0.996	14.557	0.988	14.532	1.000	0.995	0.006
2	14.547	0.999	14.192	0.963	14.451	0.994	0.985	0.019
4	14.527	0.997	14.538	0.987	14.500	0.998	0.994	0.006
6	14.488	0.995	14.512	0.985	14.493	0.997	0.992	0.006
12	14.444	0.991	14.295	0.970	14.464	0.995	0.986	0.013

Table E.13. Shelf-life study of TCE degradation by CNZVI for 0-3 months

	0 month		1 month		2month		3 month	
Time (h)	**Avg. C/C_0**	**SD**	**Avg. C/C_0**	**SD**	**Avg. C/C_0**	**SD**	**Avg. C/C_0**	**SD**
0	30.135	0.786	29.961	0.847	30.080	0.253	30.864	0.000
0.5	21.639	1.686	21.632	3.797	20.837	1.890	24.220	0.136
1	14.636	0.863	14.518	2.718	15.136	2.791	7.605	0.102
2	6.468	2.354	6.369	1.582	6.647	0.538	3.976	0.021
4	3.637	0.567	3.645	0.371	3.718	0.108	3.414	0.004
6	3.356	0.397	3.349	0.167	3.358	0.160	3.239	0.002
12	3.382	0.199	3.383	0.102	3.350	0.119	2.442	1.046

Table E.13. Shelf-life study of TCE degradation by CNZVI for 4-6 months (continued)

	4 month		5 month		6 month	
Time (h)	**Avg. C/C_0**	**SD**	**Avg. C/C_0**	**SD**	**Avg. C/C_0**	**SD**
0	29.185	0.435	29.997	0.000	29.185	0.000
0.5	17.273	1.831	24.790	0.096	17.273	1.025
1	11.399	1.532	15.209	1.292	11.399	1.003
2	4.609	0.795	7.742	1.021	4.609	1.026
4	3.399	0.189	4.343	0.904	3.399	0.702
6	3.156	0.093	3.521	0.802	3.156	0.824
12	3.268	0.540	3.030	0.046	3.268	0.033

APPENDIX F. AS(V) REMOVAL BY CNZVI AND BARE NZVI (CHAPTER 6)

Table F.1. As(V) removal by CNZVI with 10 mg/L intial As(V) concentration

	Anaerobic				Aerobic				Blank		Control	
	CNZVI		Bare NZVI		CNZVI		Bare NZVI					
Time (h)	Avg. C/C_0	SD	Avg. C/C_0	SD	Avg. C/C_0	SD	Avg. C/C_0	SD	Avg. C/C_0	SD	Avg. C/C_0	SD
0.000	1.000	0.000	1.000	0.000	1.000	0.000	1.000	0.000	1.000	0.000	1.000	0.000
0.083	0.385	0.002	0.576	0.034	0.302	0.035	0.554	0.065	0.999	0.050	0.984	0.017
0.250	0.134	0.031	0.247	0.042	0.095	0.035	0.196	0.036	0.983	0.073	0.979	0.050
0.500	0.033	0.100	0.110	0.084	0.023	0.050	0.085	0.043	0.989	0.002	0.985	0.011
0.750	0.026	0.001	0.063	0.029	0.004	0.016	0.044	0.066	0.982	0.012	0.977	0.098
1.000	0.025	0.060	0.064	0.055	0.003	0.069	0.044	0.070	0.999	0.070	0.983	0.036
1.500	0.022	0.050	0.062	0.002	0.004	0.035	0.043	0.056	0.983	0.063	0.960	0.024
2.000	0.024	0.101	0.060	0.042	0.003	0.015	0.043	0.033	0.983	0.003	0.960	0.044

Table F.2. As(V) removal by CNZVI and bare NZVI with 5 mg/L intial As(V) concentration

	Anaerobic				Aerobic				Blank		Control	
	CNZVI		Bare NZVI		CNZVI		Bare NZVI					
Time (h)	Avg. C/C_0	SD	Avg. C/C_0	SD	Avg. C/C_0	SD	Avg. C/C_0	SD	Avg. C/C_0	SD	Avg. C/C_0	SD
0	0	1	0	1	0	1	0	1	0	1	0	0
0.083	0.083	0.487	0.025	0.649	0.06	0.997	0.033	0.997	0.005	0.417	0.016	0.083
0.25	0.25	0.233	0	0.309	0.033	0.981	0.049	0.995	0.106	0.167	0.136	0.25
0.5	0.5	0.087	0.061	0.157	0.042	0.989	0.029	0.985	0.019	0.014	0.028	0.5
0.75	0.75	0.055	0.001	0.124	0.063	0.991	0.06	0.994	0.006	0.016	0.037	0.75
1	1	0.065	0.05	0.11	0.041	0.979	0.007	0.992	0.057	0.013	0.105	1
1.5	1.5	0.055	0.03	0.108	0.002	0.982	0.017	0.986	0.034	0.013	0.025	1.5
2	2	0.055	0.04	0.114	0.071	0.985	0.01	0.989	0.069	0.013	0.023	2

Table F.3. As(V) removal by CNZVI and bare NZVI with 1 mg/L intial As(V) concentration

	Anaerobic				Aerobic				Blank		Control	
	CNZVI		Bare NZVI		CNZVI		Bare NZVI					
Time (h)	Avg. C/C_0	SD	Avg. C/C_0	SD	Avg. C/C_0	SD	Avg. C/C_0	SD	Avg. C/C_0	SD	Avg. C/C_0	SD
0	1	0	1	0	1	0	1	0	1	0	1	0
0.083	0.409	0.024	0.672	0.047	0.989	0.011	0.969	0.066	0.391	0.016	0.409	0.024
0.25	0.272	0.036	0.429	0.026	0.995	0.006	0.969	0.054	0.156	0.028	0.272	0.036
0.5	0.197	0.005	0.271	0.003	0.995	0.001	0.983	0.016	0.059	0.028	0.197	0.005
0.75	0.171	0.009	0.226	0.04	0.99	0.007	0.97	0.024	0.009	0.037	0.171	0.009
1	0.166	0.008	0.208	0.033	0.996	0.003	0.969	0.036	0.005	0.026	0.166	0.008
1.5	0.164	0.006	0.204	0.028	0.996	0.001	0.971	0.037	0	0	0.164	0.006
2	0.166	0.004	0.201	0.036	0.974	0.013	0.964	0.016	0	0	0.166	0.004

Table F.4. As(V) removal by CNZVI in NaCl and $CaCl_2$ solutions

	NaCl		$CaCl_2$		Blank		Control	
Time (h)	**Avg. C/C_0**	**SD**	**Avg. C/C_0**	**SD**	**Avg. C/C_0**	**SD**	**Avg. C/C_0**	**SD**
0.000	1.000	0.000	1.000	0.000	0.992	0.000	1.000	0.000
0.083	0.554	0.048	0.686	0.004	0.979	0.047	0.391	0.016
0.250	0.225	0.049	0.295	0.003	0.995	0.026	0.156	0.028
0.500	0.158	0.051	0.181	0.012	0.985	0.003	0.059	0.028
0.750	0.052	0.053	0.092	0.028	0.990	0.040	0.009	0.037
1.000	0.056	0.054	0.091	0.036	0.966	0.033	0.009	0.026
1.500	0.056	0.069	0.079	0.067	0.996	0.028	0.009	0.025
2.000	0.052	0.071	0.090	0.084	0.974	0.036	0.009	0.023